

B.Sc. in Computer Science and Engineering Thesis

Study on Fiber Nonlinearities and Polarization Mode Dispersion on DWDM System

Submitted by

Md. Azad Hossain
201014007

Yunus Ibne Abdullah
201014012

Supervised by

Lieutenant Colonel Kazi Abu Taher,psc,te
Instructor Class-'A'
Department of Computer Science and Engineering
Military Institute of Science and Technology
Dhaka, Bangladesh



**Department of Computer Science and Engineering
Military Institute of Science and Technology**

CERTIFICATION

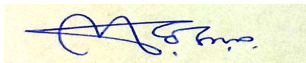
This thesis paper titled “**Study on Fiber Nonlinearities and Polarization Mode Dispersion on DWDM System**”, submitted by the group as mentioned below has been accepted as satisfactory in partial fulfillment of the requirements for the degree B.Sc. in Computer Science and Engineering on December 2013.

Group Members:

Md. Azad Hossain

Yunus Ibne Abdullah

Supervisor:



Lieutenant Colonel Kazi Abu Taher,psc,te
Instructor Class-’A’
Department of Computer Science and Engineering
Military Institute of Science and Technology
Dhaka, Bangladesh

CANDIDATES' DECLARATION

This is to certify that the work presented in this thesis paper is the outcome of the investigation and research carried out by the following students under the supervision of Lieutenant Colonel Kazi Abu Taher, psc, te Instructor Class-'A', Department of Computer Science and Engineering, Military Institute of Science and Technology, Dhaka, Bangladesh.

It is also declared that neither this thesis paper nor any part there of has been submitted anywhere else for the award of any degree, diploma or other qualifications.

Md. Azad Hossain
201014007

Yunus Ibne Abdullah
201014012

ACKNOWLEDGEMENT

We are thankful to Almighty Allah for his blessings for the successful completion of our thesis. Our heartiest gratitude, profound indebtedness and deep respect go to our supervisor Lieutenant Colonel Kazi Abu Taher, psc, te Instructor Class-'A', Department of Computer Science and Engineering, Military Institute of Science and Technology, Dhaka, Bangladesh, for his constant supervision, affectionate guidance and great encouragement and motivation. His keen interest on the topic and valuable advices throughout the study was of great help in completing thesis.

We are especially grateful to the Department of Computer Science and Engineering (CSE) of Military Institute of Science and Technology (MIST) for providing their all out support during the thesis work.

Finally, we would like to thank our families and our course mates for their appreciable assistance, patience and suggestions during the course of our thesis.

Dhaka
December 2013

Md. Azad Hossain
Yunus Ibne Abdullah

ABSTRACT

The rapid worldwide growth of data and internet traffic in telecommunication networks has resulted in a sharp increase in the demand for transmission capacity. Efficient utilization of the existing optical fiber network is an answer to this growing demand. An important step to this end is the introduction of optical communication systems with terabits per second capacity, which are based on Dense Wavelength Division Multiplexing (DWDM) system. This DWDM system has brought a big leap of transmission capacity in optical communication systems. Some research groups have already demonstrated that it is possible to transmit almost a Tbits/s bit rate over thousands of kilometers. But such higher data transmission rates impose very strict requirements on the fiber plants and transmission systems. In particular the nonlinearity effects and polarization mode dispersion (PMD) can be a serious limitation on certain fiber links, particularly on links in older legacy networks. Recent papers written on this topic argue that even fibers made and deployed in the 1990 to 2001 time frame, may be unstable due to the challenges presented by the nonlinearity and PMD effect. As network data rates continue to rise, it is becoming increasingly important to understand the nonlinearity and PMD effect and their potential impact in the network. PMD in optical fibers is considered to be the ultimate limitation in DWDM system. Many studies on first and higher-order PMD compensation have already been reported, but most of them are based on single channel systems and the nonlinear effects in optical fibers such as Cross Phase Modulation (XPM), Four Wave Mixing (FWM) are overlooked. But in DWDM system the nonlinearity and PMD phenomena both lead to pulse distortion and system impairments which adversely limit the transmission capacity of the fiber. In this paper an endeavor has been taken to cover the practical aspects and implications of nonlinearity and PMD effects on fiber transmission systems. A rigorous analysis has been carried out to quantify the effect of XPM and how they affect PMD impairments and mitigation.

TABLE OF CONTENT

<i>CERTIFICATION</i>	ii
<i>CANDIDATES' DECLARATION</i>	iii
<i>ACKNOWLEDGEMENT</i>	iv
<i>ABSTRACT</i>	v
List of Figures	xiii
List of Tables	xiv
List of Abbreviation	xv
List of Symbols	xvii
1 INTRODUCTION	1
1.1 Communication System	1
1.2 Evolution of Optical Communication	2
1.3 Review of Previous and Present State of Works	5
1.4 Research Aims	13
2 OPTICAL COMMUNICATION, FIBER NONLINEARITIES AND POLARIZATION MODE DISPERSION	14
2.1 Principles of Optical Communication	14
2.1.1 Optical Transmitter	14
2.1.2 Optical Fiber	15

2.1.3	Optical Receiver	15
2.2	Wavelength Division Multiplexing (WDM) and Dense WDM (DWDM) . .	16
2.3	Fundamentals of Nonlinear Effects in Optical Fibers	17
2.3.1	Stimulated Brillouin Scattering (SBS)	17
2.3.2	Stimulated Raman Scattering (SRS)	18
2.3.3	Optical Kerr Effect	19
2.4	Fundamentals of Polarization Mode Dispersion	24
2.4.1	Sources of Birefringence	25
2.4.2	PMD Coefficient	26
2.4.3	PMD in Short-Length and High-Birefringence Fibers	26
2.4.4	PMD in Long-Length Fibers	28
2.4.5	PMD compensators	30
2.5	Summary	30
3	THEORETICAL ANALYSIS OF XPM AND PMD ON DWDM SYSTEM	31
3.1	Introduction	31
3.2	Duobinary Line Code	32
3.2.1	Differential Encoding	34
3.2.2	Differential Encoder	35
3.2.3	Optical System for Duobinary Modulation	36
3.3	A Multi-Level Novel Optical Line Code	38
3.3.1	First Order Code	38
3.4	Theoretical Analysis of XPM	42
3.4.1	Input and Output Power Representation	43
3.4.2	Bit Error Rate (BER) Derivation	46

3.4.3	Applying Line Coding Schemes	47
3.4.4	Applying Duobinary Line Coding Schemes	47
3.4.5	Applying Novel Optical Line Coding Schemes	47
3.4.6	Summary on Theoretical Analysis of XPM	48
3.5	Theoretical Analysis of PMD	48
3.5.1	System Modeling	49
3.5.2	Summary on Theoretical Analysis of PMD	51
4	SIMULATION METHODS AND RESULTS	52
4.1	Simulation Methods for XPM	52
4.2	Split Step Fourier Method	52
4.2.1	Light Waves Beam Propagation Method using Split Step Model	53
4.2.2	Algorithm for the Split Step Model	55
4.3	Eye-opening Penalty	57
4.4	Filter Design	58
4.5	Simulation Results for XPM in the DWDM System	59
4.6	Combating XPM by Dispersion Management	78
4.7	Discussions	78
4.8	Summary	79
4.9	Simulation for PMD in the DWDM System	79
4.10	Simulation Results for PMD in the DWDM System	79
4.10.1	Simulation with Varying Dispersion	80
4.10.2	Simulation with Varying PMD Coefficient	84
4.11	Summary	90

5 CONCLUSION AND FUTURE WORK 91

5.1 Conclusion of this Study 91

5.2 Future Work 92

References 92

LIST OF FIGURES

2.1	Optical fiber communication system	14
2.2	Block Diagram of an Optical Transmitter	15
2.3	Block Diagram of an Optical Receiver	16
2.4	Graphical Representation of a Point to Point WDM Optical System	16
2.5	Experimental Setup to Demonstrate the Effects of XPM	21
2.6	Illustration of Walk-off Distance	23
2.7	Illustration of Side-Bands Generation due to FWM in Two-Channel Systems	23
2.8	Birefringence of Internal and External Sources (a) Internal sources; such as: core asymmetry and built in stress (b) External sources; such as: bend twists and external stress applied to the fiber	25
2.9	A schematic of pulse broadening due to PMD	27
3.1	Duobinary Encoder	34
3.2	Differential Encoder with an XOR Gate	35
3.3	Differential Encoder with a Divide-by-2 Counter	36
3.4	Effect of Dispersion on NRZ and Duobinary Sequences	36
3.5	NRZ and Duobinary Signal for Data Sequence [1 0 1 0 0 0 1 1 1 1 0 1 0 1 0 1]	37
3.6	(a) Elementary Signals and (b) Code State Diagram for Novel Multilevel Optical Line Code of Order one.	39
3.7	(Transmitter Model of an optical system	40
3.8	An Example Showing NRZ and Duobinary Signals for Data Sequence [0 1 1 0 0 0 1 1 1 1 0 1 0 1 0 1]	41
3.9	Block diagram for analyzing effect of PMD	50
3.10	Block diagram for optical PMD compensation	50

3.11	Simulation block for analyzing effect and compensation of PMD	51
4.1	Schematic Illustration of Symmetrized Split Step Model	55
4.2	(a) Frequency and (b) Magnitude Response of a Butterworth Lowpass Filter	59
4.3	(a) Normalized IM index in dB and (b) phase response versus the pump modulation frequency for the channel separations of 0, 0.25 and 4 nm. The average power per channel is 0 dBm. Here $\lambda_1=1550$ nm, $D = 17$ ps/km-nm, $Y_1 = 1.18W^{-1} \cdot km^{-1}$, $\alpha = 0.21$ dB/km and $L = 80$ km.	61
4.4	Total XPM induced power in a lossless system with probe power $P_1 = 0$ dBm, bit rate = 10 GHz, channel spacing = 50 GHz and fiber length = 50, 100 and 150 km for pump power (P_2) = (a) -20 to 20 and (b) -10 to 10 dBm	62
4.5	Total XPM induced power in a lossless system with pump power $P_2 = 0$ dBm, bit rate = 10 GHz, channel spacing = 50 GHz and fiber length = 50, 100 and 150 km for probe power (P_1) = (a) -20 to 20 and (b) -10 to 10 dBm	63
4.6	Total XPM induced power for a lossy system with probe power $P_1 = 0$ dBm, bit rate = 10 GHz, channel spacing = 50 GHz and fiber Length = 50, 100 and 150 km	64
4.7	Total XPM power in dB for different (a) probe powers (0, -5 and -10 dBm) and (b) pump powers (-10, -5 and 0 dBm) at 100 km	65
4.8	Plot of BER for channel spacing 50, 60, and 75 and 100 GHz with $P_2 = 0$ dBm, fiber length = 100 km and bit rate = 10 GHz	66
4.9	XPM Power with line coding, (a) analytical result for pump power = -10 and 0 dBm and (b) simulated result for probe power = -10 and 0 dBm with fiber length = 100 km, bit rate = 10 GHz and channel spacing = 50 GHz	68
4.10	(a) Analytical (b) Simulated BER for different probe powers -10, -5, 0, 5 and 10 dBm at 100 km with bit rate = 10 GHz and channel spacing = 50 GHz	69
4.11	(a) Analytical (b) Simulated BER for different pump powers -10, -5, 0, 5 and 10 dBm at 100 km	70

4.12	Plot of (a) XPM induced power and (b) BER caused by XPM with NRZ data, Duobinary and Novel Order 1 Code for probe power -10, -5, 0, 5 and 10 dBm for 100 km fiber	71
4.13	Plot of (a) XPM induced power and (b) BER caused by XPM with NRZ data, Duobinary and Novel Order 1 Code for pump power -10, -5, 0, 5 and 10 dBm for 100 km fiber	72
4.14	Plot of allowable pump power for BER of 10^{-9} at 50, 100 and 150 km	73
4.15	Plot of allowable probe power for BER of 10^{-9} at 50, 100 and 150 km	74
4.16	Plot of 512 bit (PRBS) eye-power penalty of NRZ data for 25, 50, 100, and 150 km	75
4.17	Plot of 512 bit (PRBS) eye-power penalty of Duobinary coded data for 25, 50, 100 and 150 km	76
4.18	Plot of 512 bit (PRBS) eye-power penalty of Novel Optical coded data for 25, 50, 100 and 150 km	77
4.19	Eye diagram at run 1 showing a Q value of 6.0206 dB	80
4.20	Eye diagram at run 2 showing a Q value of 7.463510 dB	81
4.21	Eye diagram at run 3 showing a Q value of 9.911912 dB	81
4.22	Eye diagram at run 4 showing a Q value of 12.561970 dB	82
4.23	Eye diagram at run 5 showing a Q value of 15.541085 dB	82
4.24	(a) Graph (b) Eye Opening Graph (c) Optical Spectrum for Transmitted Signal (d) Optical Spectrum for Received Signal for simulation 1 is shown	83
4.25	Eye diagram at run 1 showing a Q value of 21.072053 dB	84
4.26	Eye diagram at run 2 showing a Q value of 23.00 dB shows that the due to the time varying effect the eye diagram changes and thus Q value also changes	85
4.27	Eye diagram at run 3 showing a Q value of 22.850229 dB showing variations	85
4.28	Eye diagram at run 4 showing a Q value of 21.946904 dB	86

4.29	Eye diagram at run 5 showing a Q value of 11.909151 dB	86
4.30	Eye diagram at run 6 showing a Q value of 15.477207 dB	87
4.31	Eye diagram at run 7 showing a Q value of 13.984685 dB	87
4.32	(a) Graph (b) Eye Opening Graph (c) Optical Spectrum for Transmitted Signal (d) Optical Spectrum for Received Signal for simulation 2 is shown	88
4.33	(a) combined effect of Q value and dispersion (b) combined effect of Q value and PMD (c) combined effect of Q value PMD and dispersion for simulation 3 is shown	89

LIST OF TABLES

3.1	An Example Showing the Transformation of Data in a Duobinary System	38
3.2	Map containing the value of g_2	40
3.3	Encoding Rule of Novel Optical Line Code (Order1)	40
4.1	Improvement in allowable pump power in dB by applying Novel line code in comparison with NRZ data for BER of 10^{-9} at different lengths	73
4.2	Improvement in allowable probe power in dB by applying Novel line code in comparison with NRZ data for BER of 10^{-9} at different lengths	74
4.3	Eye power penalty for pump power of 0 dBm and probe power of -10 dBm	78
4.4	Simulation 1 with varying dispersion keeping other factors constant	80
4.5	Simulation 2 with varying PMD co-efficients keeping other factors constant	84

LIST OF ABBREVIATION

ABI	: Alternate Block Inversion
ASE	: Amplified Spontaneous Emission
ASK	: Amplitude Shift Keying
BER	: Bit Error Rate
CCR	: Carrier to Crosstalk Ratio
CW	: Continuous Wave
DCF	: Dispersion Compensating Fibers
DGD	: Differential Group Delay
DRA	: Distributed Raman Amplification
DPKS	: Data Pulse Known Symbol Rate
DSF	: Dispersion Shifted Fiber
DWDM	: Dense Wavelength Division Multiplexing
EDFA	: Erbium Doped Fiber Amplifier
EOAT	: Eye Opening after Transmission (with fiber)
EOBB	: Eye Opening Back-to-Back (without fiber)
EOP	: Eye Opening Penalty
FFT	: Fast Fourier Transform
FIR	: Finite Impulse Response
FWM	: Four Wave Mixing
GaAs	: Gallium Arsenide
GVD	: Group Velocity Dispersion
IrDI	: Inter-Domain Interfaces
IM	: Intensity Modulation
IM/DD	: Intensity Modulation Direct Detection
ISI	: Inter-Symbol Interference
ITU	: International Telecommunication Union
LAN	: Local Area Network
LECAF	: Large Effective Core Area Fiber
LED	: Light Emitting Diode

MMI : Monospaced Mark Inversion
MZ : Mach-Zehnder
NLSE : Nonlinear Schrödinger Equation
NRZ : Non Return to Zero
NZDSF Non Zero dispersion Shifted Fiber
OFC : Optical Fiber Communication
OSNR : Optical Signal Noise Ratio
OSSB : Optical Single Side-band
PASS : Phased Amplitude Shift Signaling
PMD : Polarization Mode Dispersion
PMDC: Polarization Mode Dispersion compensator
PSP : Principal States of Polarization
PSK : Phase Shift Keying
SBS : Simulated Brillouin Scattering
SCM : Synchronous Channel Multiplexer
SMF : Single Mode Fiber
SNR : Signal to Noise Ratio
SOP : State of Polarization
SPM : Self Phase Modulation
SRS : Simulated Raman Scattering
TAT : Transatlantic Telephone
TPC : Transpacific Crossings
WDM : Wavelength Division Multiplexing
XPM : Cross Phase Modulation
ZDSF : Zero dispersion Shifted Fiber

LIST OF SYMBOLS

Mb/s	: Mega bit per second
dB/km	: Decibel per kilometer
GHz	: Giga Hertz
THz	: Tera Hertz
Gb/s	: Gigabytes per second
Km	: Kilometer
μm	: Micrometer
Tbits/s	: Tera bits per second
gB	: Brillouin gain coefficient
ΔV_s	: Line width of the source
ΔV_B	: Brillouin line-width
$I(t)$: Optical intensity
λ	: Wavelength of optical wave
z	: Propagation distance
M	: Number of co-propagating channels in the fiber
V_g	: Group velocity
D	: Dispersion coefficient
N_{ch}	: Number of channels
A_{eff}	: Effective area of fiber
ω	: Angular frequency
n_s	: Effective indices of the slow mode
n_f	: Effective indices of the fast mode
L	: Length of the fiber
$\Delta\tau$: Difference in the propagation times
L_b	: Beat length of the fiber
β_s	: Propagation constant for slow mode
β_f	: Propagation constant for fast mode
η	: FWM efficiency
L_c	: Coupling length
d_k	: Data bits

$q(t)$: Transmitted pulse
\mathbf{T}	: Bit period
\mathbf{kT}	: Sampling instance
\oplus	: Modulo 2 subtraction
\mathbf{E}	: Electrical field
L_{eff}	: Effective length of the fiber
$\psi(\omega)$: Phase retardation factor
η_{xpm}	: XPM efficiency
Y_1	: Nonlinear coupling coefficient of the optical signal
α	: Attenuation coefficient of the fiber
\mathbf{d}	: Walk-off parameter
\mathbf{D}	: Dispersion coefficient of the fiber
R_d	: Bias or load resistance
P_s	: Receiver power
P_T	: Received optical power at the photo-detector
B_e	: Bandwidth of the photo-detector
$i_n(t)$: Sum of the various noises considered in the system
σ_{shot}^2	: Variance of the shot noise

CHAPTER 1

INTRODUCTION

1.1 Communication System

A communication system transmits information or message like voice, video, text, etc. from one place to another. Communication systems exchange signals between two or more entities in a form suitable to process and manipulate most economically. The basic principle of a communication system remains the same for different types of systems. The basic principle of a communication system is to bridge two entities at different locations. A communication system consists of many components which take part in the system activity and perform its part in a definite sequence. The function of each component of a communication system is to assist transmit the information from the source to the destination over the transmission medium with least possible distortion and attenuation. However, in any communication system with the best possible design parameters, the received signal will fall short of the true duplication of the transmitted signal.

A typical communication system consists of three basic components; transmitter, transmission medium and receiver. A transmitter receives the information from the source and transforms it into suitable form conforming to the transmission medium. The transformed information is called signal. The design parameters of the transmitter mainly takes into consideration of the facts like power, distance, type of data, bandwidth, type of the transmission medium, operating frequency, etc.

The transmission medium bridges the distance between the source and the receiver. It is the component of a communication system that determines many important aspects of the transmitter, the receiver and signal flow. As signal propagates through the medium it gets attenuated due to interaction between the signal and the medium. The signal also gets distorted due to nonlinear characteristics of the medium and other interferences. The transmission medium may be of various types. It includes physical and non-physical media. Physical

media includes copper wire, coaxial cable, optical fiber, etc. The non-physical media includes links at various frequencies like high frequency, very high frequency, microwave, etc.

The receiver transforms the signal into information that travels up to it through the transmission medium. The receiver performs all necessary steps to ensure that the received information is a faithful copy of the original information and provides required energy level to be passed to the destination.

Electrical communication systems became the first dominant modern communication method since the advent of telegraphy in the 1830s. Until the early 1980s, most of the fixed (non-radio) signal transmission was carried by metallic cable (twisted wire pairs and coaxial cable) systems. However, large attenuation and limited bandwidth of coaxial cable limited its capacity upgrade. The bit rate of the most advanced coaxial system which was put into service in 1975 was 274 Mb/s [1]. At around the same time, there was a need of conversion from analogue to digital transmission to improve transmission quality, which requires further increase of transmission bandwidth. Many efforts were made to overcome the drawbacks of coaxial cable during the 1960s and 1970s. After the invention of wireless communication system, signals could be transmitted through the atmosphere using the suitable frequencies as carrier. But the available frequency bandwidth could not meet the growing demands of communication bandwidth.

1.2 Evolution of Optical Communication

Even though an optical communication system had been conceived in the late 18th century by a French Engineer Claude Chappe who constructed an optical telegraph, electrical communication systems remained the dominant means of communication. In 1966, Kao and Hockham proposed the use of optical fiber as a guiding medium for the optical signal [2]. Four years later, a major breakthrough occurred when the fiber loss was reduced to about 20 dB/km from previous values of more than 1000 dB/km by applying improved fiber manufacture design techniques. Since that time, optical communication technology has developed rapidly to achieve larger transmission capacity and longer transmission distance. The capacity of transmission has been increased about 100 fold in every 10 years.

There were several major technological breakthroughs during the past two decades to achieve such a rapid development. In 1980, the bit rate used was 45 Bb/s with repeater spacing of 10 km. The multimode fiber was used as the transmission medium and GaAs LED as the source of the system. In 1987 the bit rate was increased to 1.7 Gb/s with repeater spacing of 50 km. By 1990 the bit rate was increased to 2.5 Gb/s with repeater spacing further increased to 60-70 km. Dispersion shifted fibers are used to minimize the bit error rate and to increase the repeater spacing and the bit rate.

In 1996 the bit rate of the optical transmission system was increased to 5 Gb/s. The development of optical amplifiers brought another important break through in optical communication system. Optical amplifiers reduced the associated delay and power requirement of the electronic amplifiers. Wavelength division multiplexing (WDM) was also introduced at this time to increase the available bandwidth capacity in terms of the channels. By 2002, the bit rate of the optical system was increased to 10 Gb/s with repeater spacing of 70-80 km. The introduction of the dense DWM (DWDM) system increased the channel capacity and the bit rate got increased to 40 GB/s.

The first generation of optical communication was designed with multi-mode fibers and direct band gap GaAs light emitting diodes (LEDs) which used to operate at the 0.8 μm - 0.9 μm wavelength range. Compared to the typical repeater spacing of coaxial system ($\sim 1\text{km}$), the longer repeater spacing ($\sim 10\text{km}$) was a major motivation. Large modal dispersion of multi-mode fibers and high fiber loss at 0.8 μm ($> 5\text{dB/km}$) limited both the transmission distance and bit rate. In the second generation, multi-mode fibers were replaced by single-mode fibers, and the center wavelength of light sources was shifted to 1.3 μm , where optical fibers have minimum dispersion and lower loss of about 0.5 dB/km.

However, there was still a strong demand to increase repeater spacing further, which could be achieved by operating at 1.55 μm where optical fibers have an intrinsic minimum loss around 0.2dB/km. Larger dispersion in the 1.55 μm window delayed moving to a new generation until dispersion shifted fiber became available. Dispersion shifted fibers reduced the large amount of dispersion in the 1.55 μm window by modifying the index profile of the fibers while keeping the benefit of low loss at the 1.55 μm window. However, growing communication traffic and demand for larger bandwidth per user revealed a significant drawback of electronic regenerator systems. Because all the regenerators are designed to operate at a

specific data rate and modulation format, all of them needed to be replaced to convert to a higher data rate.

The difficulty of upgradeability has finally been removed by optical amplifiers, which led to a completely new generation of optical communication. An important advance was that an erbium-doped single mode fiber amplifier (EDFA) at $1.55 \mu\text{m}$ was found to be ideally suited as an amplifying medium for modern fiber optic communication systems. Invention of the EDFA had a profound impact especially on the design of long-haul under-sea systems. Trans-oceanic systems installed like TAT (Transatlantic Telephone)-12/13 [3] and TPC (Transpacific Crossings)-5 were designed with EDFAs, and the transmission distance reaches over 8000 km without electronic repeaters between terminals. The broad gain spectrum ($3\sim 4\text{THz}$) of an EDFA also makes it practical to implement wavelength-division-multiplexing (WDM) systems.

It is highly likely that DWDM systems will bring another big leap of transmission capacity of optical communication systems. Some research groups have already demonstrated that it is possible to transmit almost a Tbits/s bit rate over thousands of kilometers. There are some important experimental results of DWDM systems. In 1999, a channel system was simulated experimentally with bit rate of 20 Gb/s. The system could cover 10,000 km with amplifier spacing of 50 km. The signal format used here was of soliton type. Later the number of channels was increased to 20 with NRZ type signal format. In 1997 the number of the channels was increased 32 with 45 km amplifier spacing and the distance covered was 9,300 km. In this system NRZ and soliton type signal format were used. In 1998, the number of the channels was increased to 64 at the cost of reduced transmission distance of 500 km with 100 km amplifier spacing. However by 1999 the distance could be extended to 7,200 km with 64 channel system and 10 Gb/s bit rate at the cost of reduced amplifier spacing of 50 km. In 2004, the bit rate was increased to 40 Gb/s at the cost of reduced number of channels of 34 which could cover a distance of 6,380 km.

For example, N. Bergano et al. successfully demonstrated transmission of 640 Gb/s over 7200km using a re-circulating loop while G. Vareille et al. demonstrated the transmission capacity of 340 Gb/s over 6380 km on a straight-line test bed. These results indeed show that remarkable achievements have been made in recent years, and let us forecast that optical communication systems in the next generation will have a transmission capacity of a few

hundreds of Gb/s.

1.3 Review of Previous and Present State of Works

In 1994 Chraplyvy described optical nonlinearities namely the stimulated Raman, stimulated Brillouin, four wave mixing (FWM) and carrier induced phase noise in the context of lightwave system limitations. In 1994 together with Marcuse and Tkach concluded that XPM did not limit the number of wavelength channels that a single optical fiber can support [4].

Chiang, Kagi, Fong, Marhic and Kazovsky (1994) and Chiang, Kagi, Marhic and Kazovsky (1996) have inspired many others for this research [5-6]. They presented a detailed investigation theoretically and experimentally of the impact of modulation frequency to XPM in dispersive fibers. In the case of fibers with multiple optical amplifiers, the XPM induced phase shift is smaller in system employing lumped dispersion compensation than in systems employing distributed dispersion compensation. They also concluded that in non-dispersive fibers XPM is frequency independent, while in dispersive fibers XPM frequency response is approximately inversely proportional to the product of frequency, fiber dispersion and wavelength separation.

With the application of Erbium-doped fiber amplifiers (EDFA), the fiber loss can be compensated periodically [7]. Hence, fiber loss is no longer a limiting factor in long-haul optical communication system. Fiber nonlinearities if not properly addressed, may adversely affect system performance. This reality stirs up research interests in this field, which leads to understanding nonlinear phenomenon, making attempts of quantifying and reducing their affects in DWDM optical communication. Marhic, Yang, Akasaka and Kazovsky (1999) proposed replacing EDFA by Distributed Raman Amplification (DRA) along the transmission fiber. They suggested using a Raman pump Modula at the transmitting end and reducing the transmitted power so that the received power remains the same. Hence lower transmitter powers would be possible and this would help reduce fiber nonlinear effects during transmission.

Cartaxo (1998 and 1999) accepted the pump-probe format investigating the impact of modulation frequency on XPM but extended it to IM/DD WDM systems [8-9]. At very low modulation frequency, the walk off effect does not affect the XPM-induced IM efficiency

but at higher frequency it significantly reduced it. Kim, Han and Chung (2001) reported the effect of SRS on hybrid WDM systems. Experimental results were compared with theoretical values and it was shown that the SRS induced crosstalk increased with wavelength separation. The results were used to estimate the scalability of hybrid WDM systems. The carrier to crosstalk ratio (CCR) was also presented for CATV systems taking SRS, XPM and Optical Kerr effect into account.

Djordjevic (2001) [10] derived simple expressions for maximum transmission length for dispersion compensated links using inline optical amplifiers, The non linearity's taken into consideration in the presence of ASE noise were FWM and SRS. Djordjevic investigated different dispersion compensation configurations and determined that the ZDSF and CF combination gives the maximum transmission distance while the CF and DCF could provide much denser packaging. He also showed that as the number of channels increase, the transmitting distance and the total bandwidth for optimum channels spacing decreases. He showed that the total transmitter distance is dependant on the bit rate.

Norimatsu and Yamamoto (2001) [11] studied the influence of SRS on wideband transmission systems taking into account the random modulation and the walk-off. It was shown that the power depletion due to SRS could be separated into the average power loss and the waveform distortion. Simple equations that described the GVD were derived and the waveform distortion due to SRS can be evaluated in short calculation for different system parameters such as channel allocation, bit rate, fiber input power, effective core area of fiber and so on. The evaluations were done on various types of fibers such as DSF, SMF, Large Effective Core Area Fiber (LECAF) and NZDSF and it was shown that the waveform distortion of the rectangular NRZ pulses in SMF were smaller than that in LECAF.

In 1998, Belloti, Varani, Francia and Bononi, made a new linear model for the XPM induced intensity distortion on a CW probe in a dispersion compensated transmission system [12]. The model succeeds in capturing the interaction between XPM and group velocity dispersion (GVD) hence giving an accurate prediction within the applicability model range. In this model, XPM induced intensity modulation can be treated as additive intensity noise giving allowance for SPM effects extensions. This model is of great value in the search for optimized dispersion maps. Bigo, Belloti and Chbat (1999) studied the impact of XPM on the transmission performance of a 2×10 Gb/s multiplex. They have characterized the impact

over four types of fiber infrastructures namely NZDSF-, DSF, NZDSF+ and SMF+DCF. The outcome of their study concluded that dispersion-compensated single mode fiber is virtually not affected by XPM down to 50 GHz-channel spacing.

Kowalewski, Marciniak and Sedlin in 2000 [13] reported an investigation of optical crosstalk caused by nonlinear interactions in short and long haul WDM transmission systems called inter-domain interfaces (IrDI). IrDI is a 16-Channel WDM interface that is to be used to connect two sub-networks belonging to different administrative domains. By using the parameters proposed by ITU, simulations on various nonlinear effects (FWM, SPM, XPM, stimulated Raman, stimulated Brillouin and nonlinear interactions in EDFA) showed that XPM and FWM greatly influenced the efficiency of IrDI transmission systems. However, dispersion management can be used to combat these effects effectively. For NRZ signal formats, estimates of the penalty can be obtained from calculations of the distortion of a CW probe channel, permitting the effect of XPM to be isolated from other impairments. The pump-probe technique allows rapid optimization of the link design to minimize XPM penalties.

In single mode fiber links, the pulse broadening effect of self phase modulation (SPM) severely affects the transmission distance. Lakoba and Agrawal (2000) [14] investigated the performance of dispersion maps for long haul soliton data. An effort was made to find the maximum allowed range of values for the average dispersion. They showed that positive residual dispersion can be used to counter the effects of pulse broadening. The use of positive residual dispersion effectively minimized XPM induced distortion and also reduces pulse broadening due to SPM.

Ten, Ennser, Grochosinski, Burtsev and Silva [15] compared the FWM and XPM impairments in a dense WDM system and examined the impact of different fiber dispersion slopes and effective areas. XPM and FWM were considered as noise like impairments. From the analysis done, they showed that XPM dominates FWM across the entire channel plan for all types of fibers. Increasing the fiber effective area decreases the FWM and XPM variance uniformly for all channels and reducing the dispersion slope allows for better XPM compensation resulting in smaller Q variations with wavelength.

Betti, Giaconi and Nardini (2003) [16], presented a statistical analysis that takes into account both the effect on the FWM inter-modulation products due to dispersive propagation, and

the statistics of such inter-modulation terms, which are considered as random processes. The autocorrelation function of the FWM process was calculated for the independent wavelength division multiplexing optical channel. The fiber propagation of WDM signals affected by FWM was analyzed and it was shown that the penalty values due to the FWM effect result lower than the ones obtained by analytical models considering unmodulated optical signals.

Thiele, Killey and Bayvel (1999) [17] investigated the effects of pre and post compensation in high capacity WDM systems with large inter amplifier spacing. They measured spectral broadening by using a gated, scanning interferometer. It was shown that in the case of post compensation, the eye closure was more rapid in the post compensated case, where the SPM chirp acquired led to additional pulse broadening. With 4 channel transmission little change was seen in the SPM penalty was observed. This was attributed to the XPM.

Hoon (2003) [18] investigated, theoretically and experimentally the SPM and XPM induced phase noise in a DPSK system and determined how much of this noise contributes to performance degradation. In order to accomplish this he calculated the rms intensity ratio of XPM induced noise to SPM induced noise for a two channel WDM system. The BER was then measured while varying the OSNR of the signals at the receiver. It was shown that the XPM induced phase noise becomes as large as SPM induced phase noise in a NZ-DSF link for channel spacing less than 100 GHz. BER degradation was also observed for a two channel systems as compared to a single channel system.

Sang, Hyun, Wanseok and Seung (2001) [19] suggested a SBS suppression method for WDM links based on XPM effect induced by an optical supervisory channel. It was found that the phases of the signal channels could be modulated through the XPM induced by the SV channel. The induced XPM broadened induced timing jitter and to crosstalk between channels at the receiver due to spectral broadening. For the case of precompensation in a 4 channel system, large broadening was observed due to high peak power of the compressed pulses at the start of each span increasing the effects of SPM and XPM. The limitation imposed by SPM in post compensated systems can be overcome by precompensated systems.

Keang (2002) [20] calculated the channel capacity of DWDM systems and demonstrated how constant intensity modulation formats such as phase or frequency modulation can be used to eliminate the phase shift caused by SPM and XPM. By using constant intensity modulation SPM and XPM cause only constant phase shifts thus eliminating both phase

and intensity distortion. This in turn leads to a monotonic increase in channel capacity for increased powers. They observed that constant intensity techniques provide a higher efficiency than that of in the regime in which XPM dominates over FWM. This was attributed to the fact that FWM decreases more rapidly than XPM as channel spacing increases.

Spectrum line widths of the signal by four times and effectively reduced the SBS induced error floors and power penalties in transmission. The demonstrated experimentally that this method could increase the SBS threshold and reduce the error floors irrespective of the bit rate, channel power, channel wavelength and channel spacing of the WDM channels.

Wang, Bodther and Jacobsen performed an analysis on crosstalk due to XPM in SCM-WDM video transmission systems in 1995 [21]. An analytical expression for XPM in a 2 channel system was derived. The effect of XPM for different channel spacing parameters was investigated and it was shown that the crosstalk level is smaller for larger channel spacing and larger for a higher sub-carrier frequency. The analysis was extended to a total of 16 optical channels it was found that the number of achievable optical channels is severely limited by XPM.

The same model mentioned above was improved upon by Bellotti et al. in 1998 [22]. The first approach was based on the assumption of undistorted interfering channels. The new model assumes that the intensity noise in systems at 40 Gb/s. The model was used to evaluate XPM related transmission impairments in WDM transmission systems for different dispersion compensation schemes.

Hui, Demarest and Allen (1999) [23] reported the results of an experimental and theoretical study on the frequency response of XPM induced crosstalk in multi-span WDM optical systems, both with single fiber configurations. Interference between XPM induced crosstalk effects created in different amplified optical spans was found to have a strong impact on the overall spectral feature of XPM induced crosstalk. A simple analytical expression was obtained to describe the XPM induced crosstalk and it was found that crosstalk levels are strongly dependant on fiber dispersion and optical channel spacing. The crosstalk level between high and low bit rate channels was found to be similar to that between two low bit rate channels. The effect of dispersion compensation on XPM crosstalk was also discussed. In uncompensated optical systems, a decrease in fiber dispersion will increase XPM induced phase modulation efficiency while an increase in fiber dispersion will increase phase to in-

tensity noise conversion efficiency. Compared to lumped dispersion compensation, per span dispersion compensation was found to be the most effective way to minimize the impact of XPM and SPM crosstalk.

Cartaxo (1999) [9] also investigated the effect of XPM in IM/DD optical fiber links with multiple fiber segments with different fiber characteristics and optical amplifiers theoretically and numerically. A generalized model was simulated and its validity range was present. It was shown that XPM induced IM is approximately proportional to the square frequency when the walk off effect is weak. However, when the walk off is strong the XPM induced IM is approximately linearly proportional to the frequency and inversely proportional to the wavelength separation. Cartaxo proved theoretically and numerically that the effect of XPM could be reduced by properly arranging the dispersion characteristics in each fiber in a multiple fiber segments. In non-dispersion compensated amplifier link and for weak walk off effect, the total XPM induced IM increases approximately with the square of the number of fiber segments and of modulation frequency. It was also shown that in a multi segment fiber link the best way to compensate for dispersion was to place one dispersion compensator in each fiber segment.

Thiele, Killey and Bayvel (2000) [24] investigated the variation of XPM induced distortion with transmission for dispersion managed fiber links. The experimental set up used a recirculating loop and the build up of XPM induced distortion was measured as a function of the number of recirculations. Dispersion compensating fibers (DCF) were used to perfectly compensate 40km of standard single mode fiber. It was shown that the XPM induced distortion increases almost linearly with distance after compensation.

In 2002, R. Hui, Y. Wang, K. Demarest and C. Allen [25] analyzed the performance of a fiber optic SCM transmission system a 10-Gb/s SCM fiber optic system in which 4x2.5-Gb/s data streams were combined in one wavelength . OSSB modulation was used as it was deemed an effective method to reduce the impact of fiber chromatic dispersion and increase the bandwidth efficiency. Receiver sensitivity was also evaluated and it was concluded that if a narrowband optical filter was used in front of the receiver, the signals' ASE beat noise will be reduced and an improvement in receiver sensitivity was seen. A comparison between ASK and PSK modulation formats was also made. Optical carrier suppression was suggested as a method to increase modulation efficiency. The effect of nonlinear crosstalk in fiber due to

XPM and FWM were also analyzed. Analytical expressions were presented and it was found that XPM induced crosstalk decreases monotonically with increase in number of channels and decrease of channel data rate.

In a dispersive fiber, the input pulse get broaden causing inter-symbol interference (ISI) at the receiver. This effect is due to the nonlinear shape of the fiber phase response around the optical carrier frequency. A signal with narrow bandwidth should suffer less from chromatic dispersion. A way to reduce the signal bandwidth is to apply line coding [26]. NRZ line code is a preferred format for optical transmission. Duobinary code has been successfully implemented to reduce the spectral bandwidth. But duobinary code alone is not enough to combat the interference phenomenon occurring in practice between optical marks and spaces. For highly dispersive fibers, band limiting is a necessary requirement to have a benefit from duobinary coding. Recently, other line coding schemes, called phased amplitude-shift signaling (PASS) codes based on a modification of the duobinary one, have been proposed by Stark. According to the duobinary code, marks separated by an odd number of spaces are oppositely phased. The alternate-block-inversion (ABI) PASS code establishes that marks separated by any nonzero number of spaces be oppositely phased. In monospaced-mark-inversion (MMI) PASS code, only marks separated by a single space are oppositely phased. These codes have substantially different power spectra and the power spectrum alone is not a clear indicator of transmission performance. Novel Optical Line Codes tolerant to fiber chromatic dispersion is also introduced in giving hints to try out the applicability of line codes to reduce the nonlinear effects like SPM and XPM.

All these works discussed various nonlinear phenomena with the aim to quantify and reduce their effects in optical communication system. The FWM effect could be reduced effectively by dispersion management. But the Kerr effects remained as a problem for DWDM systems with high bit rates. The dispersion management could be found effective in reducing the effects caused by nonlinear phenomena like FWM, SPM and XPM. But there is no work reported that quantifies and reduces the effect of the XPM alone. This paper will address the XPM effect with the aim to quantify and reduce its effect by applying line coding schemes.

The continuous growth of internet traffic is driving transmission system engineers to use higher and higher data rates in all segments of communication network. It is widely recognized that 40 GB/s data transmission rates impose very strict requirements on the fiber plants

and transmission systems deployed in the field. However, data rates of 10 GB/s also impose similar significant performance requirements. In particular polarization mode dispersion (PMD) can be a serious limitation on certain fiber links operating at 10 GB/s, particularly on links in older legacy networks. Recent papers written on the topic argue that even fibers made and deployed in the 1990 to 2001 time frame may be unstable for 10 GB/s and higher data rate transmission, due to the challenge presented by the PMD. As network data rates continue to rise, it is becoming increasingly important to understand PMD and its potential impact in the network.

With the ever increasing bit rates in fiber transmission PMD remains a significant transmission obstacle. Even though a large amount of PMD mitigation methods have been suggested and evaluated, they usually need to be implemented on a channel-by-channel basis in wavelength-division-multiplexing (WDM) systems, and in fact, there exist fundamental reasons for why such per channel compensation must be adopted. The central issue is that, if a broadband compensation is attempted, the compensation at one wavelength might lead to worse performance at another channel. In fact, when adding birefringence to a system, the average PMD at wavelengths not specifically compensated will increase. In WDM systems, the fiber nonlinearities that dominate are the crosstalk from four-wave mixing (FWM) and cross-phase modulation (XPM). After the move from dispersion shifted fiber in the mid-1990s to either standard fiber plus dispersion management or nonzero dispersion shifted fiber, the FWM is often negligible, and the XPM is the dominating nonlinear impairment. Most work has been devoted to two-channel (pump-probe) interaction in this respect, and significantly fewer studies discuss the more practically important case with many equal-power WDM channels.

The subject of PMD presents many challenge, including understanding the inconsistent terminologies and the statistical nature of PMD and also comprehending the background to the advanced measurement techniques employed to calculate PMD. The purpose of this paper is to provide an introduction to the topic of PMD. So this paper will also explain the origin and nature of PMD, clarify the terminology and statistical nature of PMD, and examine the impact of PMD on high speed transmission system.

1.4 Research Aims

The main objective of this research is to develop an approach to minimize the adverse effects limited by the PMD and XPM of a DWDM optical transmission system. In particular, the objectives are to carryout analysis for phase and amplitude distortions in a DWDM system with different line-coding schemes like Miller code, duobinary code, Novel optical line codes, etc. and to evaluate the eye closer penalty due to XPM and PMD for the above systems by using computer simulation and further, to determine the effectiveness of the line coding schemes in minimizing the effect of XPM and PMD in a DWDM system. It is expected that this research will be useful in designing DWDM optical transmission systems with reduced XPM and PMD effects.

CHAPTER 2

OPTICAL COMMUNICATION, FIBER NONLINEARITIES AND POLARIZATION MODE DISPERSION

2.1 Principles of Optical Communication

A typical point-to-point optical communication system consists of three major components: optical transmitter, optical fiber cable as the transmission medium and optical receiver as in Figure 2.1.

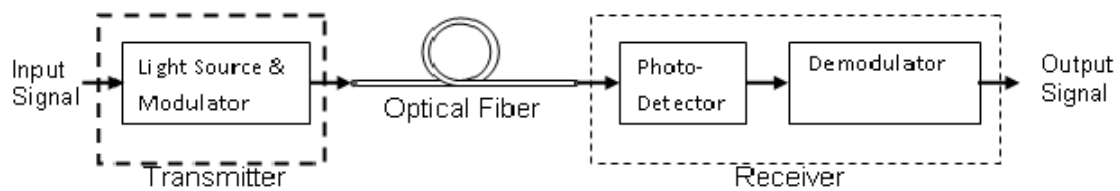


Figure 2.1: Optical fiber communication system

2.1.1 Optical Transmitter

The function of an optical transmitter is to transform the electrical signal into optical form. The electrical signal is then launched into the optical fiber. Figure 2.2 shows the block diagram of an optical transmitter. It consists of an optical source, a modulator and a channel coupler. Semiconductor lasers or light emitting diodes are used as optical source. The main consideration in selecting a source is its ability in launching maximum power into the optical fiber in the suitable wavelength. The optical signal is generated after modulating the light wave by the input signal. The coupler is generally a micro-lens that focuses the optical signal onto the entrance plane of an optical fiber with the maximum possible efficiency. The

amount of launched power is an important factor in designing the optical communication system.

2.1.2 Optical Fiber

The optical fiber bridges the distance between the optical transmitter and the optical receiver. The main consideration in designing the fiber is to ensure the propagation of the transmitted signal up to the receiver with acceptable level of attenuation and distortion so that the same information can be received at the receiver with minimum error. With the development in the field of optical fiber communication, the attenuation of the signal could be reduced to 0.2 dB/km. Factors that contributed to this reduction in the loss parameter are improved fiber design technique, low loss fiber window, dispersion compensation, etc [27]. Fiber loss, dispersion and nonlinear effects are main design considerations of optical fiber. Introduction of optical amplifiers and dispersion shifted fibers could successfully address the limitations imposed by fiber loss and dispersion. But many aspects of nonlinear characteristics of the fiber yet remained as the limitation of optical fibers.

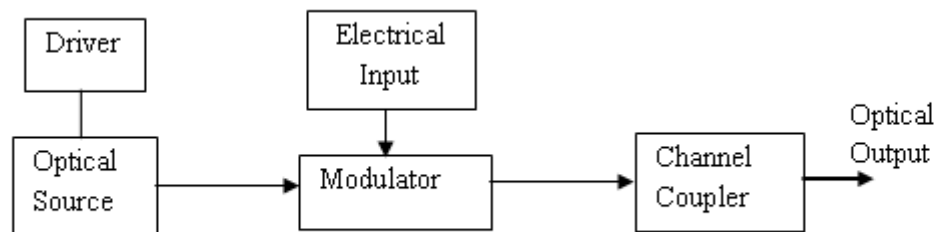


Figure 2.2: Block Diagram of an Optical Transmitter

2.1.3 Optical Receiver

The optical receiver converts the received optical signal from the fiber into the original electrical signal. Figure 2.3 shows the block diagram of an optical receiver. It consists of a coupler, a photo-detector and a demodulator. The coupler focuses the received optical signal onto the photo detector. Semiconductor photo diodes are used as photo-detectors because

of their compatibility with the whole system. The design of the modulator depends on the modulation format used in the system. Receiver sensitivity is one of the important design parameter. It is often designed to keep the system within a bit error rate of 10^{-9} .

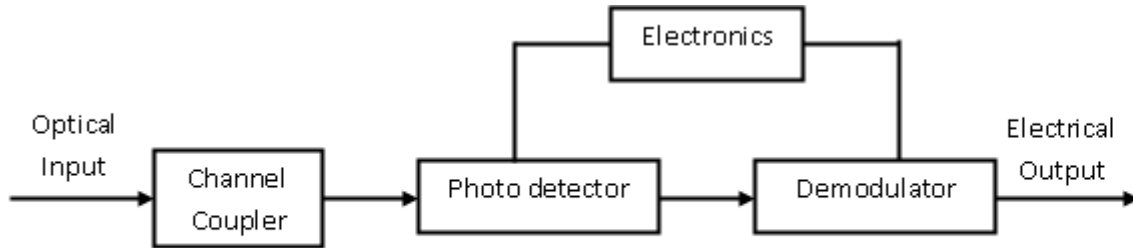


Figure 2.3: Block Diagram of an Optical Receiver

2.2 Wavelength Division Multiplexing (WDM) and Dense WDM (DWDM)

The development of WDM fiber links marks the advent of the 4th generation of light wave systems. It offers the technology to increase the bit rate and having in-line amplifiers in order to increase the transmission distance. WDM is essentially the same as frequency division multiplexing which has been used in radio systems. In DWDM, the wavelengths are selected with small channel separation like channel spacing of 100 GHz.

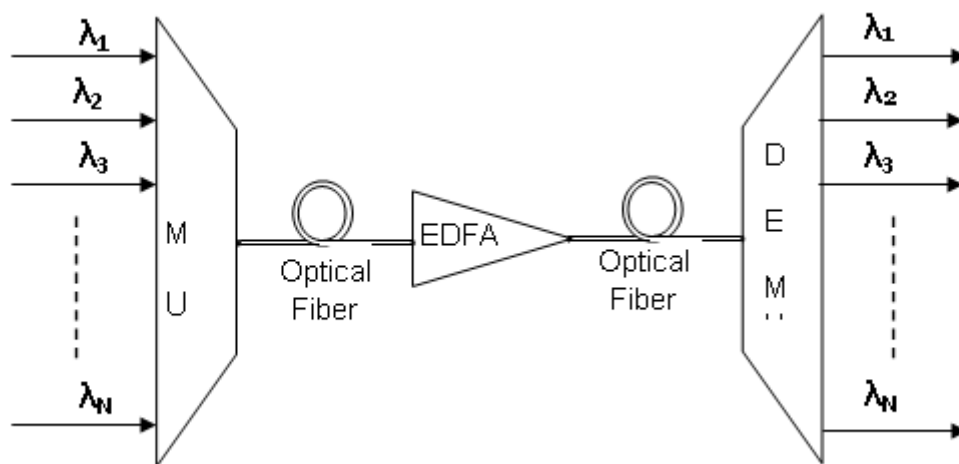


Figure 2.4: Graphical Representation of a Point to Point WDM Optical System

WDM makes use of the optical fiber's available intrinsic bandwidth by multiplexing many wavelengths of coherent light along a single mode fiber channel. Each wavelength of light can transmit encoded information at the optimum data rate. Therefore, multiplexing the distinct wavelengths of lights leads to a significant increase in the total throughput of information for the system. The key elements of a WDM optical system are: tunable semiconductor lasers, multiplexing components, electro-optical modulators, single mode optical fibers, Erbium doped fiber amplifiers (EDFA), semiconductor optical amplifier wavelength translators, demultiplexers and high speed photo detectors. Figure 2.4 shows a point to point WDM optical system.

2.3 Fundamentals of Nonlinear Effects in Optical Fibers

The nonlinearities in optical fibers fall into two categories. One is stimulated scattering (Raman and Brillouin), and the other is the optical Kerr effect due to changes in the refractive index with optical power. While stimulated scatterings are responsible for intensity dependent gain or loss, the nonlinear refractive index is responsible for intensity dependent phase shift of the optical signal. One major difference between scattering effects and the Kerr effect is that stimulated scatterings have threshold power levels at which the nonlinear effects manifest themselves while the Kerr effect does not have such a threshold.

2.3.1 Stimulated Brillouin Scattering (SBS)

Stimulated Brillouin scattering (SBS) may be defined as the light modulation through thermal molecular vibrations within the fiber. It generates acoustic phonon during the process. In SBS, a strong optical wave traveling in one direction (forward) provides narrow band gain for light propagating in the opposite direction (backward). Some of the forward-propagating signal is redirected to backward, resulting in power loss at the receiver. If the SBS threshold is defined as the input power at which the scattered power increases as large as the input power in the undepleted pump approximation, the SBS threshold power is proportional to

$$P_B^{th} \approx \frac{1}{g_B} \left(1 + \frac{\Delta V_S}{\Delta V_B} \right) \dots\dots\dots(2.1)$$

where g_B is the Brillouin gain coefficient, $\Delta\nu_S$ is the line-width of the source and $\Delta\nu_B$ is the Brillouin line-width. Equation (2.1) indicates that the threshold power will be increased as the line-width of the source increases. For optical fibers at 1550 nm, the Brillouin line-width is about 20 MHz, so optical signals modulated at higher bit rates will experience lesser effects of SBS. From a system point of view, the relatively narrow gain spectrum of SBS prevents interactions among channels in a WDM system, which makes SBS independent of channel number. Only each individual channel signal needs to be below the threshold power. Another characteristic of SBS which makes it less troublesome compared to other nonlinear effects is that the threshold of SBS does not decrease in a long amplified system because practical optical amplifiers have one or more optical isolators. The optical isolators prevent accumulations of the backscattered light from SBS. Therefore, although SBS could be a detrimental nonlinear effect in an optical communication system, system limitations are usually set by other nonlinear effects [28].

2.3.2 Stimulated Raman Scattering (SRS)

SRS is due to the interaction of photons with a fiber's molecular vibrations. High frequency optical phonons are generated in the process. Unlike SBS, SRS scatters light waves in both directions, forward and backward. However, the backward-propagating light can be eliminated by using optical isolators. Therefore, the forward scattered light is of more concern. The Raman gain coefficient is about three orders of magnitude smaller than the Brillouin gain coefficient and the SRS threshold is known to be around 1W for a single-channel system. In a single-channel system, the large threshold power makes SRS a negligible effect. Also, the gain bandwidth of SRS is of the order of 12 THz, which is about 6 orders of magnitude greater than that of SBS. The large gain bandwidth of SRS enables it to couple different channels in a WDM system. On the other hand, it can cause performance degradation through crosstalk. Chraplyvy and Tkach estimated the worst case of signal-to-noise ratio (SNR) degradation in an amplified system due to SRS. According to the estimate, the requirement to ensure an SNR degradation of less than 0.5 dB in the worst channel is that the product of total power, total bandwidth and the total effective length of the system should be less than 10 THz-mW-Mm. Although it was assumed in their estimate that all the channels are transmitting mark states simultaneously, the probability of which is very low in a

multi-channel system, it indicates that SRS may impose a fundamental limit on the capacity of future optical communication systems.

2.3.3 Optical Kerr Effect

The refractive index of silica fiber for communication is weakly dependent on optical intensity, and is given by [27],

$$n = n_o + n_2 I(t) \dots\dots\dots(2.2)$$

Where linear refractive index $n_o \approx 1.5$, nonlinear-index coefficient $n_2 \approx 2.6 \times 10^{-20} \text{ m}^2/\text{W}$, and $I(t)$ is the optical intensity. Although the refractive index is a very weak function of signal power, the higher power from optical amplifiers and long transmission distances make it no longer negligible in modern optical communication systems. In fact, phase modulation due to intensity dependent refractive index induces various nonlinear effects, namely, self-phase modulation (SPM), cross-phase modulation (XPM) and four-wave mixing (FWM).

Self-Phase Modulation (SPM)

The dependence of the refractive index on optical intensity causes a nonlinear phase shift while propagating through an optical fiber. The nonlinear phase shift is given by

$$\phi_{NL} = \frac{2\pi}{\lambda} n_2 I(t) z \dots\dots\dots(2.3)$$

Where λ is the wavelength of the optical wave and z is the propagation distance. Since the nonlinear phase shift is dependent on its own pulse shape, it is called self-phase modulation (SPM). When the optical signal is time varying, such as an intensity modulated signal, the time-varying nonlinear phase shift results in a broadened spectrum of the optical signal. If the spectrum broadening is significant, it may cause cross talk between neighboring channels in a dense wavelength division multiplexing (DWDM) system. Even in a single channel system, the broadened spectrum could cause a significant temporal broadening of optical pulses in the presence of chromatic dispersion. However, under some circumstances SPM and chromatic dispersion can be beneficial. One extreme example is the soliton [29], which

is known to be stable and dispersion-free. Even with non-return-to-zero (NRZ) pulses, it is known that pulse compression could be achieved partially in the anomalous dispersion region where the linear chirp induced by chromatic dispersion and the nonlinear one due to SPM have opposite signs. The anomalous dispersion region has a negative sign of β_2 , the second order propagation constant. When a transmission system is designed to achieve the optimum compensation of the linear chirp and the nonlinear chirp, it is often called a nonlinear assisted transmission system.

Cross-Phase Modulation (XPM)

Another nonlinear phase shift originating from the Kerr effect is cross-phase modulation (XPM). While SPM is the effect of a pulse on its own phase, XPM is a nonlinear phase effect due to optical pulses in neighboring channels. Therefore, XPM occurs only in multi-channel systems. In a multi-channel system, the nonlinear phase shift of the signal at the center wavelength λ_i is described by [27],

$$\phi_{NL} = \frac{2\pi}{\lambda_i} n_2 z \left[I_i(t) + 2 \sum_{i \neq j}^M I_j(t) \right] \dots\dots\dots(2.4)$$

Where M is the number of co-propagating channels in the fiber. The first term is responsible for SPM, and the second term is for XPM. Equation (2.4) might lead to a speculation that the effect of XPM could be at least twice as significant as that of SPM. A pump-probe approach helps isolate the effect of XPM [24] . Referring to Figure 2.5, the pump channel generates a time varying intensity signal, λ_1 while the probe generates a constant intensity continuous wave (CW) wave signal, λ_2 . Then they are transmitted through two channels of a fiber. At the receiver, both signals are demultiplexed and compared to the original condition at the transmitter. Both pump channel and probe channel signals experience amplitude variation. The amplitude variation in the pump channel is due to the SPM. On the other hand, the amplitude variations in the probe channel are caused by the XPM from the pump channel. This is because the signal in the probe has a constant intensity, which eliminates the effects of SPM.

However, XPM is effective only when pulses in the other channels are synchronized with the signal of interest. When pulses in each channel travel at different group velocities due to dispersion, the pulses slide past each other while propagating [8-9]. Figure 2.6 illustrates how

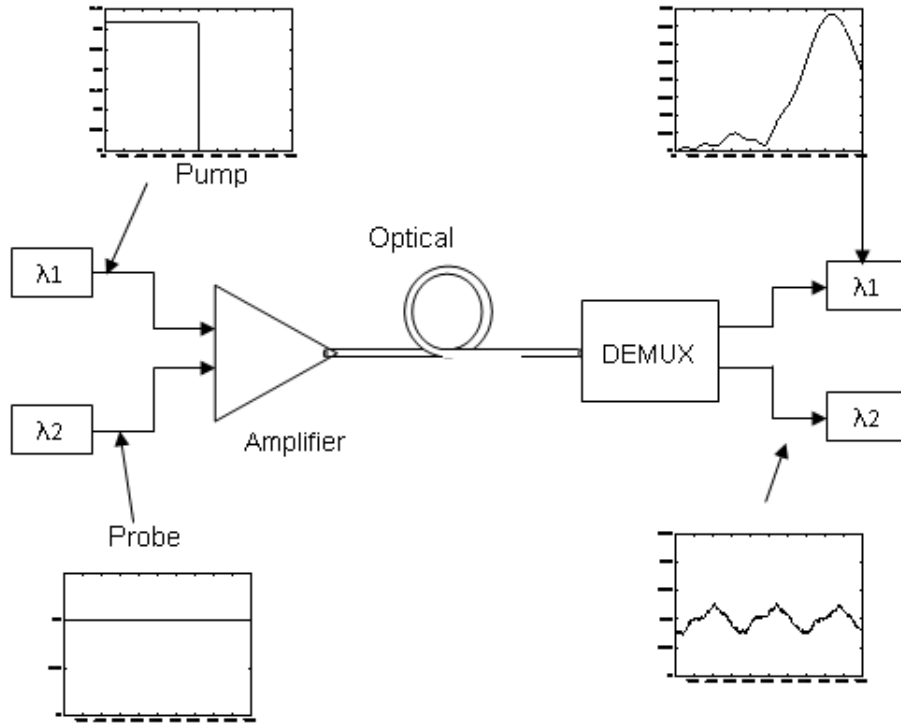


Figure 2.5: Experimental Setup to Demonstrate the Effects of XPM

two isolated pulses in different channels collide with each other. When the faster traveling pulse has completely walked through the slower traveling pulse, the XPM effect becomes negligible. The relative transmission distance for two pulses in different channels to collide with each other is called the walk-off distance, L_W [27].

$$L_W = \frac{T_o}{|v_g^1(\lambda_1) - v_g^1(\lambda_2)|} \approx \frac{T_o}{|D\Delta\lambda|} \dots\dots\dots(2.5)$$

Where T_o is the pulse width, v_g is the group velocity, and λ_1, λ_2 are the center wavelength of the two channels. D is the dispersion coefficient and $\Delta\lambda = |\lambda_1 - \lambda_2|$.

When dispersion is significant, the walk-off distance is relatively short, and the interaction between the pulses will not be significant, which leads to a reduced effect of XPM. However, the spectrum broadened due to XPM will induce more significant distortion of temporal shape of the pulse when large dispersion is present, which makes the effect of dispersion on XPM complicated.

Four-Wave Mixing (FWM)

Four-wave mixing (FWM), also known as four-photon mixing, is a parametric interaction among optical waves, which is analogous to inter-modulation distortion in electrical systems. In a multi-channel system, the beating between two or more channels causes generation of one or more new frequencies at the expense of power depletion of the original channels. When three waves at frequencies f_i , f_j , and f_k are put into a fiber, new frequency components are generated at $f_{FWM} = f_i + f_j - f_k$. In a simpler case here two continuous waves (CW) at the frequencies f_1 and f_2 are put into the fiber, the generation of side bands due to FWM is illustrated in Figure 2.6. The number of side bands due to FWM increases geometrically, and is given by,

$$M = \frac{1}{2} (N_{ch}^3 - N_{ch}^2) \dots\dots\dots(2.6)$$

Where N_{ch} is the number of channels, and M is the number of newly generated sidebands. For example, eight channels can produce 224 side bands. Since these mixing products can fall directly on signal channels, proper FWM suppression is required to avoid significant interference between signal channels and FWM frequency components. When all channels have the same input power, the FWM efficiency, η , can be expressed as the ratio of the FWM power to the output power per channel, and is proportional to:

$$\eta \propto \left[\frac{n_2}{A_{eff}D(\Delta\lambda)^2} \right]^2 \dots\dots\dots(2.7)$$

Where A_{eff} is the effective area of fiber.

Equation (2.7) indicates that FWM of a fiber can be suppressed either by increasing channel spacing or by increasing dispersion. Large dispersion can cause unacceptable power penalties especially in high bit rate systems. However, careful design of the dispersion map (often called dispersion management) which allows large local dispersion but limits the total average dispersion to be below a certain level is found to be very effective to combat both dispersion and FWM induced degradations.

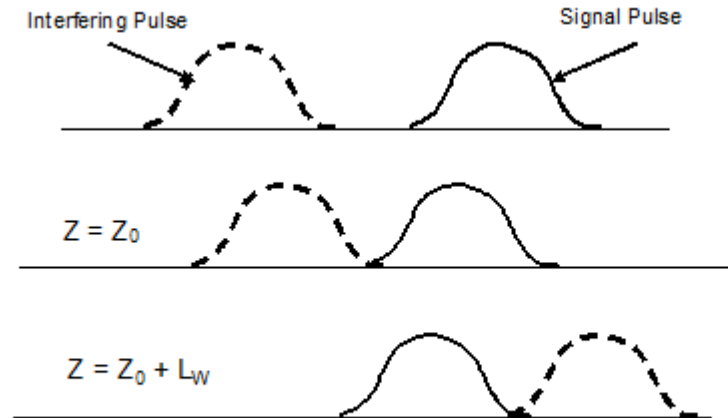


Figure 2.6: Illustration of Walk-off Distance

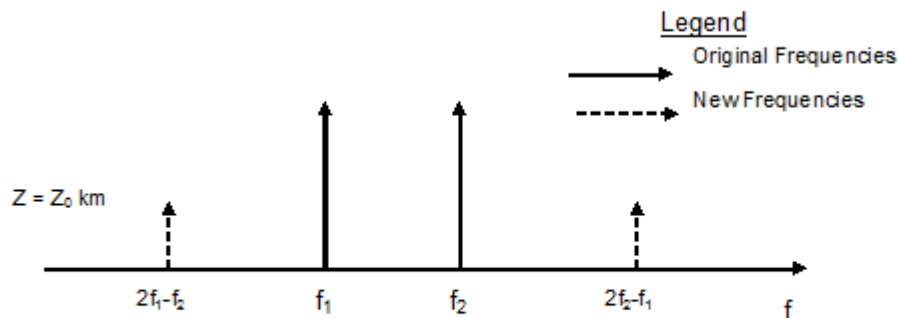


Figure 2.7: Illustration of Side-Bands Generation due to FWM in Two-Channel Systems

Three different effects from the nonlinear refractive index, namely, SPM, XPM, and FWM have been discussed. However, in a real system, especially in a DWDM system where channels are packed very closely to each other, the broadened spectrum due to the three nonlinear effects is usually indistinguishable. The system performance degradations by fiber nonlinearities are, in general, assessable by solving the nonlinear Schrödinger equation (NLSE). The NLSE and a numerical algorithm to solve the NLSE - the split-step Fourier method - will be introduced in Chapter 3.

2.4 Fundamentals of Polarization Mode Dispersion

Let us discuss the detrimental aspect of birefringence in optical fibers-namely, PMD. The existence of birefringence in a fiber implies that the fiber supports two orthogonally polarized modes that have different effective indices and hence propagate with different group velocities in the fiber. An optical pulse launched into such a fiber would be split into two orthogonally polarized pulses, which would then propagate with different propagation constants and group velocities. The two pulses thus reach the output end of the fiber at slightly different time and with different phases. The superimposition of these two pulses leads to the generation of an optical pulse that is now temporally more broadened as compared to the input pulse. Thus, the pulse becomes dispersed due to the effect of fiber birefringence, and the phenomenon is called PMD. PMD is a serious limitation in the case of ultrahigh-bit-rate (>10 Gb) fiber communication links, as it puts a cap on the bit rate of the link as well as causes errors in data transmission. In the following subparagraphs, we shall discuss some basic concepts involved in the understanding of PMD in optical fibers.

PMD in optical fibers is considered as the ultimate limitation in wavelength division multiplexing (WDM) transmission systems with bit rate per channel of 40 Gb/s or higher. Many studies on firsthand higher-order PMD compensation have already been reported, but most of them are based on single channel systems, and the nonlinear effects in optical fibers such as cross phase modulation (XPM), four wave mixing (FWM) in WDM systems are overlooked. PMD is a phenomenon that arises because of the polarization properties of light propagated in an optical fiber. In fact, a so called single mode fiber (SMF) supports two polarization modes of input optical signals. Ideally, perfect optical fibers with geometrical uniformity, homogeneous material, and no tension effects, would propagate these two polarization modes at exactly the same velocity and the two polarization modes degenerate. However, due to internal and external factors, real optical fibers are far from being perfect and, consequently, polarization modes travel at slightly different velocity. This difference in velocity translates into a difference in transmission time through the fiber link, called differential group delay (DGD), which leads to a broadening of the transmitted bits and increases the system bit error rate (BER). In WDM systems, despite the factors mentioned above, the polarization evolution in a channel along the fiber is also affected by the XPM effects from other channels. In this paper, by solving coupled non-linear Schrödinger equation in split-

step Fourier method, the impact of XPM on a post 1st-order PMD compensator (PMDC) is investigated by numerical simulations for a 40 Gb/s WDM transmission system.

2.4.1 Sources of Birefringence

There are many ways in which a fiber can become birefringent. Birefringence can arise due to an asymmetric fiber core or can be introduced through internal stresses during fiber manufacture or through external stress during cabling and installation. Optical fiber manufacturing processes are designed to yield fiber with a circular cross section. Any deviation from this form will generally result in an elliptical core, which in turn will result in a refractive index difference between the X and Y axis of the elliptical core. Even if the fiber core is manufactured with an ideal circular cross section, its refractive index can be asymmetric across its cross section due to stress built in to the fiber during the manufacturing process or stress that is externally applied during deployment or operation. External asymmetric stress can be introduced to the fiber during cabling and installation. Any non uniform loading of the fiber cross section, or bends or twist that are introduced to the fiber by sub-optimal cabling or installation will result in an asymmetric external stress being placed on the fiber. An optical fiber will exhibit birefringence as a consequence of all the above sources of internal and external stress.

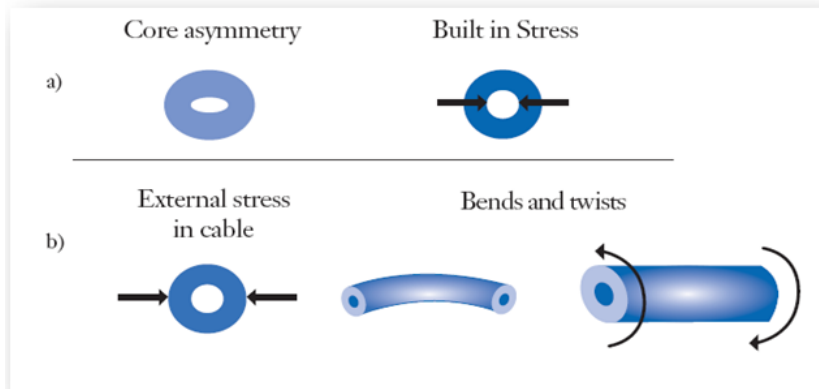


Figure 2.8: Birefringence of Internal and External Sources (a) Internal sources; such as: core asymmetry and built in stress (b) External sources; such as: bend twists and external stress applied to the fiber

2.4.2 PMD Coefficient

The PMD coefficient is an average of random DGDs at the output of the fiber. By itself, for a given fiber, the PMD coefficient is not a random number, in the same way as an average is not a random number, but it is a characteristic of the random distribution of DGDs. However, in the cable, the PMD coefficient is treated as a random number because the fiber sections making up the cable are drawn randomly from the fiber distribution in the cable manufacture inventory and consequently the information about the PMD coefficients of the individual fiber sections is lost [59].

2.4.3 PMD in Short-Length and High-Birefringence Fibers

In short-length SMFs or Hi-Bi fibers, one can assume that the birefringence is constant in magnitude as well as in direction so that there is no polarization mode coupling. In such cases, the two polarization modes—namely, slow and fast—are fixed, so PMD is completely deterministic and not random. If n_s and n_f are the effective indices of the slow and fast modes, respectively, the corresponding propagation constants will be given by [58]

$$\beta_s = \frac{\omega}{c}n_s \text{ and } \beta_f = \frac{\omega}{c}n_f \dots\dots\dots(2.8)$$

Where ω is the angular frequency. The two orthogonally polarized pulses will be traveling with different group velocities given by

$$\frac{1}{v_{gs}} = \frac{d\beta_s}{d\omega}, \text{ and } \frac{1}{v_{gf}} = \frac{d\beta_f}{d\omega} \dots\dots\dots(2.9)$$

Thus, the two pulses will take different times to travel a given length L of the fiber. The difference in the propagation times $\Delta\tau$ is known as the differential group delay (DGD) of the fiber and is given by

$$\Delta\tau = \frac{L}{v_{gs}} - \frac{L}{v_{gf}} = L \frac{d}{d\omega} [\beta_s - \beta_f] = L\Delta\beta' \dots\dots\dots(2.10)$$

Where $\Delta\beta = (\beta_s - \beta_f)$ and $\Delta\beta'$ represents the derivative of $\Delta\beta$ with respect to ω . The DGD is taken as the measure of PMD of a given fiber. Figure 2.9 shows the effect of the PMD on the input pulse in the time domain, demonstrating that an input pulse is divided into two

orthogonally polarized pulses that are separated in time by $\Delta\tau$ at the output end. It should be noted that in short-length fibers, the DGD grows linearly with fiber length [see Equation (2.3)]. It is clear from Equation (2.1) that the two polarized modes will accumulate a phase difference between them, which at a distance z from the input end is given by

$$\delta(\omega, z) = (\beta_s - \beta_f) z = \frac{\omega}{c} (n_s - n_f) z = \frac{\omega}{c} (\Delta n_{eff}) z \dots\dots\dots(2.11)$$

Where $\Delta n_{eff} = (n_s - n_f)$. The phase difference $\delta(\omega, z)$ depends on both frequency and distance. As a result, the SOP of a polarized incident pulse will change with both distance and input frequency.

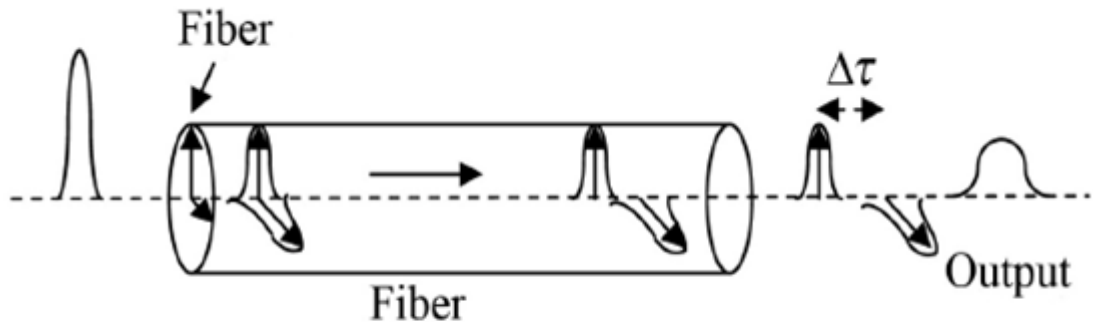


Figure 2.9: A schematic of pulse broadening due to PMD

Equation (2.3) can also be put in the form:

$$\Delta\tau = \frac{d}{d\omega} [L (\beta_s - \beta_f)] = \frac{d}{d\omega} \delta(\omega, L) \dots\dots\dots(2.12)$$

Equation (2.5) shows that $\Delta\tau$ is equal to the rate of change of $\delta(\omega, L)$ with respect to frequency ω . A change in the phase difference $\delta(\omega, L)$ means a change in the output SOP, so it is implied that $\Delta\tau$ can be obtained by knowing the rate of change of the output SOP with respect to the input frequency ω . For example, if the change $\Delta\omega$ in the input frequency ω is such that the output SOP repeats itself, the change in $\delta(\omega, L)$ will be equal to 2Π , and hence, $\Delta\tau$ will be given by $\Delta\tau = \frac{2\Pi}{\Delta\omega}$.

This is the frequency domain picture of the PMD. In fact, as discussed later in this chapter, by measuring the rate of change of the output SOP with respect to the frequency (or wavelength) of input light, one can determine the PMD. This, in fact, is the working principle of several PMD measuring techniques. It may be noted that Equation (2.12) can also be recast as:

$$\Delta\tau = L \frac{d}{d\omega} \left[\frac{\omega}{c} (n_s - n_f) \right] = \frac{L}{c} \left[\Delta n_{eff} + \omega \frac{d}{d\omega} \Delta n_{eff} \right] \dots\dots\dots(2.13)$$

In a special case, if the dispersion of eff Δn can be neglected, then

$$\Delta\tau = \frac{L}{c} \Delta n_{eff} = \frac{\lambda_o}{c} \frac{L}{L_b} \dots\dots\dots(2.14)$$

Where L_b represents the beat length of the fiber given by

$$L_b = \frac{2\pi}{\Delta\beta} = \frac{\lambda_o}{\Delta n_{eff}} \dots\dots\dots(2.15)$$

2.4.4 PMD in Long-Length Fibers

In a long-distance fiber communication link, the fiber experiences stresses, bends, temperature changes, twists, etc., in a random fashion along the length of the link. Therefore, the birefringence along the fiber keeps changing both in magnitude as well as in direction. As a result, the birefringence is no longer additive; hence, the PMD does not grow linearly with the fiber length. Instead, it grows as a square root of the propagation distance, as will be discussed later in this section. Due to random mode coupling, the calculation of PMD becomes very complicated. Fortunately, in a long-length fiber, there exist two orthogonal input polarization states, of which the output polarization states are independent of frequency to the first order. These input polarization states are known as the principal states of polarization (PSPs) of a given fiber length. Pulses launched in these polarization states emerge into two fixed output polarization states, which are also orthogonal to each other. Thus, if the input pulse is launched along one of the input PSPs, there is no splitting of the pulse, similar to the case with short length or Hi-Bi fibers. The PSP model was proposed by Poole and Wagner¹ in 1986 and is extensively used in the calculation and understanding of PMD in long-length fibers. It should be noted that due to random time variation of the birefringence

along a long-length fiber link, PMD also varies randomly, so a statistical approach must be adopted when studying PMD. Using the coupled mode theory, Poole² has studied the effect of random mode coupling between the PSPs on the DGD and has arrived at an elegant expression for the root-mean-square (rms). DGD given by

$$\Delta\tau_{rms}(L) = \Delta\tau_o \left(\sqrt{2} \frac{L_c}{L} \right) \left(e^{-\frac{L}{L_c}} - 1 + \frac{L}{L_c} \right)^{\frac{1}{2}} \dots\dots\dots(2.16)$$

Where $\Delta\tau_{rms} = \sqrt{(\Delta\tau^2)}$, L is the fiber length, and L_c is a constant known as the coupling length and is a measure of magnitude of the mode coupling along the fiber length.

Further, is the DGD in the absence of mode coupling and hence will be given by Equation (2.16) i.e., $\Delta\tau_o = \Delta\beta'L$. Equation (2.16) is valid for all values of L. For $L \ll L_c$,

$$\Delta\tau_{rms}(L) = \Delta\tau_o \left(\sqrt{2} \frac{L_c}{L} \right) \left(\frac{L}{\sqrt{2}L_c} \right) = \Delta\tau_o = \Delta\beta'L \dots\dots\dots(2.17)$$

Showing that the DGD varies linearly with L. On the other hand, for $L \gg L_c$,

$$\Delta\tau_{rms}(L) = \Delta\tau_o \left(\sqrt{2} \frac{L_c}{L} \right) \left(\frac{L}{L_c} \right)^{\frac{1}{2}} = \Delta\beta' \sqrt{2L_c L} \dots\dots\dots(2.18)$$

Where we have used $\Delta\tau_o = \Delta\beta'L$. Equation (2.17) shows that in long-length fibers, the DGD grows as the square root of the length of the fiber. The parameter L_c is generally used to define the short-length and the long-length regimes of PMD as $L \ll L_c$ for the short-length regime, and $L \gg L_c$ for the long-length regime.

Equation (2.18) suggests that PMD in a long-length fiber can be reduced by reducing $\Delta\beta'$ and L_c . Reducing $\Delta\beta'$ means that the birefringence in the fiber should be reduced, which obviously reduces PMD. Reducing L_c means that the coupling between the polarization modes should be increased. This is achieved in spun fibers, which are fabricated by spinning the fiber during the fiber-drawing process. Such fibers were first fabricated for their applications in fiber sensors. Galtarossa and coworkers have done extensive work on the PMD characteristics of spun fibers. Their studies have shown that periodic spinning in optical fibers is much more effective than uniform spinning for reducing the PMD in optical fibers.

2.4.5 PMD compensators

The second approach to PMD mitigation is to use a PMD compensator. It should be mentioned that it is extremely difficult to completely compensate for PMD, as it is a complex phenomenon due to its randomly varying nature.

2.5 Summary

This chapter describes briefly the optical transmission system including various nonlinear characteristics and PMD effects. The linear characteristics such as loss and dispersion parameters are not discussed here. It is evident from the discussion that the limitations offered by nonlinear parameters and PMD in optical fiber communication become more and more detrimental with the increase of distance and bit rate, and decrease in the channel spacing.

CHAPTER 3

THEORETICAL ANALYSIS OF XPM AND PMD ON DWDM SYSTEM

3.1 Introduction

The rapid worldwide growth of data and internet traffic in telecommunication networks results in a sharp increase in the demand for transmission capacity. Efficient utilization of the existing optical fiber network is an answer to this growing demand. It also provides the solution from the economical point of view. An important step to this end is the introduction of optical communication systems with terabits per second capacity, which are based on DWDM technology. Thus for the first time bandwidth efficiency, which is an important feature in wireless communication has appeared as an important issue in fiber optics.

There are several approaches to achieve overall bandwidth efficiency like improved modulation format, line-coding techniques, management of chromatic and PMD including equalization, wideband optical amplifiers, improved WDM multiplexers and demultiplexers. Modeling of the WDM optical channel including nonlinear effects is necessary in order to investigate the impact of the various methods. For practical reasons it is important (to avoid high complexity algorithms) to end up with structures that are realizable at these high frequencies.

Therefore research engineers focus mainly on bandwidth efficient modulation formats at channel data rates 40 Gbps. By saving bandwidth both the dispersion problems and the channel density are improved. A promising approach is multilevel signal line coding. Optical systems by and large use RZ and NRZ modulation format. RZ and NRZ modulations are suitable for long haul systems in which the dispersion in the single mode fiber is compensated for by another fiber with negative dispersion. But it is not the best choice for uncompensated single mode fiber. Optical line codes are more resilient to dispersion and are found superior to NRZ modulation for the uncompensated optical fiber channel.

The popular line coding formats such as RZ and NRZ worked well up to 10 Gbps per channel in long haul high-speed optical communication networks. Recent analysis and investigations have shown that RZ turned out to be superior compared to conventional NRZ systems, at least as long as standard single mode fibers are used as transmission media. The RZ format has been reported to be effective against self phase modulation (SPM) in standard single mode fiber links. SPM and XPM resulting from fiber non-linearity effects caused by group velocity dispersion (GVD) lead to waveform distortion that limits the maximum transmission distance and capacity of high-speed optical links. Thus tolerance with respect to SPM, XPM and GVD are essential for reliable network operation. On the other hand, because of the narrower optical spectrum of NRZ format, NRZ enables higher spectral efficiency in wavelength division multiplexing (WDM) systems compared to RZ in the linear region. However the tolerable dispersion range is limited in both RZ and NRZ modulation formats. In addition, they limit the potential transmitted distance of the signal due to the non-linearity effects of fiber, when they are used in terabit capacity optical communication networks.

In this section generation of multilevel coding formats such as duobinary and novel optical coding are discussed in detail. In section 3.2 duobinary coding is discussed in detail, while in section 3.3 a detail description of novel optical line coding of order one is presented along with its generation example. The XPM changes the state-of-polarization (SOP) of the channels that leads to amplitude modulation of the propagating waves in a wave-division multiplexing (WDM) system. The theoretical analysis of XPM is presented in section 3.4. Due to the presence of PMD, the angles between the SOP of the channels change randomly and the modulation amplitude fluctuation in the perturbed channel becomes random. Finally the effect of XPM on the performance of first order PMD compensation in the DWDM system is analyzed and numerically simulated. The theoretical analysis of PMD is thus discussed in section 3.5.

3.2 Duobinary Line Code

Duobinary signal is a pseudo-binary coded signal in which a "0" bit is represented by a zero level electric current or voltage; a "1" bit is represented by a positive level current or voltage if the quantity of '0' bits since the last "1" bit is even, and by a negative level current or voltage if the quantity of '0' bits since the last "1" bit is odd [52]. In this scheme R

bits/sec can be transmitted using less than R/2 Hz of bandwidth. In order to realize practical transmitting and receiving filters for zero inter symbol interference (ISI) fulfilling Nyquist rate, minimum R/2 Hz of bandwidth is required to transmit R bits/sec. The condition of zero ISI may be relaxed to achieve a symbol transmission rate of r bits/sec. By allowing for a controlled amount of ISI so that it can be subtracted out to recover the original signal values, we can achieve this symbol rate. This result implies that duobinary pulses will have ISI. Let the transmitted signal be

$$X(t) = \sum_{k=-\infty}^{\infty} d_k q(t - kT), d_k = 0, 1 \dots\dots\dots(3.1)$$

Here, d_k are the data bits, $q(t)$ is the transmitted pulse and $T = 1/R$ is the bit period. The pulse $q(t)$ is usually chosen such that there is no ISI at the sampling instances ($t = kt, k = 0, \pm 1, \dots$ are the sampling instances):

$$q(kT) = \begin{cases} 1 & k = 0 \\ 0 & k \neq 0 \end{cases} \dots\dots\dots(3.2)$$

NRZ is one such scheme that requires a bandwidth of R Hz to transmit R bits/sec. This is twice as large as the Nyquist bandwidth of R/2 Hz. The simplest duobinary scheme transmits pulses with ISI as follows:

$$q(kT) = \begin{cases} 1 & k = 0, 1 \\ 0 & \text{otherwise} \end{cases} \dots\dots\dots(3.3)$$

For a channel with bandwidth W and with controlled ISI for $T = \frac{1}{2W}$, we get from Equation (2.2),

$$X(f) = \begin{cases} \frac{1}{2W} [1 + e^{-j\frac{fT}{W}}], & |f| < W \\ 0, & \text{otherwise} \end{cases}$$

$$X(f) = \begin{cases} \frac{1}{W} e^{-j\frac{fT}{2W} \cos(\frac{fT}{2W})}, & |f| < W \\ 0, & \text{otherwise} \end{cases} \dots\dots\dots(3.4)$$

Therefore, $x(t)$ is given by

$$X(t) = \text{sinc}(2Wt) + \text{sinc}(2Wt - 1) \dots \dots \dots (3.5)$$

It is evident from Equations 3.1 to 3.5 that at the sampling instance kT , the receiver does not recover the data bit d_k , but rather $(d_{k-1} + d_k)$. However this scheme allows for pulses with a smaller bandwidth. By allowing some ISI, the transmitted pulse $q(t)$ can be made longer in the time domain. Thus its spectrum becomes narrower in the frequency domain. With a narrower spectrum the distortion effects of the channel are also fewer. This outcome is one of the reasons why duobinary modulation is resilient to dispersion.

One way of generating duobinary signals is to digitally filter the data bits with a two-tap finite impulse response (FIR) filter with equal weights and then low-pass filter the resulting signal to obtain the analog waveform with the property in (3.3) as in Figure 3.1. When the input to the FIR filter is binary (let these binary values be -1 and 1), then the output can take one of these values: $0.5*(-1+1) = -1$; $0.5*(-1+1) = 0$; or $0.5*(1+1) = 1$. Hence the duobinary signal is a three-level signal.

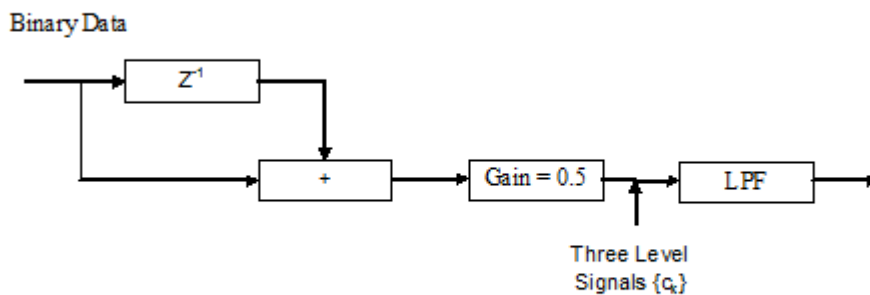


Figure 3.1: Duobinary Encoder

3.2.1 Differential Encoding

The ISI introduced at the transmitter can be revealed at the receiver by differential decoding. At each sampling instance kT , the receiver assumes the value of $X_k = (d_k + d_{k-1})$ where $X_k =$

$x(kT)$ and $x(t)$ satisfies Equation (3.3). If the previous decision at the output of the receiver is \hat{d}_{k-1} , this decision can be subtracted from the sampled value to obtain \hat{d} :

$$\hat{d} = X_k - \hat{d}_{k-1} \dots\dots\dots(3.6)$$

However, a single error at the receiver will propagate forever, causing a catastrophic decoding error. To avoid this catastrophic error propagation, it is better to differentially pre-code the data at the transmitter. The data bits d_k are differentially encoded as follows:

$$c_k = c_{k-1} \oplus d_k \text{ (} \oplus \text{ is modulo 2 subtraction) } \dots\dots\dots(3.7)$$

The transmitted signal is now

$$X(t) = \sum_{k=-\infty}^{\infty} c_k q(t - kT) \dots\dots\dots(3.8)$$

with $q(t)$ satisfying (3.3). Hence at the sampling instance kT , the receiver samples the value:

$$c_k \oplus c_{k-1} = c_{k-1} \oplus d_k \oplus c_{k-1} = d_k \dots\dots\dots(3.9)$$

3.2.2 Differential Encoder

Differential encoder can be implemented using an exclusive-OR (XOR) gate as in Figure 3.2. However, it can be difficult to implement the 1-bit delay in the feedback path at high data rates such as 10 Gb/sec.

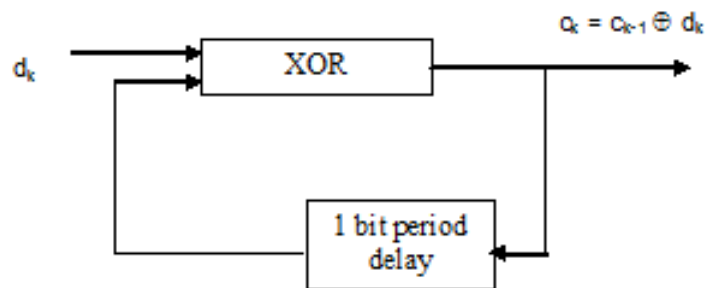


Figure 3.2: Differential Encoder with an XOR Gate

Another circuit that does not involve in the feedback path is shown in Figure 3.3. Here, a divide-by-2 counter has a clock gated with the data. When the data is high, the counter changes state, which is equivalent to adding a 1 modulo 2. When the data is low, the counter state remains the same, which is equivalent to adding a 0 modulo 2.

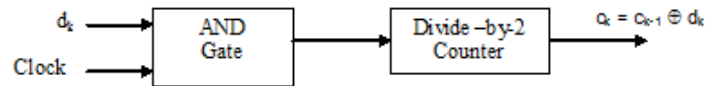


Figure 3.3: Differential Encoder with a Divide-by-2 Counter

3.2.3 Optical System for Duobinary Modulation

The final step is to modulate the light with the three-level duobinary signal, which implies a three-level optical signal. This result is achieved with a Mach-Zehnder (MZ) modulator biased at its null point. With a zero input, no light is transmitted, but with the +1 and -1 inputs are transmitted as +E and -E electrical fields. While this is a three level signal in terms of the electrical field, it is a two-level signal in terms of optical power. This choice significantly reduces the complexity of the receiver.

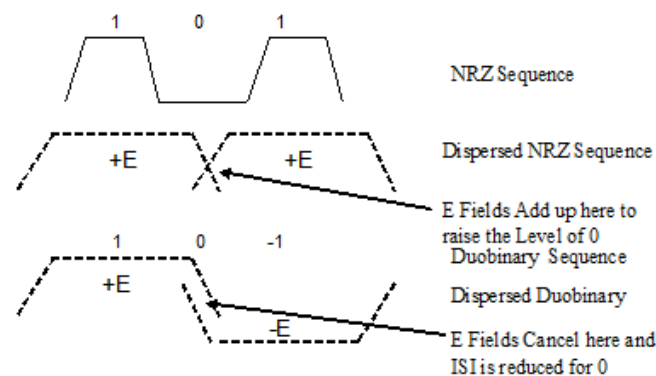


Figure 3.4: Effect of Dispersion on NRZ and Duobinary Sequences

The combination of the duobinary encoder and the above mapping to electric fields help further reduce the effects of dispersion in the fiber. As the pulses travel down the fiber, they spread out in time owing to dispersion. In an NRZ scheme, a data sequence of 1 0 1 is mapped onto the optical domain as $+E$ 0 $+E$. In the encoded duobinary sequence, a 1 0 1 sequence cannot occur, but a 1 0 -1 does occur, which is mapped as $+E$ 0 $-E$ in the optical domain. The effect of dispersion in the two cases is shown in Figure 3.4. It depicts why the resulting dispersion is less in duobinary modulation.

The same receiver that is used for a NRZ modulation scheme can be used for the duobinary modulation. The power detector squares the electric field to detect power and hence $+E$ and $-E$ outputs of the fiber get mapped to the same power level and are detected as logical 1s. Figure 3.5 shows an example of the transformation of data in a duobinary system and its electrical modulating signal.

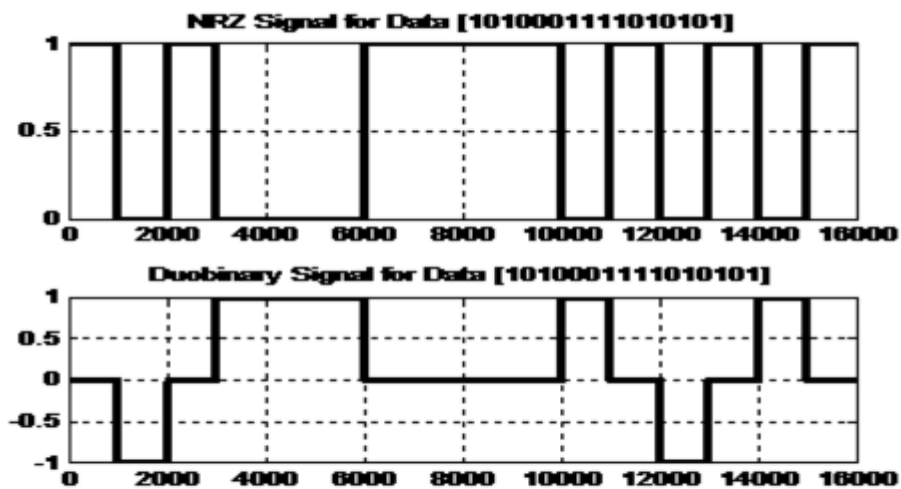


Figure 3.5: NRZ and Duobinary Signal for Data Sequence [1 0 1 0 0 0 1 1 1 1 0 1 0 1 0 1]

Table 3.1: An Example Showing the Transformation of Data in a Duobinary System

K	-1	0	1	2	3	4	5	6	7	8	9	10	11	12	13	14	15
dk	0	1	0	1	1	1	0	0	0	0	1	0	1	0	1	0	
\hat{d}_k	1	0	1	0	0	0	1	1	1	1	0	1	0	1	0	1	
Diff Encoder	0	1	1	0	0	0	0	1	0	1	0	0	1	1	0	0	1
Bit-Voltage	-1	1	1	-1	-1	-1	-1	1	-1	1	-1	-1	1	1	-1	-1	1
Duobinary	0	1	0	-1	-1	-1	0	0	0	0	-1	0	1	0	-1	0	
Electric	0	+E	0	-E	-E	-E	0	0	0	0	-E	0	E	0	-E	0	
Opt Power	0	E2	0	E2	E2	E2	0	0	0	0	E2	0	E2	0	E2	0	
Rx Bits	0	1	0	1	1	1	0	0	0	0	1	0	1	0	1	0	

3.3 A Multi-Level Novel Optical Line Code

Training is the act of presenting the network with some samples and modifying the weights to better approximate the desired Novel optical line coding is similar to conventional Miller coding with the difference being that two of them are scaled by a factor $\alpha \neq 1$ and transmitted in sequence according to the duobinary logic. Novel optical codes are ranging from order 1, 2, ..., n and here only order one novel optical codes are used.

3.3.1 First Order Code

The first order code uses four wave forms $s_i(t)$, and the state diagram is shown in the Figure 3.6, where Σ_1, Σ_2 are the code states, the elementary signals are $s_i(t)$, where $i = 1, 2, 3, 4$.

Elementary signals form two pairs with $s_1(t) = -s_4(t)$ and $s_2(t) = -s_3(t)$. In addition two of the elementary signals $s_2(t)$ and $s_3(t)$ are scaled by α . In this thesis α is chosen as 0.5 to produce best spectral shape. The information sequence $\{u_k\}$ is encoded as shown in Figure 3.7 to form the signal:

$$X_e(t) = \sum_{k=-\infty}^{\infty} g_1(\sigma_k) S_e(t - kT; U_k) \dots\dots\dots(3.10)$$

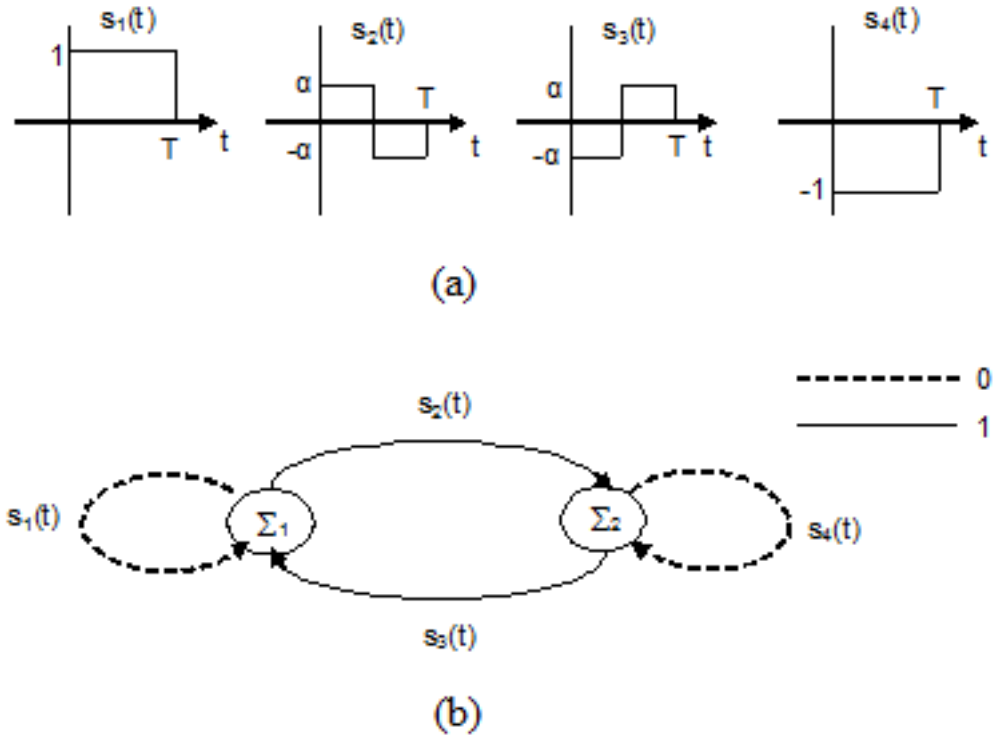


Figure 3.6: (a) Elementary Signals and (b) Code State Diagram for Novel Multilevel Optical Line Code of Order one.

where σ_k stands for the generic encoder state and $g_1(\sigma_k)$ is a coefficient defined by the following rule:

$$g_1(\sigma_k) = \begin{cases} 1, & \text{if } \sigma_k = \Sigma_1 \\ -1, & \text{if } \sigma_k = \Sigma_2 \end{cases} \dots\dots\dots(3.11)$$

where Σ_1 and Σ_2 indicate the states allowed to the encoder, and $s_e(t; u_k)$ is one of the two elementary signals $s_1(t)$ or $s_2(t)$ selected in accordance to the following rule:

$$s_e(t; u_k) = \begin{cases} s_1(t), & \text{if } u_k = 0 \\ s_2(t), & \text{if } u_k = 1 \end{cases} \dots\dots\dots(3.12)$$

Hence, the actual elementary signal output from the encoder will be one of $s_1(t)$ or $s_2(t)$ or their negatives [i.e., $s_4(t)$ or $s_3(t)$ respectively] depending on the value of $g_1(\sigma_k)$ as shown in Figure 3.6. The sequence of the encoder is defined by the following rule:

$$\sigma_{k+1} = g_2(u_k, \sigma_k) \dots\dots\dots(3.13)$$

where the value of the function g_2 is described by the following map:

Table 3.2: Map containing the value of g_2

$\frac{u_k}{\sigma_k}$	Σ_1	Σ_2
0	Σ_1	Σ_2
1	Σ_2	Σ_1

It may noticed that for $\alpha = 0$, $s_2(t) = s_3(t) = 0$, and the code reduces to duobinary code. The above coding rule for order 1 code is summarized in Table-3.3.

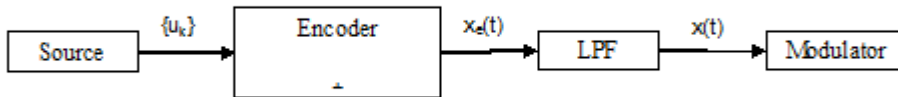


Figure 3.7: (Transmitter Model of an optical system)

Table 3.3: Encoding Rule of Novel Optical Line Code (Order1)

Data Seq $\{u_k\}$	Encoder State (σ_k)	State of Encoder (g_2)	Encoded Signal $x_e(t)$
0	Σ_1	Σ_1	$s_1(t)$
0	Σ_2	Σ_2	$-s_1(t) = s_4(t)$
1	Σ_1	Σ_2	$s_2(t)$
1	Σ_2	Σ_1	$-s_2(t) = s_3(t)$

The power spectral density of the signal $x_e(t)$ in (3.10), coded in accordance to the state diagram of Figure 2.6 is given as

$$G_e(f) = \frac{1}{T} |S_1(f)|^2 \cos^2(\Pi fT) + \frac{1}{T} |S_2(f)|^2 \sin^2(\Pi fT) + j \frac{1}{T} S_1(f) S_2^*(f) \sin(2\Pi fT) \dots\dots\dots(3.14)$$

where $S_1(f)$ and $S_2(f)$ are the Fourier transforms of the elementary signals $s_1(t)$ and $s_2(t)$ respectively. Elementary signals of order one code can be generated by expressing four elementary signals of Figure 3.6 as linear combinations of the rectangular pulses of duration $T/2$.

$$p(t) = \begin{cases} 1, & 0 < t < \frac{T}{2} \\ 0, & \text{elsewhere} \end{cases} \dots\dots\dots(3.15)$$

In this case, we get, for the elementary signals $s_i(t)$, and $i = 1, 2, 3, 4$ the following expressions:

- $s_1(t) = p(t) + p(t - \frac{T}{2})$
- $s_2(t) = \alpha [p(t) + p(t - \frac{T}{2})]$
- $s_3(t) = -s_2(t)$
- $s_4(t) = -s_1(t) \dots\dots\dots (3.16)$

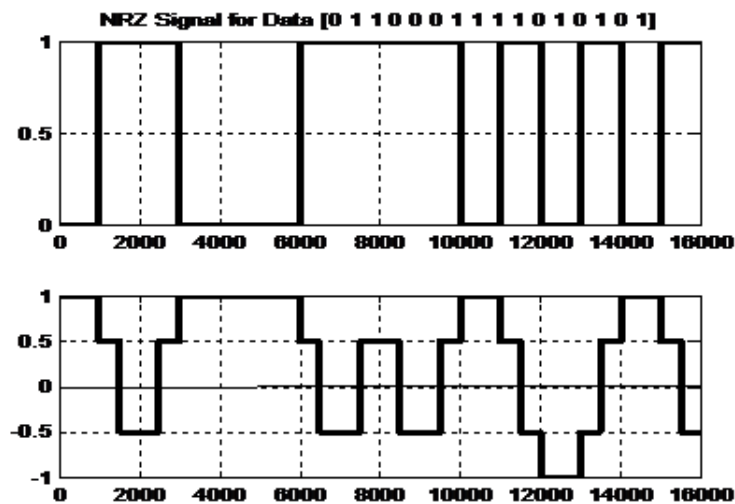


Figure 3.8: An Example Showing NRZ and Duobinary Signals for Data Sequence [0 1 1 0 0 1 1 1 1 0 1 0 1]

3.4 Theoretical Analysis of XPM

In theoretical analysis of XPM, a mathematical model is presented to quantify the XPM in a two channel optical system. An approach is adopted here to isolate in this effect from other nonlinear effects of optical fiber.

The WDM transmission employs intensity modulation direct detection (IM/DD) modulation scheme. This is described in three sections. First, the input and output power are described taking into consideration of in-line amplifications and filters. Secondly the derivation of total XPM induced phase shift in a single segment transmission line is presented. Finally an approach on calculating the BER is presented.

There are two major detection schemes widely used at present; coherent and direct detection schemes. The term coherent refers to any technique employing nonlinear mixing between two optical waves. To send information, one can modulate the amplitude, frequency or phase of the carrier. In direct detection system, electrical signal coming into the transmitter amplitude-modulates the optical power level of the light source. Thus, the optical power is proportional to the signal current level.

Coherent system offers improved receiver sensitivity and channel selectivity over direct detection technique. Advantages of coherent optical communication schemes are a nearly ideal receiver sensitivity (20 dB over direct detection) and high degree of frequency selectivity. Selectivity of coherent system is due to the fact that narrow band electronic filters pick out the neighboring channels like broadband optical filters.

To synchronize the sampling, the digital signal clock must be recovered at the receiver by means of a base band phase locked loop. The advantage of IM-DD is that it offers system simplicity and low cost but suffers from the limited sensitivity and does not take full advantage of band width capabilities of the fiber. The choice of modulation and detection schemes determines the fundamental receiver sensitivity. Receiver sensitivity in terms of SNR is proportional to received optical signal power. Receiver sensitivity for various coherent and direct detection techniques has been described in terms of the average number of photons required to achieve 10^{-9} BER.

3.4.1 Input and Output Power Representation

XPM occurs in systems having at least two channels. The group velocity dispersion (GVD) converts the XPM induced phase modulation (PM) to IM. Here, the analytical model to study the effects of XPM in DWDM transmission is based on in an IM/DD system. The two input channels considered in the system are sent to the transmitter where the electrical signals modulate the optical output. Channel 1 or probe is a continuous wave (CW) and channel 2 is the pump channel which is sinusoidally modulated. The intensity modulated input pump signal has an angular frequency ω . Considering a small section of fiber length where fiber nonlinearity and dispersion are assumed to act independently, the XPM induced phase shift in probe channel when optical pulse in pump channel traveled a distance z from fiber input can be expressed by [8-9]:

$$\phi_{xpm,1}(z, \omega) = -2\gamma_1 P_2(z, \omega) \dots\dots\dots(3.17)$$

where

$$P_2(z, \omega) = P_2(0, \omega) \cos(qz) \exp(-\alpha z) \exp\left(\frac{-j\omega z}{v_{g2}}\right) \dots\dots\dots(3.18)$$

Equation (3.18) represents the pump power fluctuation after propagating at distance z from the fiber input that modulates the phase of the probe signal through XPM. $P_2(0, \omega)$ is a complex amplitude of pump signal power at fiber input and it is given by $P_2(0, \omega) = P_{20}e^{j\theta}$. Here, $q = \frac{(\omega^2 D \lambda_2^2)}{(4\pi c)}$ with D is the fiber dispersion coefficient, λ_2 is the wavelength of pump signal and c is the speed of light. The total XPM induced phase shift of probe signal after propagating a distance L is given by [30]:

$$\phi_{xpm,1}(L, \omega) = \int_0^L \phi_{xpm}(z, \omega) dz = |H(\omega)| |P_2(z, \omega)| \cos\left(\frac{\omega L}{v_{g1}} + \angle P_2(z, \omega) + \angle H(\omega)\right) \dots\dots\dots(3.19)$$

Equation (4.3) shows that XPM is a phase modulation process with the frequency response given by [30]:

$$H(\omega) = 2Y_1 P_1 \sqrt{\eta_{xpm}(\omega)} L_{eff} \exp(j\psi(\omega)) \dots\dots\dots(3.20)$$

Without the phase term of equation (3.4), the equation is known as XPM index:

$$\Delta\phi_1 = 2Y_1P_1\sqrt{\eta_{xpm}(\omega)}L_{eff} \dots\dots\dots(3.21)$$

In (4.4) and (4.5), L_{eff} is the effective length of the fiber, $\psi(\omega)$ is the phase retardation factor, η_{xpm} is the XPM efficiency and Y_1 is the nonlinear coupling coefficient of the optical signal. These parameters are defined as:

$$L_{eff} = \frac{(1-\exp(-\alpha L))}{\alpha} \dots\dots\dots(3.22)$$

$$\psi = -\arg(-\alpha + j\omega d) + \arg[-(1 - \exp(-\alpha L) \cos(\omega d L) + j \exp(-\alpha L) \sin(\omega d L))] \dots\dots\dots(3.23)$$

$$\eta_{xpm} = \frac{\alpha^2}{\omega^2 d^2 + \alpha^2} \left[1 + \frac{4 \sin^2\left(\frac{\omega d L}{2} \exp(-\alpha L)\right)}{(1 - \exp(-\alpha L))^2} \right] \dots\dots\dots(3.24)$$

In (4.6-8), α is the attenuation coefficient of the fiber, L is the fiber length, d is the walk-off parameter defined as:

$$d_{12} = D\Delta\lambda \dots\dots\dots(3.25)$$

where $\Delta\lambda$ is the wavelength separation between channel 1 (λ_1) and channel 2 (λ_2), and D is the dispersion coefficient of the fiber. The nonlinear coupling coefficient is defined as:

$$Y_1 = \frac{2n_2\Pi}{\lambda_1 A_{eff}} \dots\dots\dots(3.26)$$

where n_2 is the nonlinear refractive index of the fiber. A_{eff} is the effective core area of the fiber expressed as:

$$A_{eff} = \Pi r^2 \dots\dots\dots(3.27)$$

where r is the radius of the fiber. The total XPM induced phase shift in time domain can be obtained by taking the real part of inverse Fourier Transform of equation (4.3)

$$\phi_{xpm}(L, t) = Re\left(\frac{1}{\Pi} \int_0^\infty \phi_{xpm}(L, \omega) \exp(-j\omega t) \partial t\right) \dots\dots\dots(3.28)$$

Equation (4.12) represents the XPM induced phase shift in probe signal at fiber output after propagating at distance L. This XPM induced phase shift will be converted to XPM induced intensity modulation (IM) by GVD effect [31]. In order to determine the strength of XPM induced IM in probe channel, the expression of power fluctuations on probe signal at fiber output induced by XPM at infinitesimal distance z from fiber input is given by [9]:

$$P_{xpm,1}(z, \omega) = -2P_1(z) \exp\left(-\alpha(L-z) \exp(-j\omega) \frac{(L-z)}{v_{g1}} \sin(b(L-z))\right) \phi_{xpm,1}(z, \omega) \dots\dots\dots(3.29)$$

Here $P_1(z) = P_1(0) \exp(-\alpha z)$ is the average power of probe channel at distance z, $P_1(0)$ is the average power of probe channel at fiber input and b is defined as $b = \frac{\omega^2 D \lambda_1^2}{4\pi c}$. The total XPM induced IM at probe channel at fiber output is the sum of the XPM induced IM at infinitesimal section z along the fiber with length with length L is given by:

$$P_{xpm}(\omega) = 2Y_1 P_1(0) P_2(\omega) \exp(-\alpha L) \exp\left(\frac{-j\omega L}{v_{g1}}\right) \dots\dots\dots(3.30)$$

From equation (3.30) the magnitude and phase responses of XPM induced IM can be easily found out as shown in Figure 4.3. The normalized magnitude response induced by XPM in the probe channel, called normalized IM index is given by [27]:

$$m_{IM}^{XPM} = \left| \frac{P_{xpm}(\omega)}{(P_2(z, \omega) \exp(-\alpha L))} \right| \dots\dots\dots(3.31)$$

On the other hand the phase response is given by

$$\Psi_{IM}^{XPM}(\omega) = \arg \left[\frac{P_{xpm}(\omega)}{\left(P_2(z, \omega) \exp\left(\frac{-j\omega L}{v_{g1}}\right)\right)} \right] \dots\dots\dots(3.32)$$

The total XPM induced IM in the time domain at probe channel at fiber output is obtained by inverse Fourier transform of equation (4.14)

$$P_{xpm}(L, t) = \left| \frac{1}{\pi} \int_0^\infty P_{xpm}(\omega) \exp(-j\omega t) \partial t \right| \dots\dots\dots(3.33)$$

3.4.2 Bit Error Rate (BER) Derivation

The demultiplexed optical signals are then sent to the receiver. The photo-detector in the receiver senses the varying optical intensity falling upon it and converts them into varying electric current, using the direct detection method. The photo-detector output current is given by:

$$i(t) = R_d |E|^2 + i_n(t) = R_d |S_{out}(t)|^2 + i_n(t) = 2R_d P_s G L \cos(\Delta\phi_{xpm}(L,t)) + i_n(t) \dots\dots\dots(3.34)$$

R_d is the bias or load resistance, P_s is the receiver power. G and L are the gain and loss of the transmission link respectively. $\Delta\phi_{xpm}(L,t)$ represents the random phase distortion introduced by XPM which can be obtained from (3.28). $i_n(t)$ is the sum of the various noises considered in the system. The noise considered in this system are the receiver shot noise, thermal noise and beat noise due to beating of the spontaneous emission of the amplifier.

Considering the thermal noise to be predominant, it is assumed that the noise for transmitted "1" and "0" are of same magnitude. The total noise variance is obtained by summing the variances of the individual noise components:

$$\sigma_n^2 = \sigma_{shot}^2 + \sigma_{thermal}^2 + \sigma_{s-sp}^2 \dots\dots\dots(3.35)$$

The variance of the shot noise is given by:

$$\sigma_{shot}^2 = 2eR_d P_T B_e \dots\dots\dots(3.36)$$

where R_d is the bias or load resistance of the photo-detector receiver, B_e is the bandwidth of the photo-detector and P_T is the received optical power at the photo-detector. The variance of the thermal noise is:

$$\sigma_{thermal}^2 = I_{th} B_e \dots\dots\dots(3.37)$$

where I_{th} is the thermal noise current generated by the detector bias resistance in the photo-detector receiver. The variance of the signal spontaneous noise is given by:

$$\sigma_{s-sp}^2 = n_{sp} (G - 1) hv2R_d^2 P_T GLB_e \dots\dots\dots(3.38)$$

where G is the gain of the amplifier, v is the optical frequency and n_{sp} is the spontaneous emission factor or population inversion factor. Then the BER can be directly found out from [26]:

$$BER = 0.5_{erfc} \left[\frac{2R_d P_s GL \cos(\bar{\phi}_{xpm})}{\sqrt{(\sigma_n^2 + \sigma_{xpm}^2)}} \right] \dots\dots\dots(3.39)$$

Here $\bar{\phi}_{xpm}$ is the mean phase shift due to XPM, σ_{xpm}^2 is the mean amplitude fluctuation of the probe signal due to XPM.

3.4.3 Applying Line Coding Schemes

For applying the line coding, the input data are passed through the line coder and data will have the form as shown in Equation (3.17) or (3.20). These data are then passed to the transmitter. The mathematical representation of the line coded data $\bar{P}_2(0, \omega)$ replaces $P_2(0, \omega)$ of Equation (3.18). The subsequent procedures are the same as given in Equation (3.30)

3.4.4 Applying Duobinary Line Coding Schemes

For duobinary line coding scheme the expression for the input power is expressed as:

$$\bar{P}_i(0, \omega) = X_i(0, \omega) \cos(qz) \exp(-\alpha z) \exp\left(\frac{-j\omega z}{v_{g2}}\right) \dots\dots\dots(3.40)$$

where $X_i(0, \omega)$ is the power spectrum of the ith channel and is defined as following with W as the bandwidth:

3.4.5 Applying Novel Optical Line Coding Schemes

The input power of a system with Novel optical coding is expressed as

$$\bar{P}_2(0, \omega) = P_2(z, \omega) = G_e(f) \cos(qz) \exp(-\alpha z) \exp\left(\frac{-j\omega z}{v_{g2}}\right) \dots\dots\dots(3.41)$$

where $G_e(f)$ is defined in Equation (3.14).

3.4.6 Summary on Theoretical Analysis of XPM

Duobinary and Novel optical line codes described in this chapter will be applied in a modeled optical system in the later chapter. In this chapter, the methods of generating the line codes along with examples are described. These methods will be applied in this study in the subsequent chapters. However there are other multilevel line codes like alternate block inversion (ABI), monospaced mark inversion (MMI), etc. which are not discussed here in this study. Subsequent chapters are dedicated mainly to find out the effectiveness of these line codes in combating the nonlinear effects. Efforts will also be taken to quantify such effectiveness in terms realizable practically following several approaches. The quantified expression of XPM and its effect in terms of BER as expressed in Equations 3.20, 3.30 and 3.39 will be applied in the simulation in subsequent chapters. This result helps the author to go forward to apply the line codes.

3.5 Theoretical Analysis of PMD

Optical Fiber Communication is used not only in telecommunication field but also in internet and Local Area network. The advantage of Optical Fiber Communication is low data loss, long distance amplifier, high data carrying capacity. As number of channel increases, dispersion began to show up as obstacles. PMD effects occur only in single mode fiber the resulting the PMD to limit the transmission capacity of fiber. The PMD of installed fiber fluctuates with temperature and stress changes. So, adaptive PMD is needed for Optical Fiber Communication. PMD which is a time changing quantity is a problem, reduces distances and data rates in a single-mode OFC system. In general, the effect of PMD on an optical fiber communication link at different bit rates shows that it causes several undesirable effects and it can be compensated through various compensation techniques. The goal of this work is to analyze the effect PMD and its compensation. The effect of PMD on a fiber link and an optical compensation method is also proposed. By which the degradation due to PMD can be mitigated to a certain extent. A suitable delay is provided to one of the polarization states and no delay to the other state. Finally the two signals are added and as a result the two components experience a differential delay.

The maximum channel density for digital transmission can be achieved by increasing the bit

rate. When the bit rate crosses the 2.5Gbps, the PMD degrades the transmission characteristics. PMD occurs in single mode fiber and because of PMD it is impossible to transmit data reliably at high speed. This effect results in the widening of the pulses and reduces the capacity of transmission of the fiber. This work analyzes the effect of PMD in optical fiber in one hundred km link fiber. The eye diagram, Q value and bit rate are used for analyzing the PMD. Also an optical compensation technique by which the effect of PMD can be reduced is also analyzed. Bit error rate can be achieved by simulating with OptSim, which includes the algorithms to guarantee the maximum possible accuracy and correct results.

3.5.1 System Modeling

In high speed transmission PMD will occur and it broadens the pulses and causes intersymbol interference. Compensation can be achieved by electronic equalization or by using dispersion compensating fibers or by optical equalization. PMD is a physical phenomenon in OFC that causes light pulses to spread. PMD severely reduces the system performance. The PMD is due to geometrical variations in concentricity or ellipticity of fiber core or cladding during manufacture. Therefore in this work an optical compensation method is proposed to compensate for the effect of PMD. Thus PMD varies randomly along the fiber length and therefore the effect of PMD can be reduced by introducing better fiber manufacturing techniques or by compensating for PMD effects. Electronic compensation is not sensitive to the phase and polarization information of the received signal and also it is bit rate dependent so optical compensation is advantageous compared to electronic compensation. The block diagram of the work is shown in Figure 3.9 and 3.10. It describes the basic components used for the analysis of the effect of PMD and its compensation. In Figure 3.9 the effect of PMD in a fiber optic link is analyzed using an emulator and in Figure 3.10 the optical compensation technique of using an emulator and a deterministic differential group delay is analyzed. An emulator is used after the fiber link to recreate the behavior of an optical field fiber in the laboratory. Then the signal is passed through the fiber channel of 100km. As the signal travels through the fiber the effect of PMD affects the transmitted signal. The simulation is done in OptSim which is one of the costliest simulation software used for optical communication. [36]

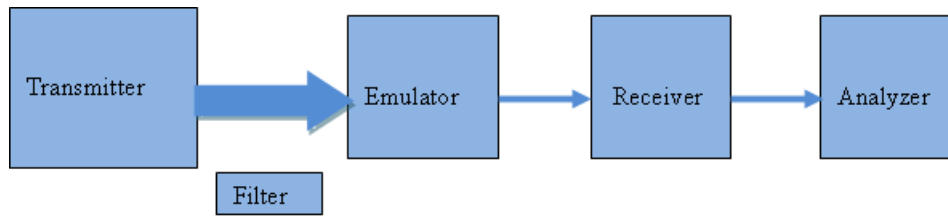


Figure 3.9: Block diagram for analyzing effect of PMD

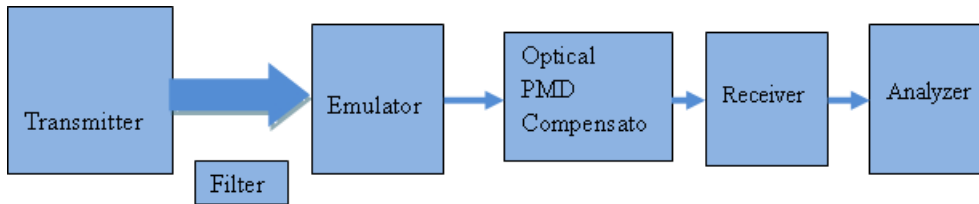


Figure 3.10: Block diagram for optical PMD compensation

The below setup shown in Figure 3.11 simulates PMD effects with and without compensation. The compensation is done by using a Deterministic DGD. The effect can be analyzed through eye diagrams and Q estimator. The light carrier is generated by Lorentzian laser source at the 1550 nm wavelength. The light can be modulated by the input signal by passing through the amplitude modulator. The transmitted signal is formed by modulating the light carrier by the NRZ data source signal. This delay provided negates the distorted signal through the emulator and thus compensation of PMD is achieved which can be seen from the eye diagrams. The distorted signal is received by the receiver and is analyzed through eye diagrams. For analyzing the optical compensation the signal emulated by the emulator is passed through a deterministic DGD element which splits the signal into two and provides a determined delay to one of the signal.

For this setup, a transmitter consists of a 40-Gbps PRBS generator, CW Laser source at 1550 nm, electrical driver, external modulator, and optical power normalizer. A 40-Gbps RZ-modulated signal then is launched into a fiber span. The output from the fiber span is inserted into a receiver. PMD is a statistical effect caused by randomly varying fiber birefringence, therefore the simulation results will be different for different settings of the random seed parameter. PMD causes differential group delay (DGD) between x- and y- polarization components during propagation in fiber, and, hence, eye distortion at the receiver. One can run a parameter scan to obtain DGD and BER/Q for different values of the PMD coefficient

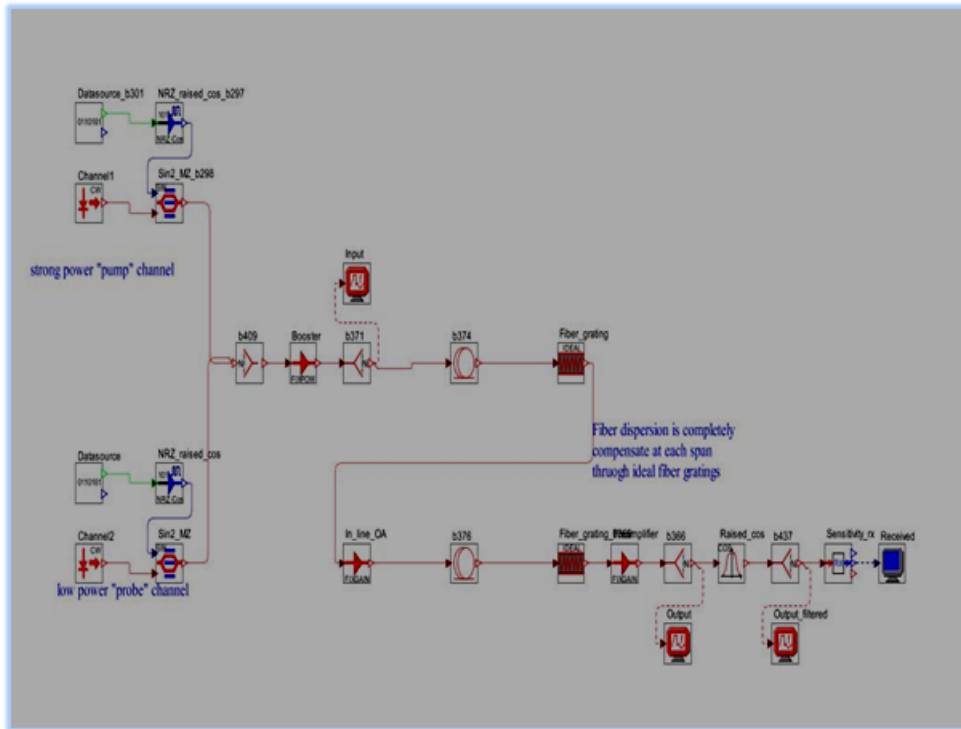


Figure 3.11: Simulation block for analyzing effect and compensation of PMD

and different random seeds. After the simulation run is finished one can double-click on various analysis blocks to view the signal plot, eye diagram, DGD, Stokes parameters on Poincare Sphere, and BER/Q values

3.5.2 Summary on Theoretical Analysis of PMD

The PMD-induced DGD degrades system performance with penalties more severe at higher bit rates and higher PMD coefficients in fibers. We can see that the XPM reduces the eye opening to some extent and results in weakening the performance of first order PMD compensation.

CHAPTER 4

SIMULATION METHODS AND RESULTS

4.1 Simulation Methods for XPM

The nonlinear Schrodinger equation (NLSE) given in equation (4.1) governs the propagation of optical pulses inside single mode fibers. The NLSE is a partial differential equation that does not generally lend itself to analytical solutions except some specific cases in which the inverse scattering method can be employed. A numerical approach is often necessary for an understanding of the interplay between GVD Kerr effects of optical fibers. The method that has been used extensively to solve the pulse propagation in nonlinear dispersive media is the split step Fourier method. The relative speed of this method compared with most finite-difference methods can be attributed in part to the use of the fast Fourier transform (FFT) algorithm.

4.2 Split Step Fourier Method

Pulse propagation in optical fiber is simulated by applying the split-step Fourier method to numerically solve the NLSE, which includes the effect of first order and second order GVD, self phase modulation (SPM) and cross phase modulation (XPM) due to fiber nonlinearity and fiber attenuation. This is a well established mathematical model and is extensively modeled for all fibers in the transmission system, i.e. for DSF and DCF. Considering a slow varying pulse envelope $A(z,t)$ which can be the envelop of a summation of a number of optical channels of the WDM system, which propagates inside a nonlinear dispersive optical fiber in the following manner:

$$\frac{\partial A}{\partial z} + \frac{\alpha}{2}A + \frac{j}{2}\beta_2 \frac{\sigma^2 A}{\sigma T^2} - \frac{1}{6}\beta_3 \frac{\sigma^3 A}{\sigma T^3} = j\gamma_k \left[|A_k|^2 + \sum_{i=1, i \neq k}^N 2|A_i|^2 \right] A_k \dots\dots\dots(4.1)$$

where α is the fiber loss, β_2 and β_3 are the second and third order GVD factors respectively, γ is the nonlinearity parameter, and $T = t - \frac{z}{v_g}$ is a frame of reference moving with the pulse

at group velocity v_g . The first and second terms on the right hand side account for self phase modulation and cross phase modulation of the optical field with the N-1 adjacent channels respectively. If we consider a two channel system what is considered in this paper, then the field propagation can be expressed as the coupled NLSE [27]:

$$\frac{\partial A_1}{\partial z} + \frac{j}{2}\beta_{21}\frac{\partial^2 A_1}{\partial T^2} + \frac{\alpha}{2}A_1 = jY_1 \left[|A_1|^2 + 2|A_2|^2 \right] A_1 \dots\dots\dots(4.2.a)$$

$$\frac{\partial A_2}{\partial z} + d\frac{\partial A_2}{\partial T} + \frac{j}{2}\beta_{22}\frac{\partial^2 A_2}{\partial T^2} + \frac{\alpha}{2}A_2 = jY_2 \left[|A_2|^2 + 2|A_1|^2 \right] A_2 \dots\dots\dots(4.2.b)$$

The walk-off parameter $d = v_{g2}^{-1} - v_{g1}^{-1}$ where v_{gj} is the group velocity of channel j. The walk-off parameter can also be expressed in terms of the dispersion coefficient D. Then, $d = \int_{\lambda_1}^{\lambda_2} D(\lambda) d\lambda = D|\lambda_2 - \lambda_1| = D\Delta\lambda$.

4.2.1 Light Waves Beam Propagation Method using Split Step Model

The instantaneous pulse envelope $A(z,t)$ propagating inside the fiber is calculated by solving equation (4.1) numerically using the split-step Fourier method. Expressing equation [32] as

$$\frac{\partial A}{\partial z} = (\hat{D} + \hat{N})A \dots\dots\dots(4.3)$$

where \hat{D} is the dispersion differential operator and \hat{N} is the nonlinearity operator. \hat{D} and \hat{N} are defined by:

$$\hat{D} = -\frac{\alpha}{2} - \frac{j}{2}\beta_2\frac{\partial^2}{\partial T^2} + \frac{1}{6}\beta_3\frac{\partial^3}{\partial T^3} \dots\dots\dots(4.4.a)$$

$$\hat{N} = j\gamma_k \left[|A_k|^2 + \sum_{i=1, i \neq k}^N 2|A_i|^2 \right] \dots\dots\dots(4.4.b)$$

As these two operators appear to add by superposition, dispersive and nonlinear effects can be considered to act independently. That is, the two effects split. Next consider dividing the fiber length into small steps of length h. The exact solution of (4.1) describes the pulse envelope in segment z+h relative to its shape in the preceding segment z:

$$A(z+h, T) = \exp(h\hat{D}) \exp(h\hat{N}) A(z, T) \dots\dots\dots(4.5)$$

where the exponential operator $\exp(h\hat{D})$ is evaluated in the Fourier domain by replacing the differential operator by $\frac{\partial}{\partial T}$ by $(j\omega)$:

$$\exp(h\hat{D})B(z, T) = F^{-1} [\exp\{h\hat{D}(j\omega)\} F(B(z, T))] \dots\dots\dots(4.6)$$

This equation is numerically solved using the Finite-Fourier-Transform (FFT) algorithm. To improve the accuracy of the split-step Fourier method, the pulse is made to propagate in the following pattern:

$$A(z+h, T) = \exp\left(\frac{h}{2}\hat{D}\right) \exp\left(\int_z^{z+h} N(z') dz'\right) \exp\left(\frac{h}{2}\hat{D}\right) A(z, T) \dots\dots\dots(4.7)$$

Intuitively, this equation says that a pulse emerges out of the preceding fiber segment and enters the current segment would propagate in a purely dispersive medium in the first half of the segment, then stops at middle of the segment and picks up all nonlinear effects in that segment, then set off to complete the remaining half of the purely dispersive segment. The pulse would then propagate through the subsequent segments in the same manner until it reaches the receiving end of the fiber.

The SPM refers to the nonlinear phase shift in the optical wave caused by the optical field itself. Such effect is generally negligible at low power levels (normally below 10 mW) but becomes significant when the peak intensity of the pulse is sufficiently high to cause appreciable change in the refractive index of silica fiber [32]. This intensity induced index variation, referred to as the Kerr nonlinearity, produces a nonlinear phase shift in the carrier wave and leads to spectral broadening of the pulse. For WDM systems, the nonlinear effects are expected to further enhance with the phase shift for a channel depends not only on the power of that channel but also on the power in the adjacent channels, the so called cross phase modulation (XPM).

In general, dispersion and nonlinearity act together along the length of the fiber. The Split Step Method obtains an approximate solution by assuming that in propagating the optical field over a small distance h , the dispersive and nonlinear effects can be pretended to act independently. More specifically, propagation from z to $z+h$ is carried out in two steps as shown in Figure 4.1. The algorithm for this model is implemented in MATLAB.

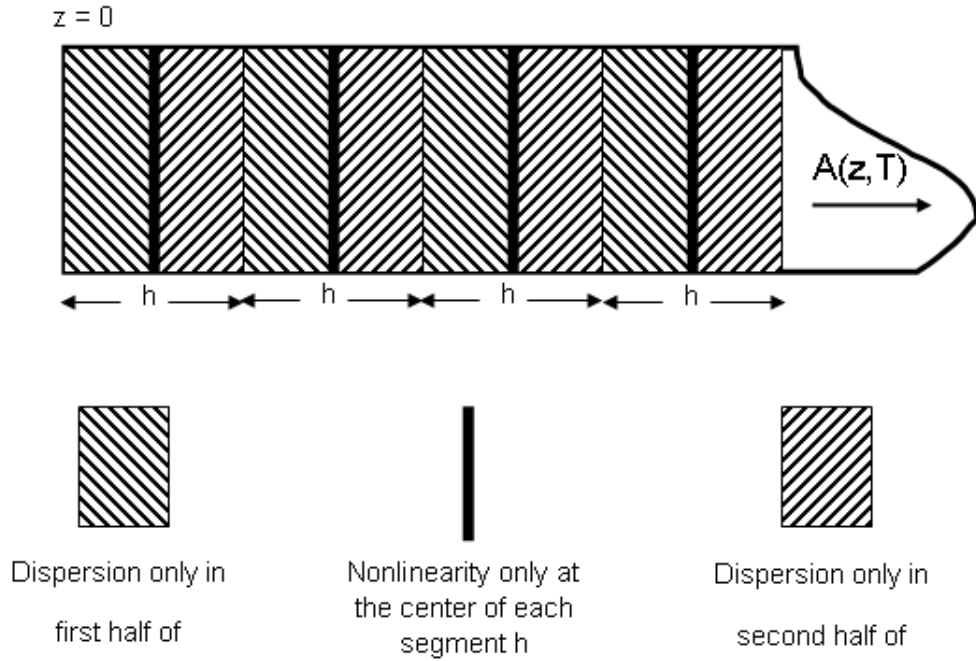


Figure 4.1: Schematic Illustration of Symmetrized Split Step Model

4.2.2 Algorithm for the Split Step Model

This algorithm is developed to synthesize the Split Step Model using the numerical methods. The algorithm is developed for the MATLAB platform.

Step 1: This step corresponds to the first half dispersion only region shown in Figure 4.1. In this process, only the dispersion (the linear operator part) acts alone and nonlinearity = 0. Thus, we have

$$A_{D1} \left(z + \frac{h}{2}, T \right) = F^{-1} \left[\exp \left(\frac{h}{2} \tilde{D}(j\omega) \right) F \{ A_o(0, T) \} \right] \dots\dots\dots(4.8)$$

where F is the Fast Fourier Transform and $A_o(0, T)$ is the optical multiplexed signals of the optical channels of different carriers or that of a single channel. The WDM signals is in fact a summation of all the electric fields representing the optical intensity channels propagated along the optical fiber transmission line. The linear operator $D(j\omega)$ is obtained by replacing differential operator by $(j\omega)$ where ω is the Fourier frequency. Thus, the equation is given by

$$\tilde{D}(j\omega) = \frac{j}{2}\beta_2\omega^2 - \frac{j}{6}\beta_3\omega^3 - \frac{\alpha}{2} \dots\dots\dots(4.9)$$

Step 2: The Split Step Model can be expressed in the following expression:

$$A(z+h, T) = \exp\left(\frac{h}{2}\tilde{D}\right) \exp\left(\int_z^{z+h} \tilde{N}(z') dz'\right) \exp\left(\frac{h}{2}\tilde{D}\right) A(z, T) \dots\dots\dots(4.10)$$

where the integral has to be evaluated more accurately by employing the trapezoidal rule and the approximated integral is given by

$$\left(\int_z^{z+h} N(z') dz'\right) \approx \frac{h}{2} \{\tilde{N}(z) + \tilde{N}(z+h)\} \dots\dots\dots(4.11)$$

However, the implementation of (4.11) is not simple since $\tilde{N}(z+h)$ is unknown at the mid segment located at $z+h/2$ as marked by thick black line in Figure 4.1. It is necessary to follow an iterative procedure that is initiated by replacing $\tilde{N}(z+h)$ by $\tilde{N}(z)$. Equation (4.10) is then used to estimate $A(z+h, T)$ which in turn to calculate the new value of $\tilde{N}(z+h)$ from (4.7). Thus, the overall algorithm of Step 2 can be expressed in the following steps:

$$A_{D1}\left(z + \frac{h}{2}, T\right) = F^{-1} \left[\exp\left(\frac{h}{2}\tilde{D}(j\omega)\right) F \{A(z, T)\} \right] \dots\dots\dots(4.12)$$

$$A_{N1}\left(z + \frac{h}{2}, T\right) = \exp\left[\frac{h}{2} \{\tilde{N}(z) + \tilde{N}(z+h)\}\right] A_{D1}\left(z + \frac{h}{2}, T\right) \dots\dots\dots(4.13)$$

$$A_{D1+N1}\left(z + \frac{h}{2}, T\right) = F^{-1} \left[\exp\left(\frac{h}{2}\tilde{D}(j\omega)\right) \cdot F \{A_{N1}\left(z + \frac{h}{2}, T\right)\} \right] \dots\dots\dots(4.14)$$

Hence, the predicted $\tilde{N}(z+h)$ is found to be:

$$\tilde{N}(z+h) = jY \left\{ \left| A_{D1+N1}\left(z + \frac{h}{2}, T\right) \right|^2 \right\} \dots\dots\dots(4.15)$$

The predicted $N(z+h)$ will be substituted into (4.13) in order to get a more accurate prediction of (4.15). Thus, this process is done iteratively.

Step 3: The predicted $N(z+h)$ would then be used to calculate the lumped region which is shown in Figure 4.1. In this process, only the nonlinear (nonlinear operator part) acts alone and $D = 0$.

$$A_{N2}\left(z + \frac{h}{2}, T\right) = \exp\left[\frac{h}{2} \{\tilde{N}(z) + \tilde{N}(z+h)\}\right] A_{D1}\left(z + \frac{h}{2}, T\right) \dots\dots\dots(4.16)$$

Step 4: This step corresponds to the second half dispersion only region shown in Figure 4.1. In this process, only the dispersion (linear operator part) acts alone and $\hat{N} = 0$. Thus, we have

$$A(z+h, T) = F^{-1} \left[\exp\left(\frac{h}{2}\tilde{D}(j\omega)\right) \cdot F \left\{ A_{N2}\left(z + \frac{h}{2}, T\right) \right\} \right] \dots\dots\dots(4.17)$$

Step 5: Repeat Step 1 by substituting $A(z+h, T)$ from equation (3.17) into $A_o(0, T)$ of (4.8) for further propagation into the next segment defined in Figure 4.1.

4.3 Eye-opening Penalty

In a digital communication link, bit error rate (BER) is the most important parameter to measure the performance of the communication link between a transmitter and a receiver. In an optical fiber communication system, BER may often be measured only experimentally. This is because the high quality performance of a conventional optical fiber communication link (BER = 10^{-9}) requires an extremely large number of bits to evaluate BER, which makes numerical simulation of BER generally impractical. BER is often evaluated indirectly using Q-factor, which is commonly used to measure system performance. Another simpler way of estimating performance is to observe eye-opening. The eye-opening is quantified by measuring the minimum value between the sampled values of marks (ones) and spaces (zeros) in the received bit sequence, $r(t)$. The eye opening is a useful system performance metric when signal distortion is a more limiting factor than noise. Mathematically, it is defined as below [30].

$$Eye - opening = \frac{\min(r_j(t_j, b=1)) - \max(r_j(t_j, b=0))}{\sqrt{P_o}} \dots\dots\dots(4.18)$$

where t_j represents the sampling instant of the j^{th} -bit interval and P_o is the peak power of $r(t)$. The first term in the numerator represents the minimum value at the sampling instant when a mark is transmitted, and the second term is the maximum value when a space is transmitted. In this chapter, the sampling instant of the received signal is assumed to be at the center of each bit period.

To assess system performance degradation due to signal transmission through the fiber, eye-opening penalty (EOP) is often used. EOP is the measure of the relative eye opening after

transmission compared to eye opening in the back-to-back case (no transmission effect). That is,

$$EOP(dB) = -10\log \left[\frac{EOAT}{EOBB} \right] \dots\dots\dots(4.19)$$

where EOAT and EOBB denote eye-opening after transmission (with fiber) and eye-opening back-to-back (without fiber) respectively. EOP will be used in this paper to quantify the system performance.

4.4 Filter Design

There are several methods commonly used to design filter, such as Butterworth, Chebyshev and Elliptic filter designs. Amongst these, Butterworth response is normally called the "maximally flat" response with minimum ripple in the passband and stopband region. Its magnitude squared function is defined by:

$$|H_{LP}(j\omega)|^2 = \frac{1}{1+(\frac{\omega}{\omega_c})^{2N}} \dots\dots\dots(4.20)$$

N is the order of the filter and ω_c is the cutoff frequency where the filter magnitude is $\frac{1}{\sqrt{2}}$ times the dc gain at $\omega = 0$, which is also 3 dB cutoff. For a cutoff or critical frequency of 1, the result is called a normalized prototype lowpass filter. Cutoff frequency of 1 is used in the simulations of this paper. For Butterworth filter responses, the poles of $H_{LP}(s)H_{LP}(-s)$ are the roots of:

$$(-1)^N s^{2N} = -1 = e^{j(2k-1)\Pi} \quad k=0,1,2,\dots,2N-1 \dots\dots\dots(4.21)$$

Therefore, the poles of S_k are given by

$$S_k = e^{j\left[\frac{(2k+N-1)}{2N}\right]\Pi} \quad k=0,1,2,\dots,2N \dots\dots\dots(4.22)$$

S_k is also expressed as $S_k = \sigma_k + j\omega_k$, where the real and imaginary parts are given by:

$$\sigma_k = \sin\left(\frac{2k-1}{N}\right)\frac{\Pi}{2}, \omega_k = \cos\left(\frac{2k-1}{N}\right)\frac{\Pi}{2} \dots\dots\dots(4.23)$$

With (4.22) and (4.23), the transfer function of the Butterworth lowpass prototype response for specific order could easily be found out. The magnitude and phase response of a Butterworth lowpass filter with $N = 2$, $f_c = 1$ and sampling frequency of $1000 \times f_c$ are shown in Figure 4.2 and Figure 4.3.

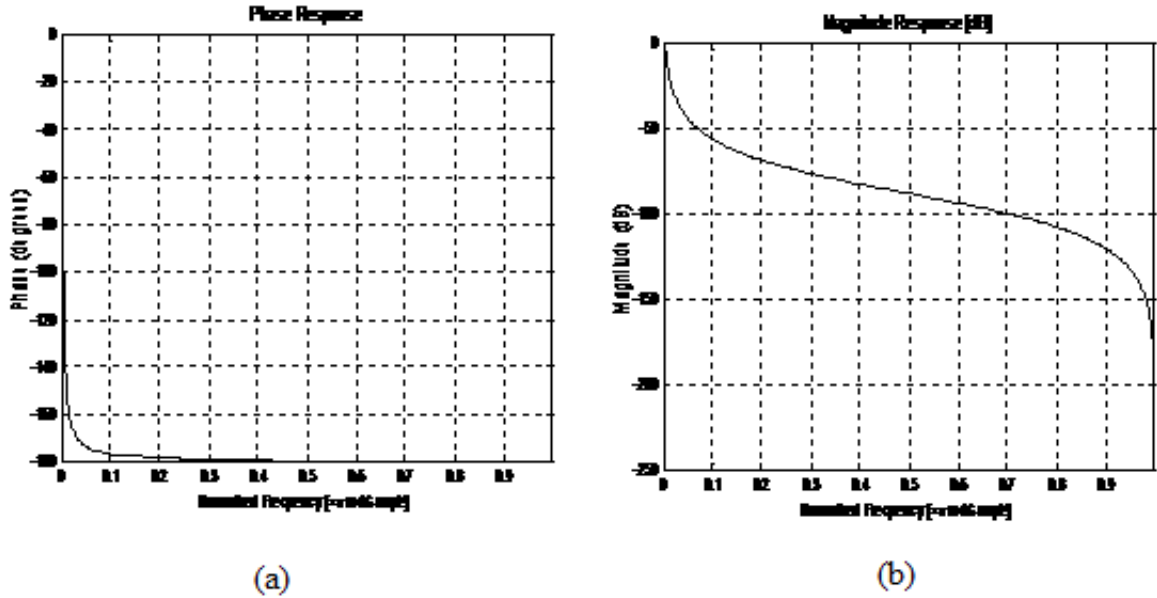


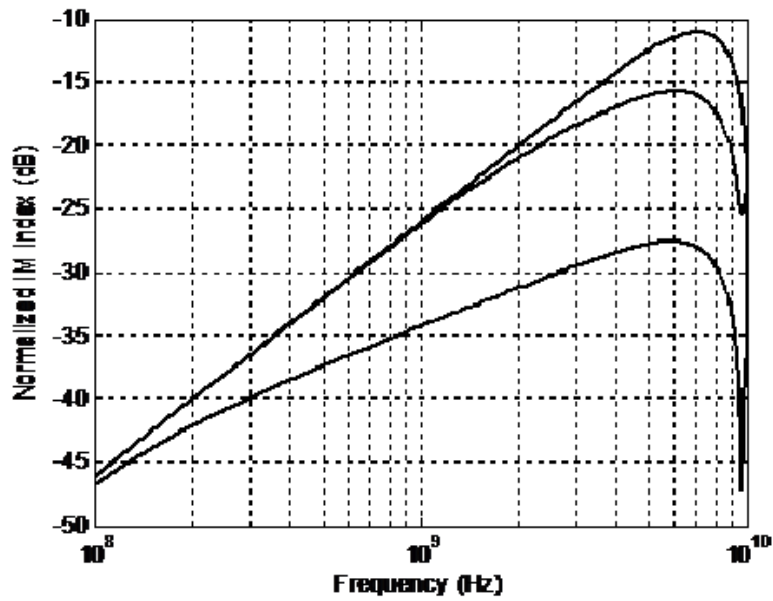
Figure 4.2: (a) Frequency and (b) Magnitude Response of a Butterworth Lowpass Filter

4.5 Simulation Results for XPM in the DWDM System

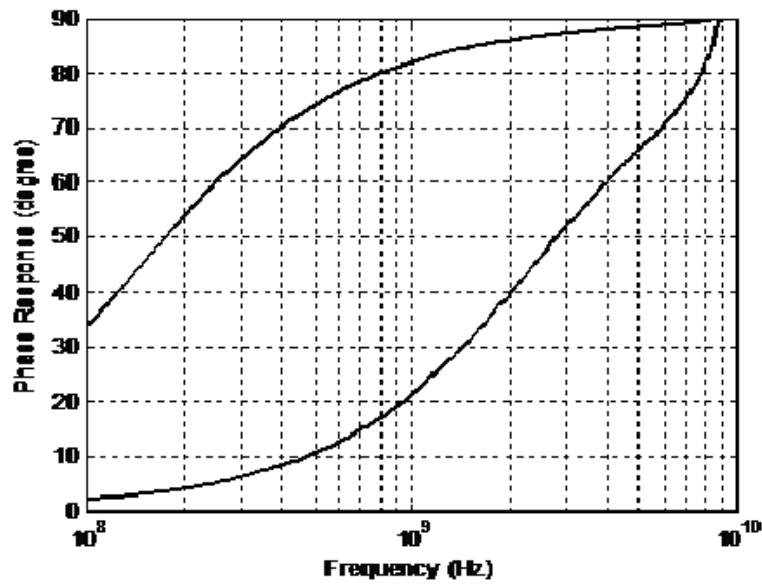
In this section, first, the reader is introduced to the effect of XPM induced phase shift considering the pump-probe approach. The XPM effects will be shown for different probe power, pump power, distance, channel separation and bit rates. Then line code will be applied for the same parameters to visualize its effect on XPM. Thereafter the allowable probe and pump power will be found out for the BER of 10^{-9} with and without line code to quantify the improvement in power penalty achieved by the application of the line code. At last a two channel DWDM system will be examined to verify the effects of XPM by applying 1024 bit sequence with and without line code where eye penalty will be applied to verify the effect of the XPM.

For a consistent and gradual development of the study some of the parameters are kept unchanged. The bit pattern used is PRBS 512 bits, nonlinear refractive index (n_2) is $2.6 \times 10^{-20} \frac{m^2}{W}$ and fiber core effective area (A_{eff}) is $5.28e^{-11} m^2$. According to Equation (3.33) that the XPM induced power depends on factors such as probe power, pump power, distance, channel separation, bit rate, etc. Normalized IM index and phase response due to XPM for the channel separations of 0, 0.25 and 4 nm; the average power per channel is 0 dBm, $\lambda_1=1550$ nm, $D = 17$ ps/km-nm, $Y_1 = 1.18W^{-1} \cdot km^{-1}$, $\alpha = 0.21$ dB/km and $L = 80$ km are depicted in Figure 4.3

Figure 4.4 and 4.5 shows the total XPM induced power for analytical and simulated approach in a lossless system. Figure 4.4 exhibits XPM induced power for a range of pump power with probe power $P_1 = 0$ dBm. Bit rate = 10 GHz, channel spacing = 50 GHz and fiber length = 50, 100 and 150 km. Figure 4.5 exhibits XPM induced power for a range of probe power with probe power $P_1 = 0$ dBm. Bit rate = 10 GHz, channel spacing = 50 GHz and fiber length = 50, 100 and 150 km. These two figures show that the XPM induced power increases proportionately with distance and input powers which conforms to the Equation (3.33).

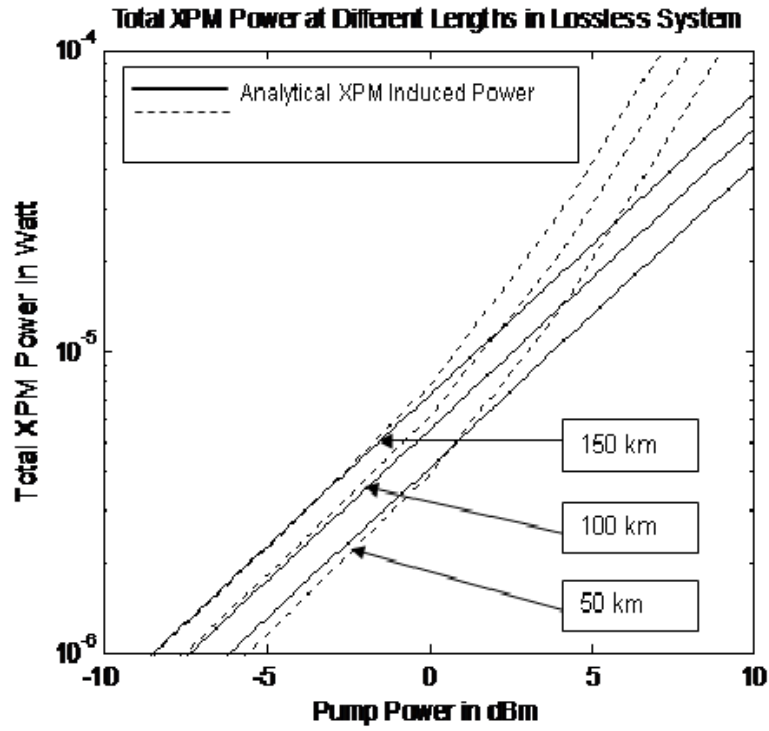


(a)

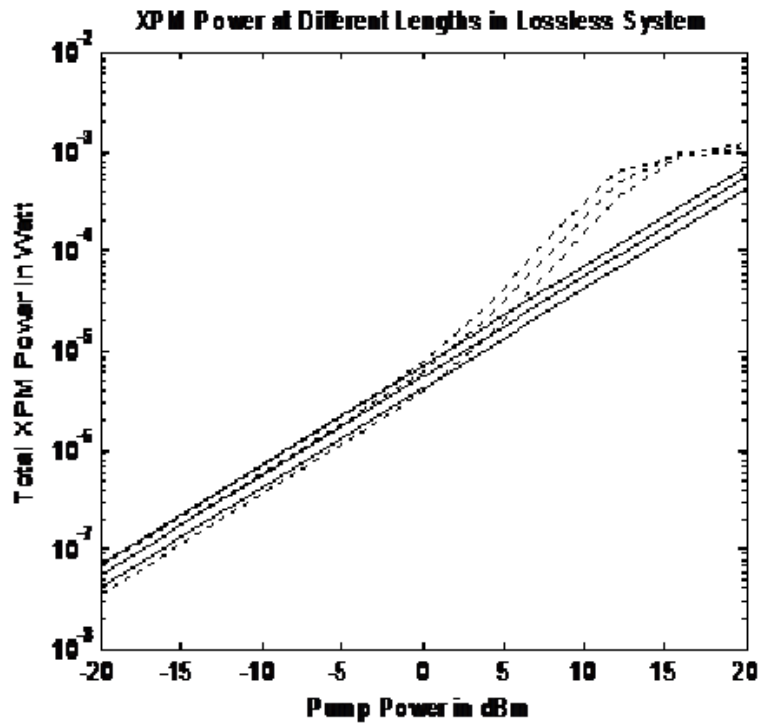


(b)

Figure 4.3: (a) Normalized IM index in dB and (b) phase response versus the pump modulation frequency for the channel separations of 0, 0.25 and 4 nm. The average power per channel is 0 dBm. Here $\lambda_1=1550$ nm, $D = 17$ ps/km-nm, $Y_1 = 1.18W^{-1} \cdot km^{-1}$, $\alpha = 0.21$ dB/km and $L = 80$ km.



(a)



(b)

Figure 4.4: Total XPM induced power in a lossless system with probe power $P_1 = 0$ dBm, bit rate = 10 GHz, channel spacing = 50 GHz and fiber length = 50, 100 and 150 km for pump power (P_2) = (a) -20 to 20 and (b) -10 to 10 dBm

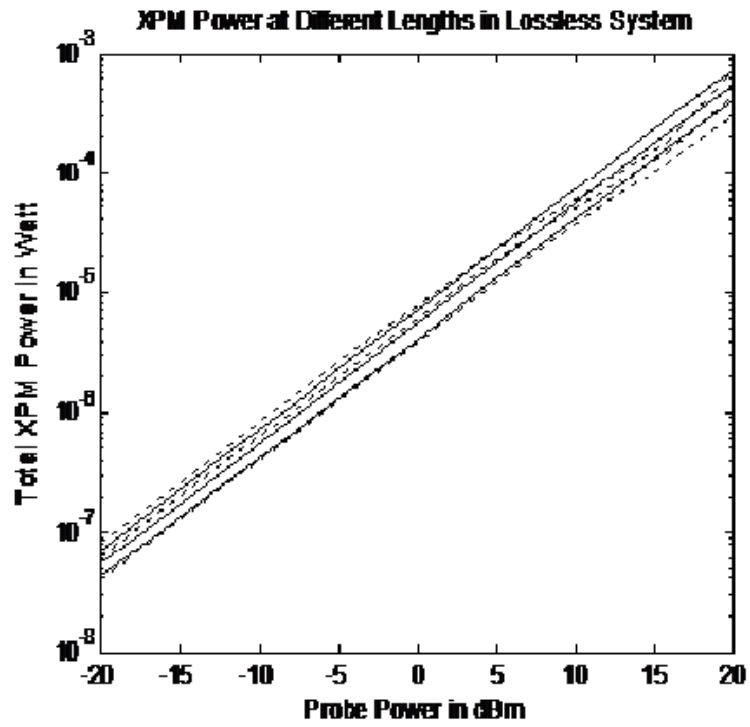
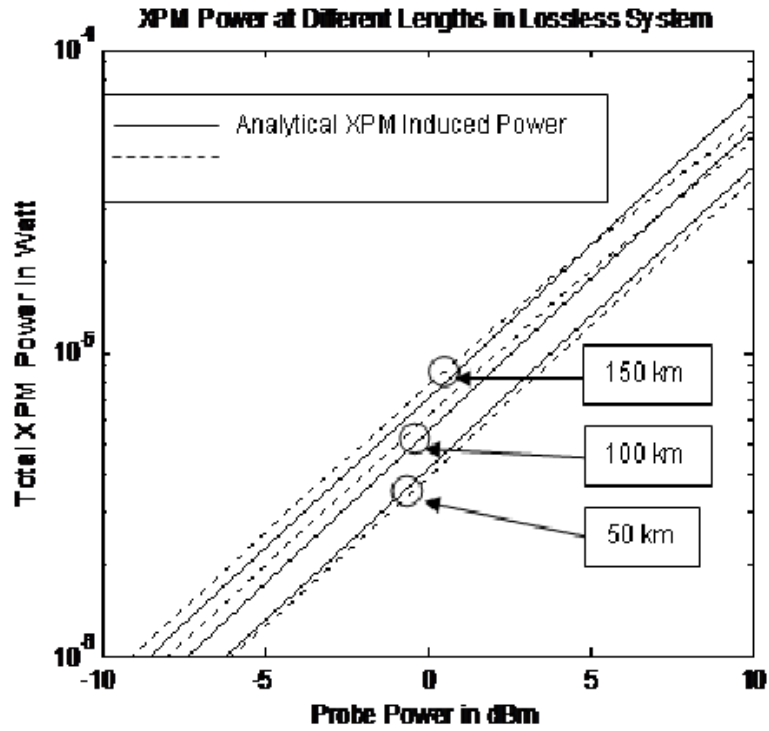


Figure 4.5: Total XPM induced power in a lossless system with pump power $P_2 = 0$ dBm, bit rate = 10 GHz, channel spacing = 50 GHz and fiber length = 50, 100 and 150 km for probe power (P_1) = (a) -20 to 20 and (b) -10 to 10 dBm

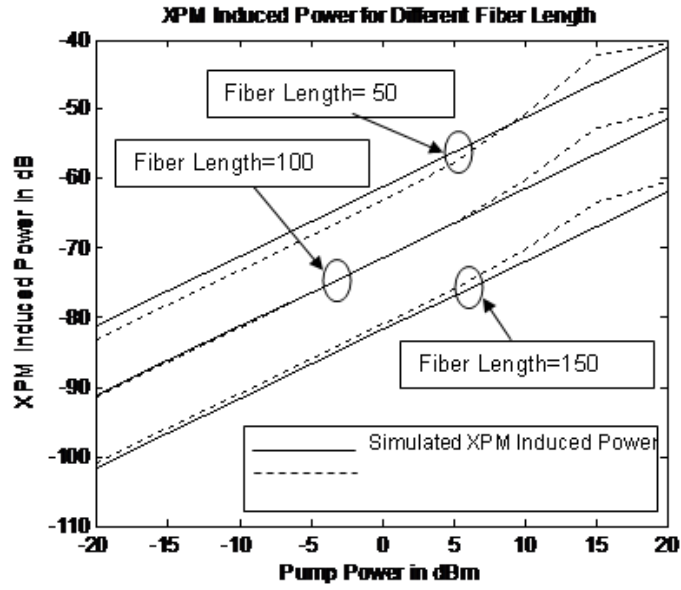
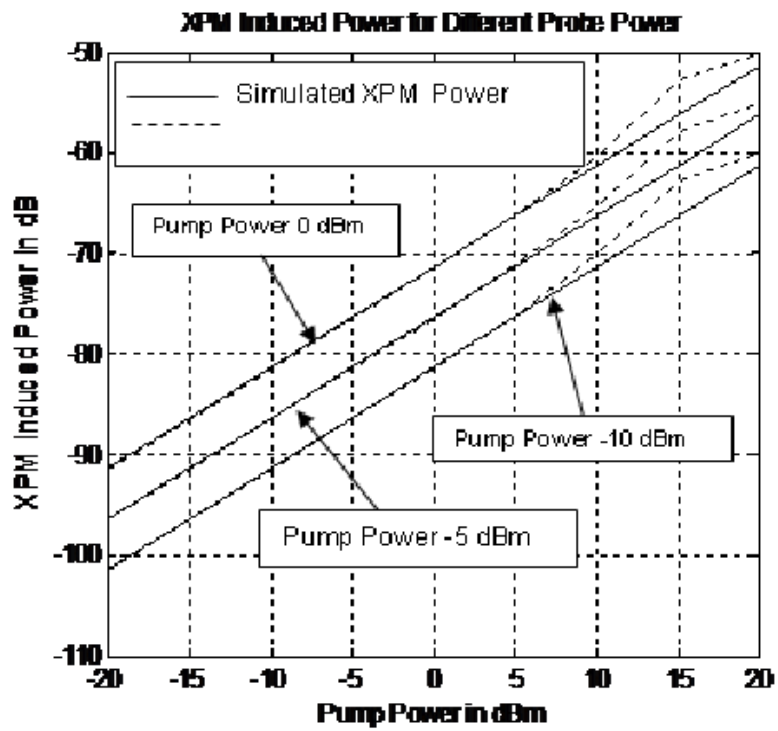


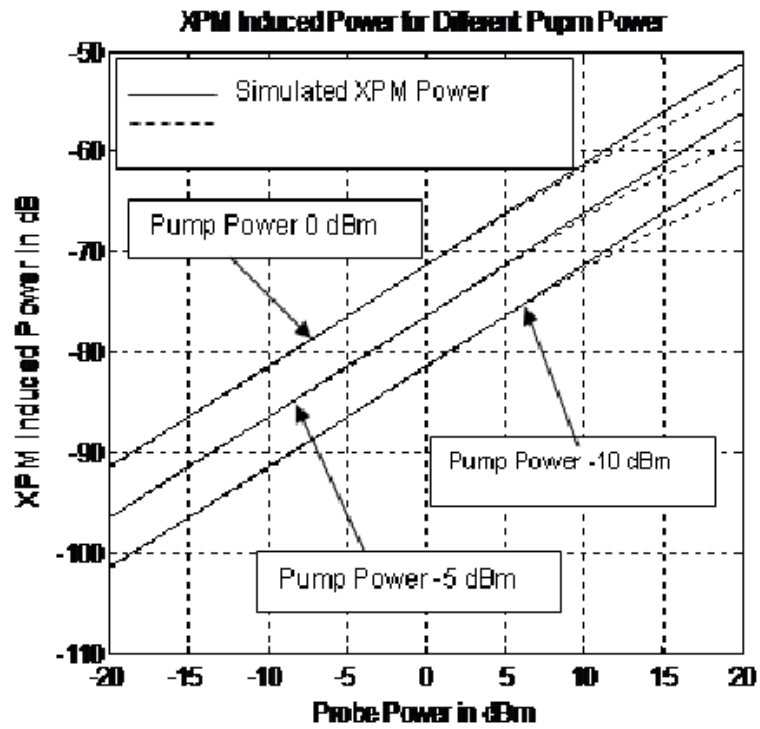
Figure 4.6: Total XPM induced power for a lossy system with probe power $P_1 = 0$ dBm, bit rate = 10 GHz, channel spacing = 50 GHz and fiber Length = 50, 100 and 150 km

Figure 4.6 shows analytical and simulated XPM power for a lossy system ($\alpha > 0$) for different lengths with probe power $P_1 = 0$ dBm, bit rate = 10 GHz and channel spacing = 50 GHz. This figure conforms to Figure 4.3 and 4.4 which was lossless, with the difference that total XPM induced power for a particular input pump power decreases proportionately with distance. This phenomenon is due to the reason that the input powers at higher distances gets decreased due to loss effect and so as to the induced XPM power due to those input powers.

Figure 4.7 shows total XPM power in dB for different probe and pump powers at 100 km, bit rate = 10 GHz and channel spacing = 50 GHz. Here also the figure conforms to the mathematical expression of Equation (3.33). The XPM induced power increases proportionately with input powers, the higher the input power either probe power or pump power the more is the XPM induced power.



(a)



(b)

Figure 4.7: Total XPM power in dB for different (a) probe powers (0, -5 and -10 dBm) and (b) pump powers (-10, -5 and 0 dBm) at 100 km

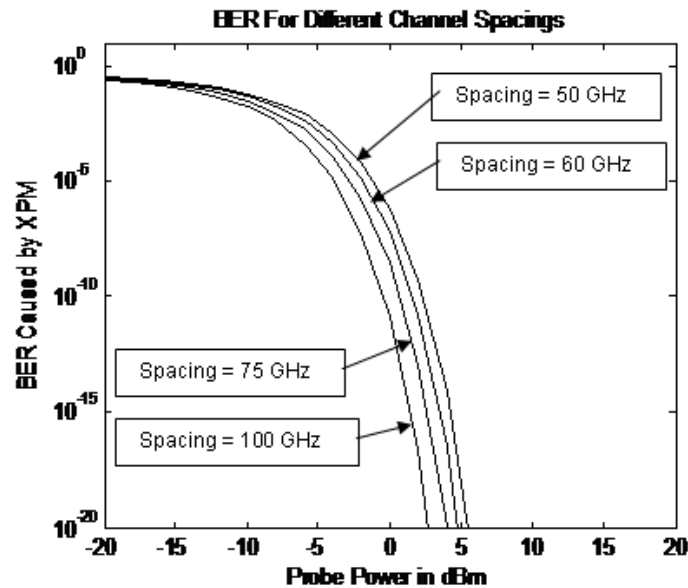


Figure 4.8: Plot of BER for channel spacing 50, 60, and 75 and 100 GHz with $P_2 = 0$ dBm, fiber length = 100 km and bit rate = 10 GHz

Figure 4.8 shows the Plot of BER for channel spacing 50, 60, and 75 and 100 GHz with $P_2 = 0$ dBm, fiber length = 100 km and bit rate = 10 GHz. The figure shows that with lower channel spacing the BER increases.

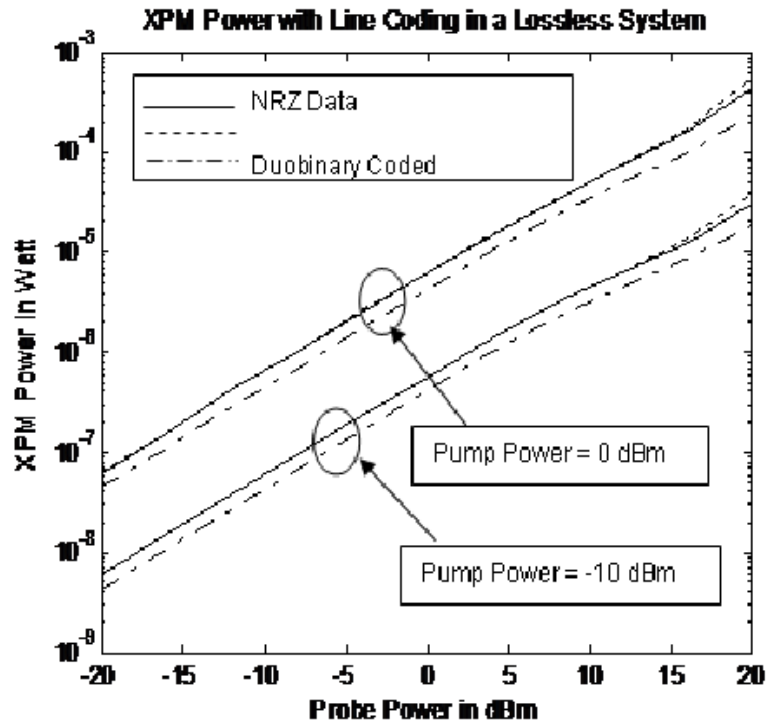
Figure 4.9 shows XPM Power with line coding for both analytical and simulated result for different pump and probe powers. Figure 6.7 shows a very important finding that the XPM induced power is less for Novel line coded scheme. Two coding schemes are applied in this simulation. It is evident from the plot that the application of duobinary coding does not reduce the XPM much but the Novel Order one coding scheme shows a remarkable reduction of XPM induced power.

In Figure 4.10 the analytical and simulated BER for different probe powers at 100 km with bit rate = 10 GHz and channel spacing = 50 GHz exhibits an important characteristics of XPM. It is evident from Equation (3.17) that the influence of pump power is more than the probe power. The analytical and simulated results show similar pattern of the curves in terms of shape and related values are also without much discrimination. It is very clear from the plot that when the probe power is low in comparison with the pump power, the BER is more. As the probe power is increased the BER also reduced. From this figure we can conclude that the BER due to XPM will be more if the probe power is less in comparison

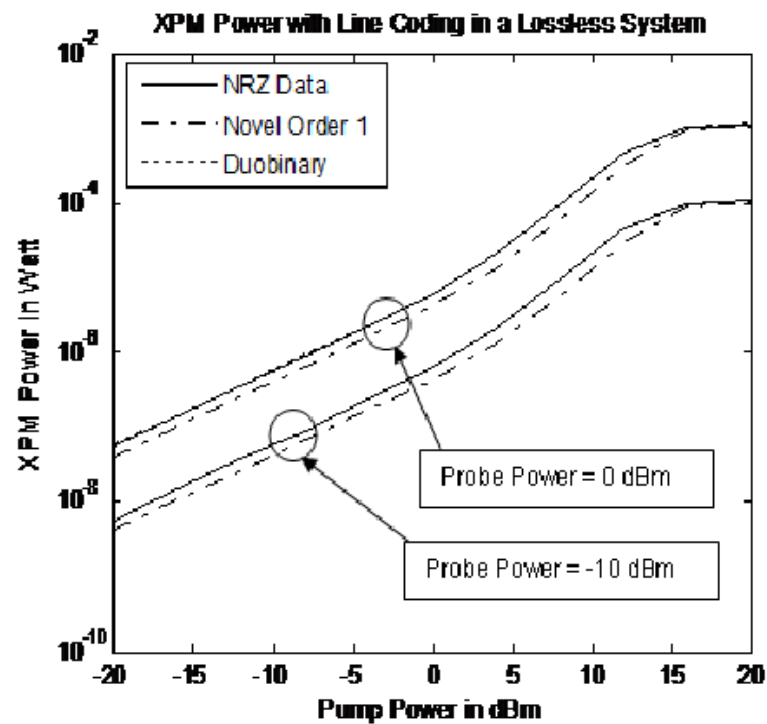
with the pump power.

In Figure 4.11 the analytical and simulated BER for different pump powers at 100 km with bit rate = 10 GHz and channel spacing = 50 GHz exhibits another important characteristics of XPM induced power and the related effects. It is evident from Equation (3.17) that the probe power contributes directly to the XPM. Here also the analytical and simulated results show similar pattern of the curves in terms of shape and related values are also without much disagreement. It is very clear from the plot that when the pump power is low in comparison with the probe power, the BER is also low. As the pump power is increased the BER also increases. From this figure we can conclude that the BER due to XPM will be more if the pump power is more in comparison with the probe power.

Figure 4.12 shows the effect of the application of line coding scheme in a DWDM system with bit rate of 10 GHz, channel spacing of 50 GHz and fiber length of 100 km. XPM induced power and BER caused by XPM with for different probe powers for NRZ data, Duobinary code and Novel Order 1 code shows that Novel Order 1 code could successfully reduce the XPM induced power and in the same token the BER also reduced. Figure 4.13 shows exhibits the same characteristics for different pump powers.

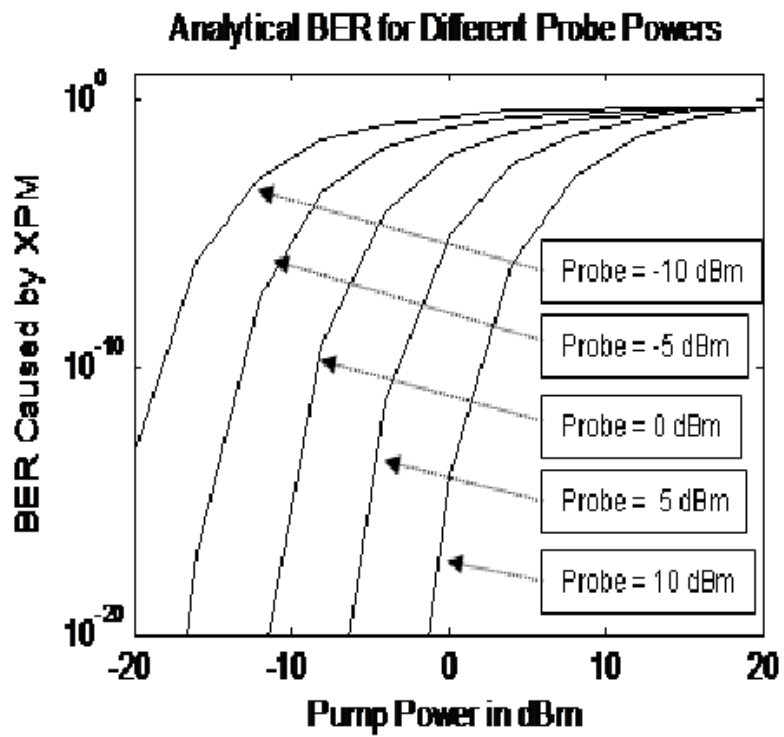


(a)

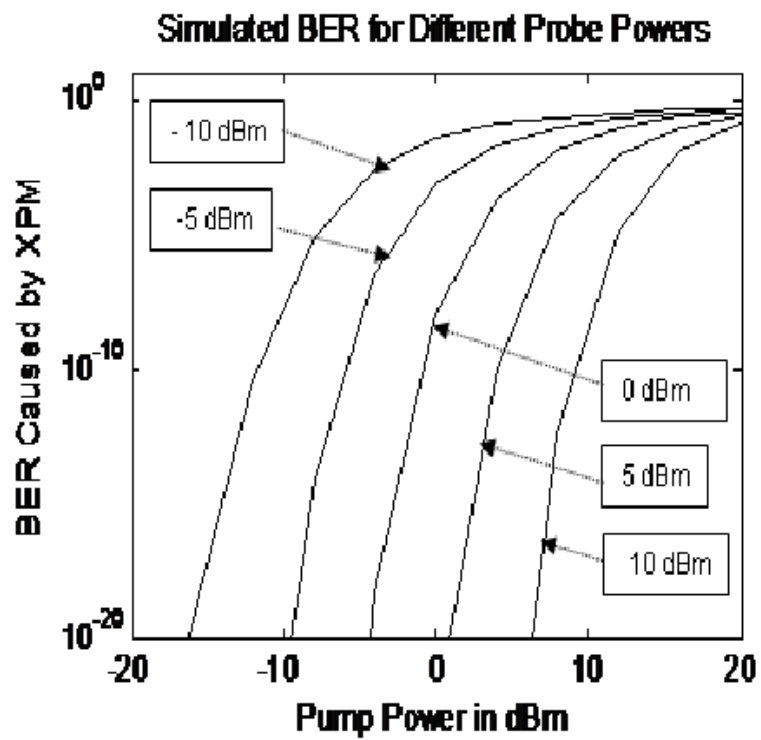


(b)

Figure 4.9: XPM Power with line coding, (a) analytical result for pump power = -10 and 0 dBm and (b) simulated result for probe power = -10 and 0 dBm with fiber length = 100 km, bit rate = 10 GHz and channel spacing = 50 GHz

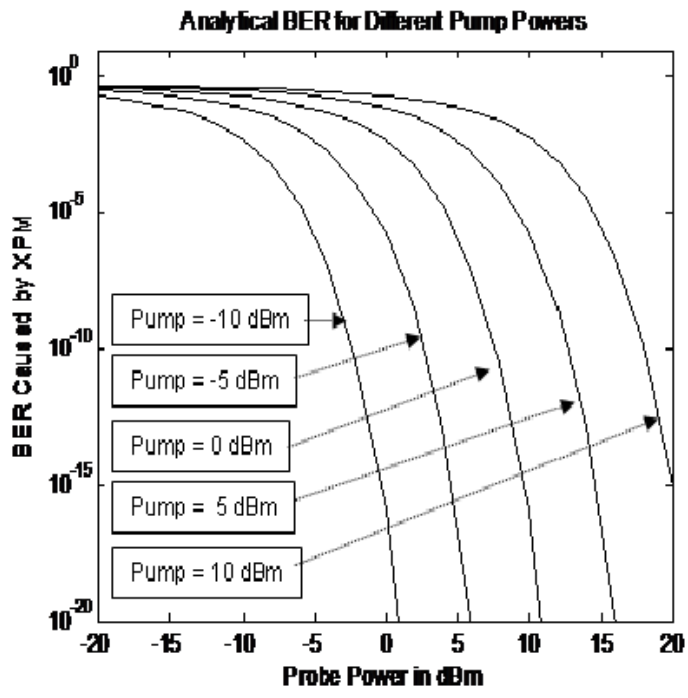


(a)

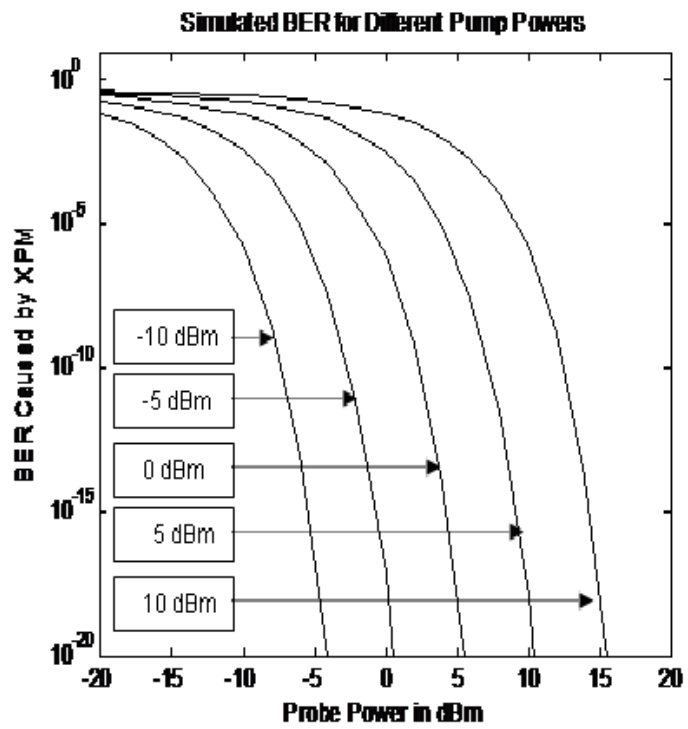


(b)

Figure 4.10: (a) Analytical (b) Simulated BER for different probe powers -10, -5, 0, 5 and 10 dBm at 100 km with bit rate = 10 GHz and channel spacing = 50 GHz

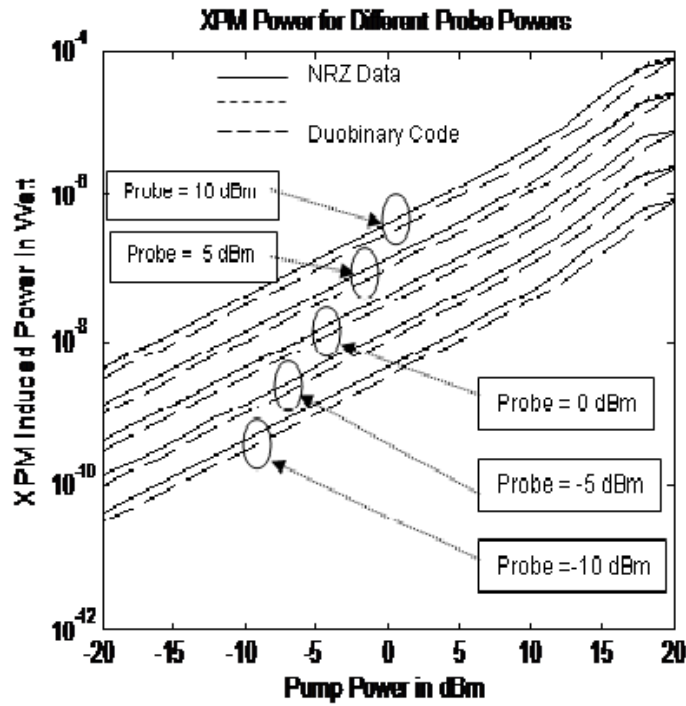


(a)

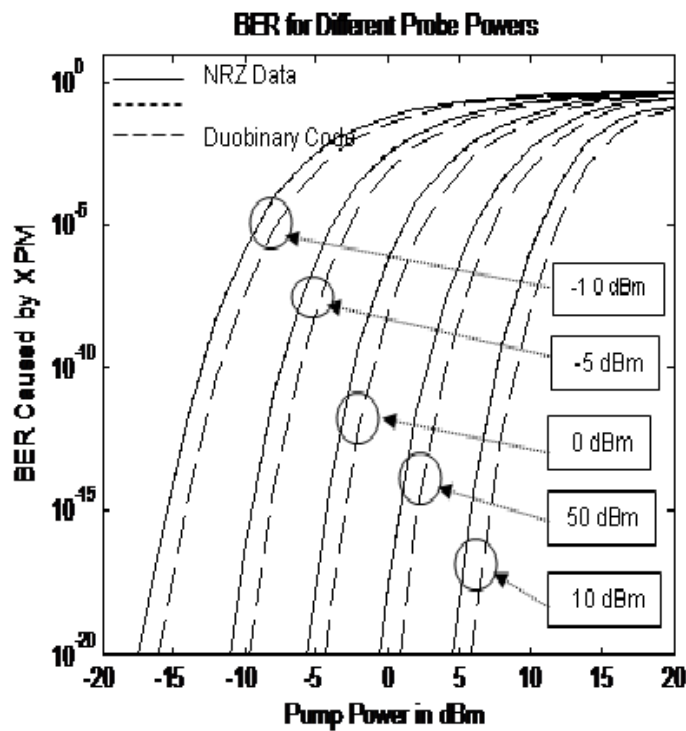


(b)

Figure 4.11: (a) Analytical (b) Simulated BER for different pump powers -10, -5, 0, 5 and 10 dBm at 100 km

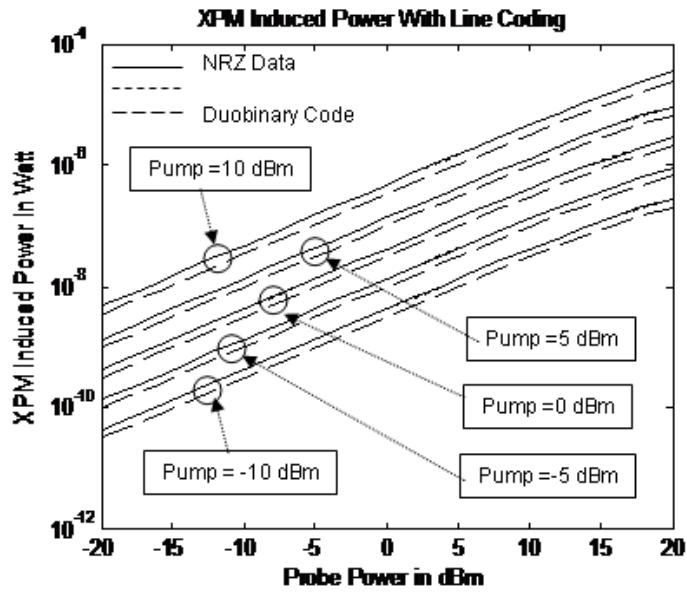


(a)

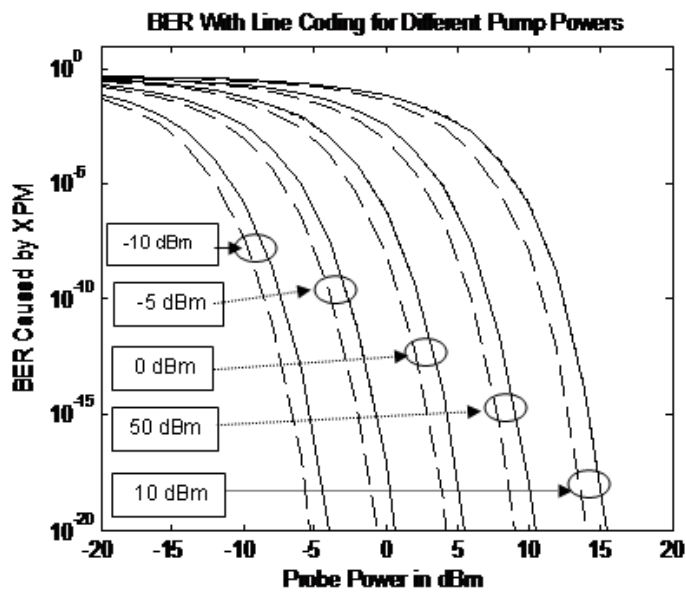


(b)

Figure 4.12: Plot of (a) XPM induced power and (b) BER caused by XPM with NRZ data, Duobinary and Novel Order 1 Code for probe power -10, -5, 0, 5 and 10 dBm for 100 km fiber



(a)



(b)

Figure 4.13: Plot of (a) XPM induced power and (b) BER caused by XPM with NRZ data, Duobinary and Novel Order 1 Code for pump power -10, -5, 0, 5 and 10 dBm for 100 km fiber

Figure 4.14 shows the allowable pump power at different distances applying line codes. Table 4.1 quantifies the allowable pump power. It is evident from Figure 4.14 that with Novel Order 1 code, the allowable pump power is more for the same BER. Table 4.1 shows that the improvement is about 1.29 dB. This improvement is the main finding of this study.

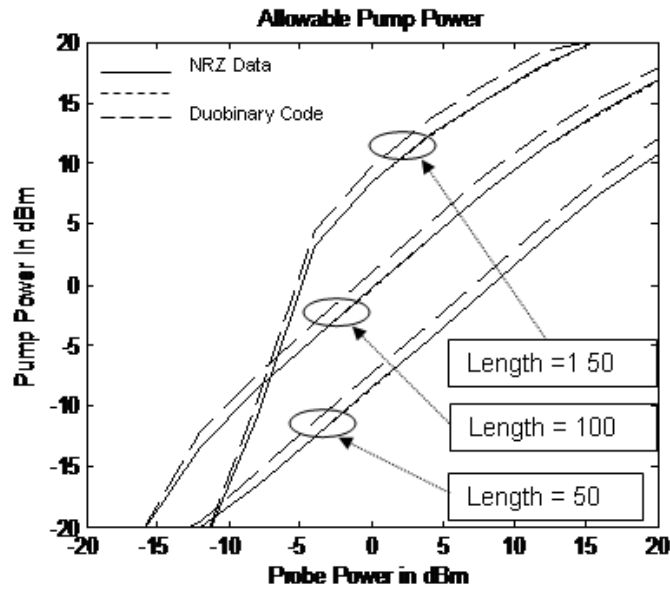


Figure 4.14: Plot of allowable pump power for BER of 10^{-9} at 50, 100 and 150 km

Table 4.1: Improvement in allowable pump power in dB by applying Novel line code in comparison with NRZ data for BER of 10^{-9} at different lengths

Length	-20	-16	-12	-8	-4	0	4	8	12	16	20
50	0	0	0.563	1.290	1.291	1.290	1.289	1.288	1.284	1.271	1.254
100	0	.238	1.293	1.292	1.291	1.29	1.287	1.281	1.266	1.253	1.23
150	0	0	0	1.286	1.288	1.282	1.271	1.249	1.2	0	0

Figure 4.15 shows the allowable probe power at different distances applying line codes. Table 4.3 quantifies the allowable probe power. It is evident from Figure 4.15 that with Novel Order 1 code, the allowable probe power is decreased for the same BER. Table 4.2 shows that the improvement is about 1.3 dB with maximum improvement of 1.89 dB at 100 km. It is also evident that the improvement is not the same for all the combinations of power. This improvement is also the main finding of this study. Figure 4.16-18 shows the simulated

eye diagram of probe channel for 512 PRBS data.

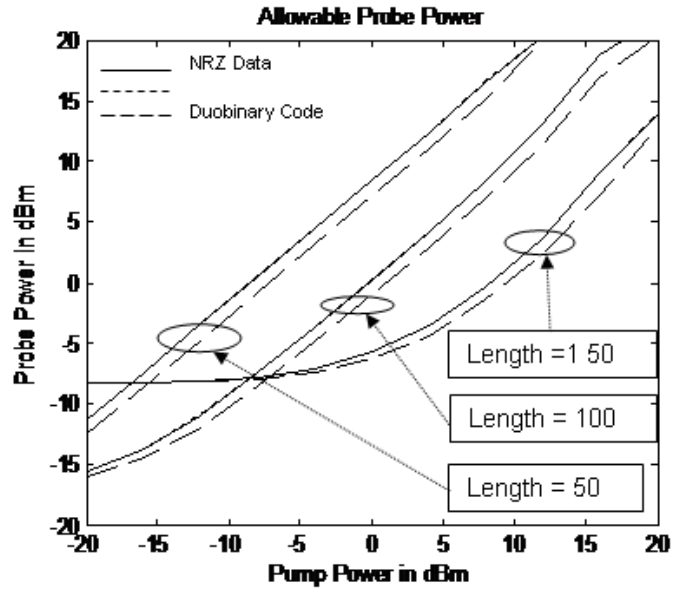
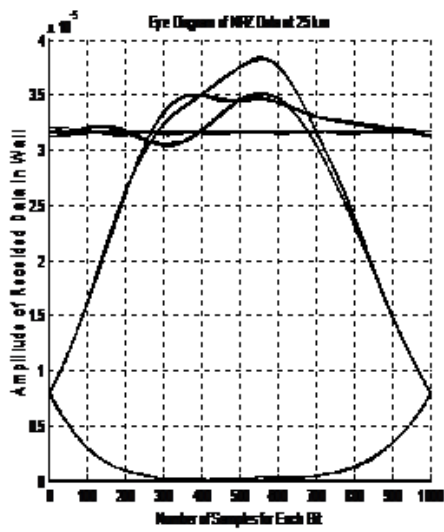


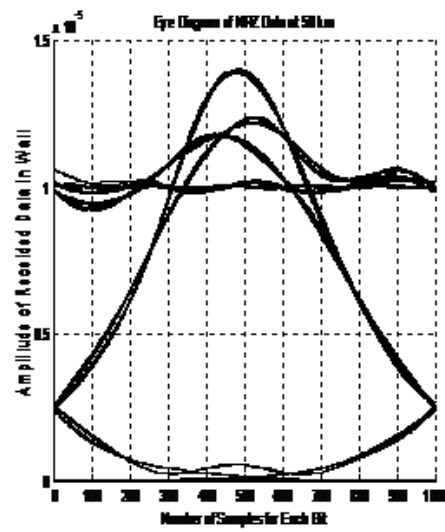
Figure 4.15: Plot of allowable probe power for BER of 10^{-9} at 50, 100 and 150 km

Table 4.2: Improvement in allowable probe power in dB by applying Novel line code in comparison with NRZ data for BER of 10^{-9} at different lengths

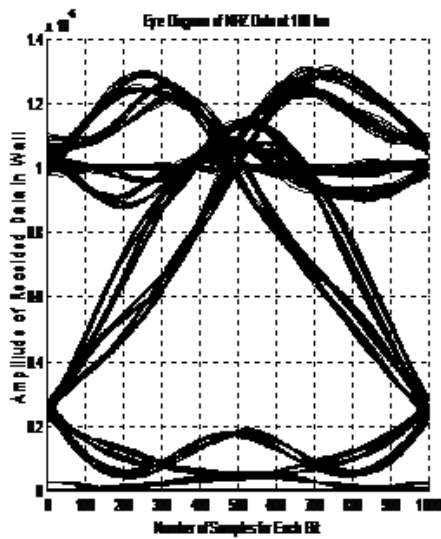
Length	-20	-16	-12	-8	-4	0	4	8	12	16	20
50	1.193	1.267	1.28	1.285	1.27	1.269	1.26	1.38	0.444	0	0
100	0.376	0.698	1.00	1.168	1.24	1.268	1.28	1.33	1.595	1.89	1.34
150	0.008	0.022	0.05	0.127	0.27	0.525	0.82	1.09	1.422	1.81	0.94



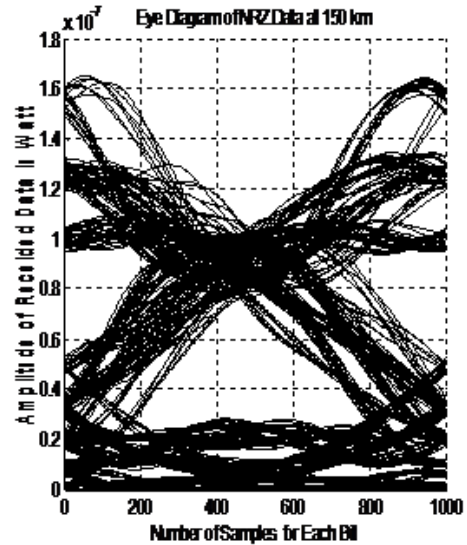
(a)



(b)

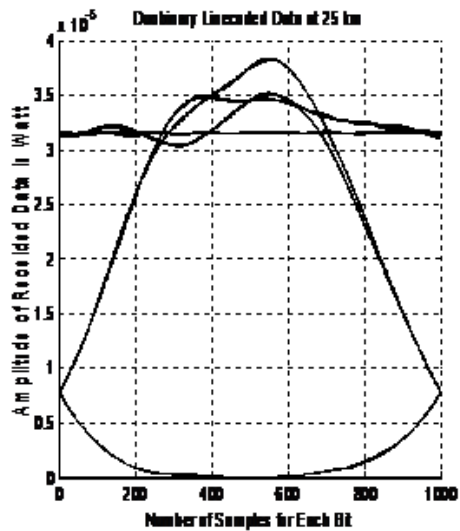


(c)

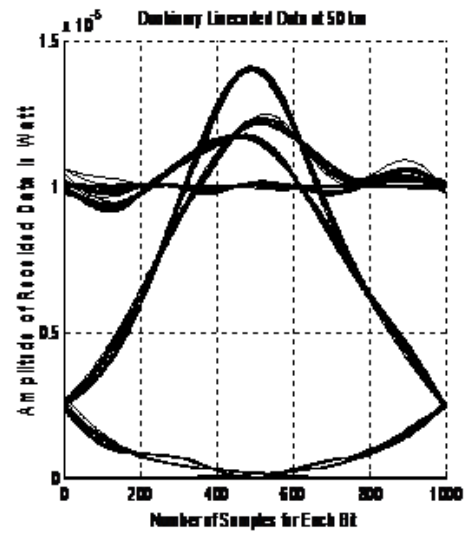


(d)

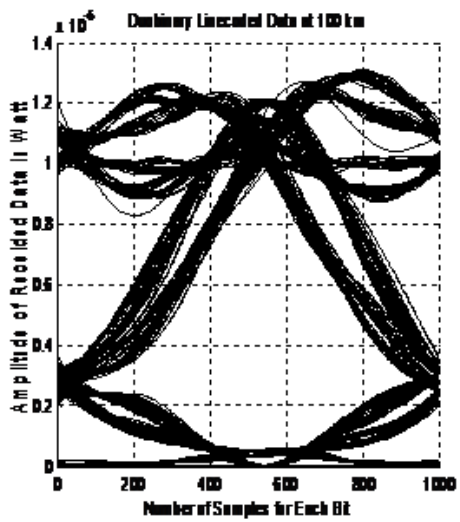
Figure 4.16: Plot of 512 bit (PRBS) eye-power penalty of NRZ data for 25, 50, 100, and 150 km



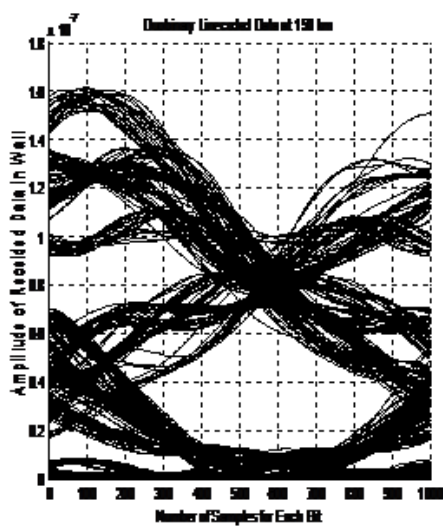
(a)



(b)

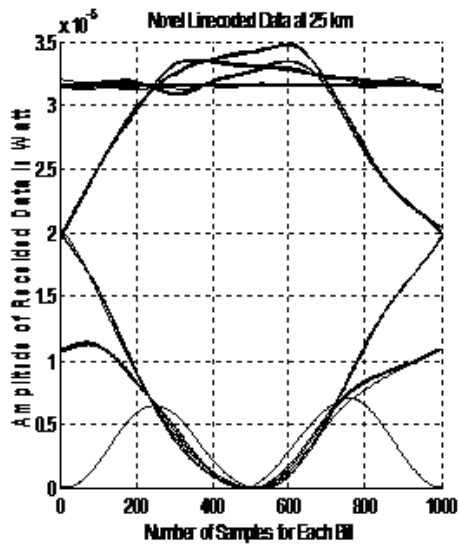


(c)

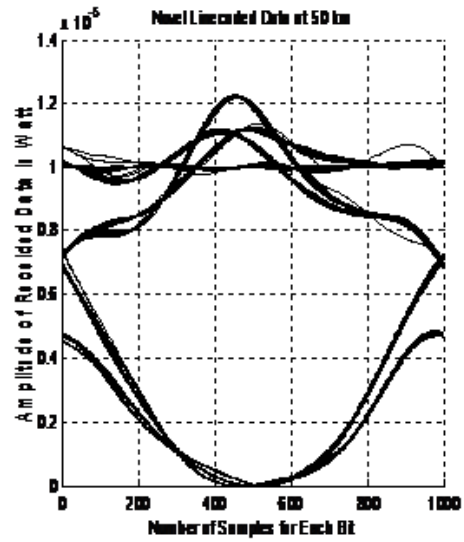


(d)

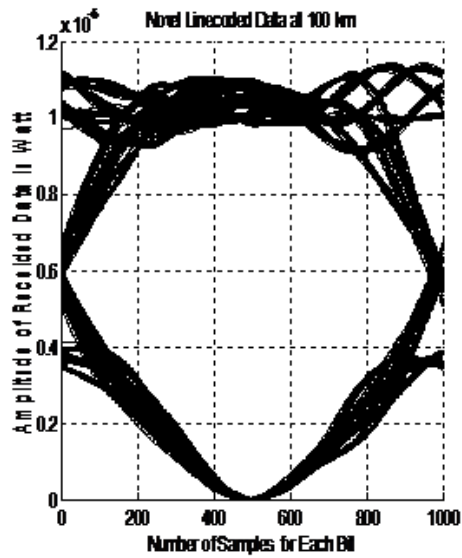
Figure 4.17: Plot of 512 bit (PRBS) eye-power penalty of Duobinary coded data for 25, 50, 100 and 150 km



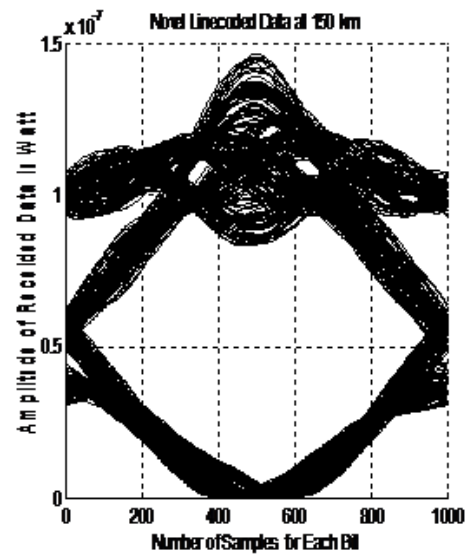
(a)



(b)



(c)



(d)

Figure 4.18: Plot of 512 bit (PRBS) eye-power penalty of Novel Optical coded data for 25, 50, 100 and 150 km

Table 4.3: Eye power penalty for pump power of 0 dBm and probe power of -10 dBm

Length of Fiber in km	25	50	75	100	125	150
NRZ Data	4.6257	9.3113	14.5882	20.0822	25.5588	30.8877
Duobinary	4.6157	9.2144	14.5235	19.7558	25.3566	30.8043
Vovel Code	4.8264	9.5936	15.0597	19.8245	24.5400	29.5663

Table 4.3 also shows that the improvement obtained by using the Novel Order 1 code, is about 1.3 dB which conforms to the allowable probe and pump power improvement. Thus we can conclude here that the application of multilevel optical line code especially the Novel Optical code is effective in combating the effect of XPM. It gives an improvement of about 1.3 dB in terms of pump or probe power.

4.6 Combating XPM by Dispersion Management

Cartaxo [9] showed that XPM-induced IM in fiber links with multiple optical amplifiers can be enhanced or reduced by properly arranging the dispersion characteristics in each fiber segment of a multiple segment fiber system. In a non-dispersion compensated amplified link and for weak walk-off effect, the total XPM induced IM increases approximately with the square of the number of fiber segments and of modulation frequency. However, if the dispersion is compensated for within each fiber segment the total XPM induced IM increases proportionately to the number of fiber segments and to the square frequency.

4.7 Discussions

There are many texts where efforts are taken to reduce optical nonlinear effects as a whole including FWM, SPM and XPM by managing the dispersion. But, to the best knowledge of this author, there is no text reported so far that directly quantifies the reduction of XPM effect alone in terms BER and input powers. Cartaxo [9] discussed an approach to combat XPM by dispersion management in links with multiple fiber segments in terms of XPM index. The improvement in XPM index does not provide any indication about the power penalty or BER. But this paper addresses the XPM effect in a single segment by reducing it applying line coding schemes without dispersion management. Hence, the findings of

this paper could not be compared with the findings of similar kind which could help better establish the findings of this study.

4.8 Summary

This section presented the simulated expressions of XPM in the MATLAB environment. Different parameters related to XPM are also presented. Parameters like the input powers in probe and pump channel, channel spacing and bit rate are discussed here showing their effects on XPM. Two line codes are applied here. They are duobinary and Novel optical coding. For performance evaluation two methods are applied. They are BER calculation and eye-power penalty determination. For calculating BER, the input in the probe channel was a CW signal and the input in the pump channel was spaces for "0" and rectangular pulses for "1". For calculating the eye-power penalty, both probe and pump channel inputs were spaces for "0" and rectangular pulses for "1". Finally the result shows that maximum 1.89 dB improvement can be achieved by using the Novel optical line code whereas the duobinary coding did not show mentionable improvement. However, the findings of this study could not be compared with the findings of same kind as such findings are not reported so far.

4.9 Simulation for PMD in the DWDM System

The effect of PMD in a fiber link and the compensation of PMD by using an optical compensation technique is simulated using OptSim 5.3. The effect of PMD in an optical fiber link and an optical compensation technique is analyzed through various eye diagrams and optical Spectrum for receptions and transmission by performing several parametric runs. A parametric run is performed to simulate the time varying property of the emulator. The eye diagrams give the Q values at each run, from which the results can be interpreted.

4.10 Simulation Results for PMD in the DWDM System

We have performed three simulations; simulation-1 one with varying dispersion, simulation-2 with varying PMD coefficient and simulation-3 with the combination of varying both dispersion and PMD co-efficient. We have considered length of cable to be 100 km, fiber non-linearity co-efficient 3.0, non-linear refractive index $5e^{20}$, band gap between two carrier

50 GB, bit rate 10 GB, low power -30 dBm and high power to be -10 dBm. The results of the two simulations are shown below [33].

4.10.1 Simulation with Varying Dispersion

Table 4.4: Simulation 1 with varying dispersion keeping other factors constant

Run	1	2	3	4	5
Dispersion	0.0	1.0	2	3	4
BER	0.02227501	0.00759213	0.000748404	$1.32446e^{-5}$	$8.92931e^{-10}$
Q Value	6.0206	7.463510	9.911912	12.561970	15.541085

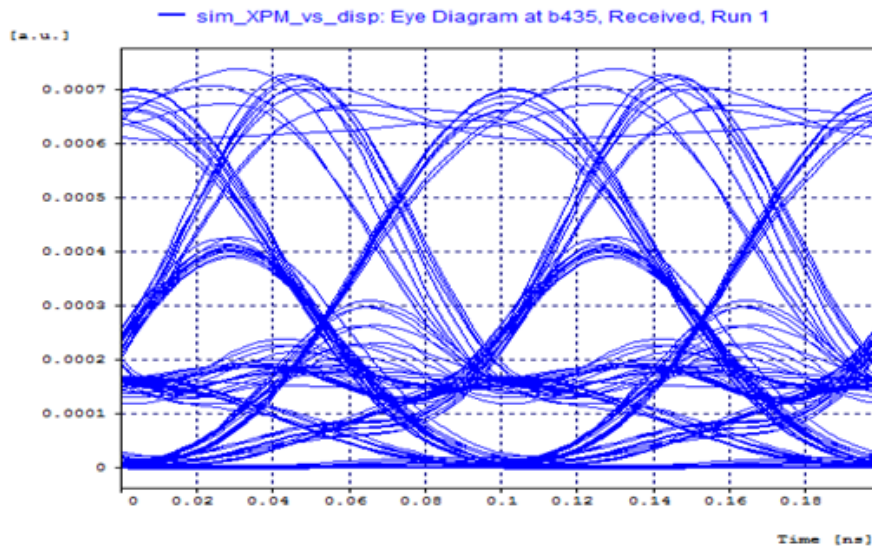


Figure 4.19: Eye diagram at run 1 showing a Q value of 6.0206 dB

Figure 4.19, above shows the eye diagram having a Q value of 6.0206 at run1. The effect PMD is analyzed by performing a parametric run which shows the time varying property of PMD.

Figure 4.20 below shows that the due to the time varying effect the eye diagram changes and thus Q value also changes.

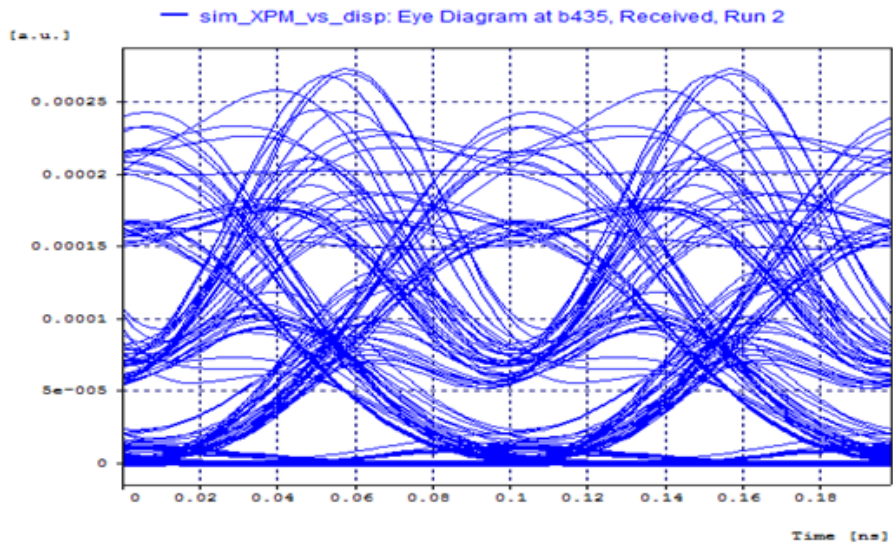


Figure 4.20: Eye diagram at run 2 showing a Q value of 7.463510 dB

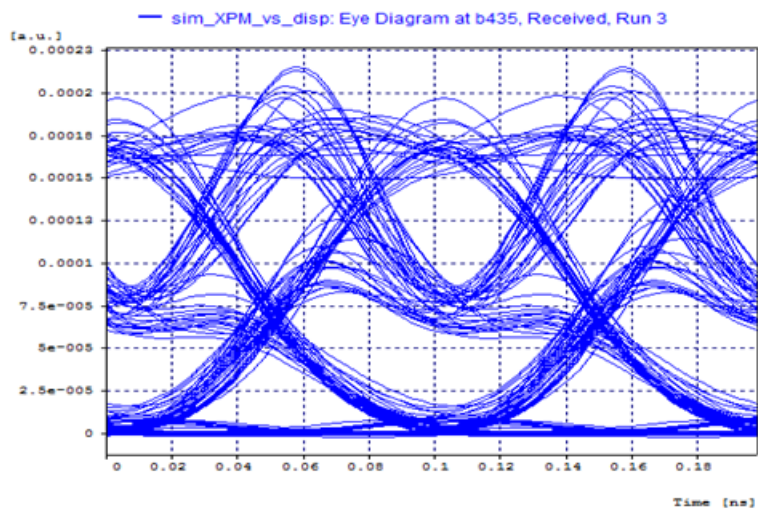


Figure 4.21: Eye diagram at run 3 showing a Q value of 9.911912 dB

Figure 4.21 shows that the variations in the eye diagram. Thus Figures 4.19 to 4.21 shows the effect of PMD in an optical fiber link of 100 km.

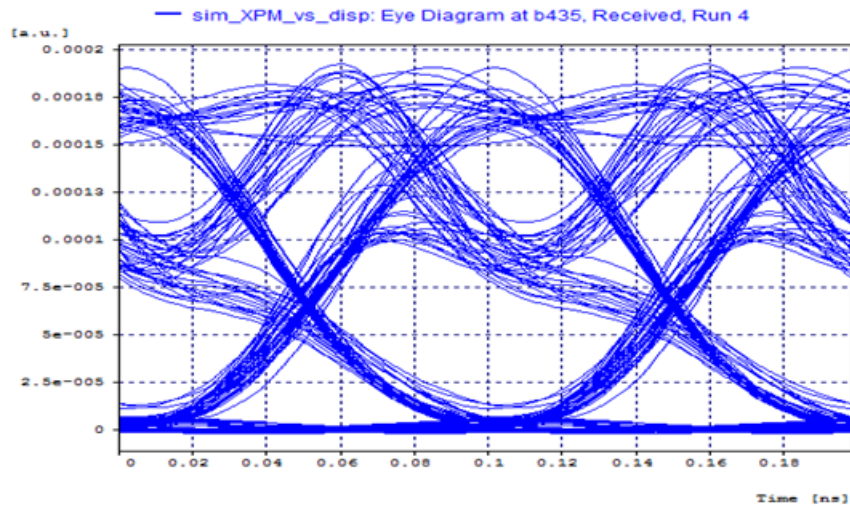


Figure 4.22: Eye diagram at run 4 showing a Q value of 12.561970 dB

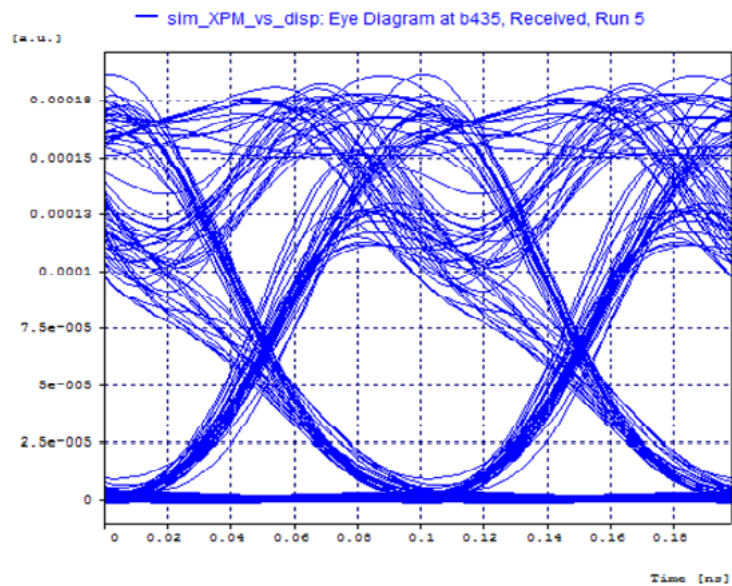
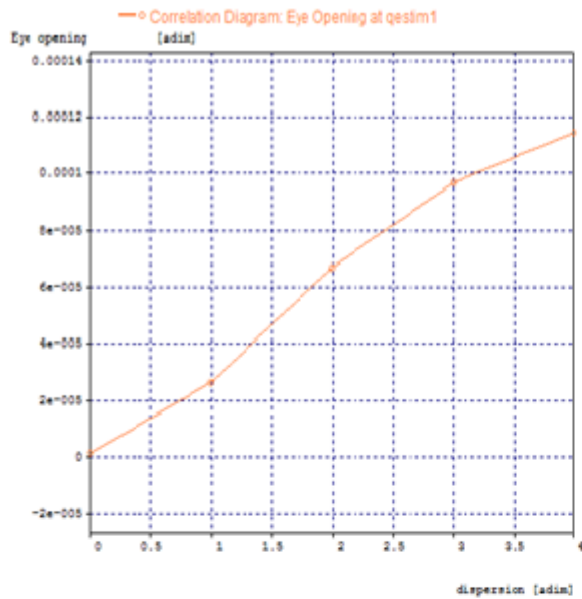
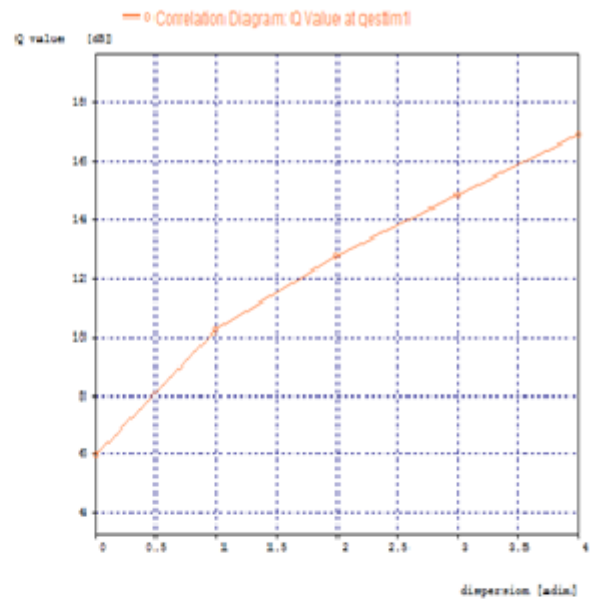


Figure 4.23: Eye diagram at run 5 showing a Q value of 15.541085 dB

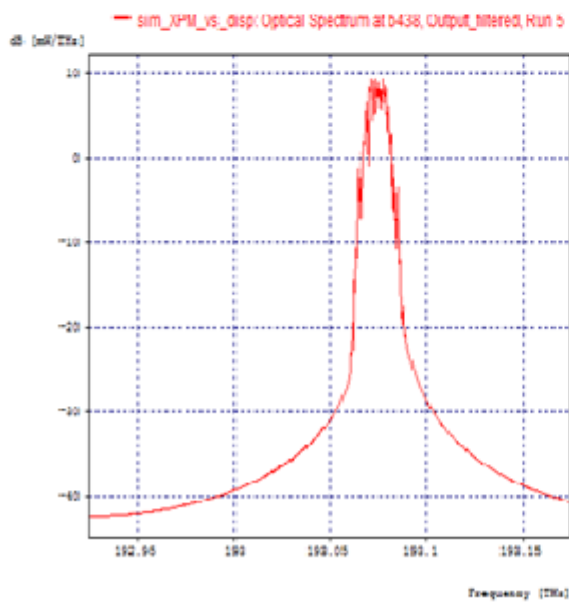
Figures 4.22 and 4.23 shows the effect of optical compensation at 2 different runs by which the Q value is increased.



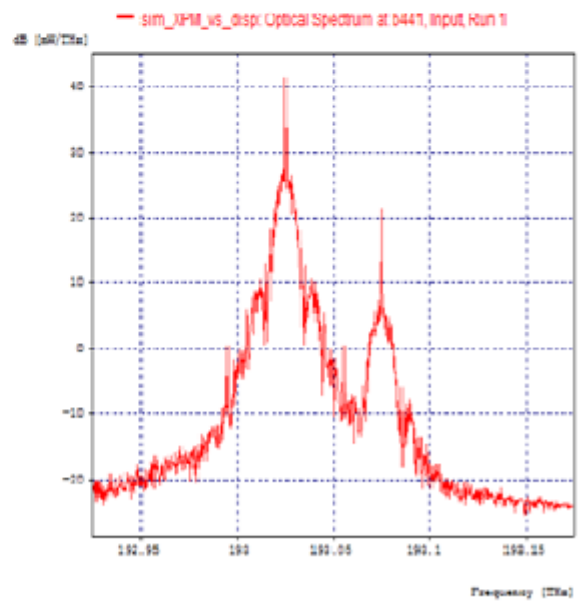
(a)



(b)



(c)



(d)

Figure 4.24: (a) Graph (b) Eye Opening Graph (c) Optical Spectrum for Transmitted Signal (d) Optical Spectrum for Received Signal for simulation 1 is shown

4.10.2 Simulation with Varying PMD Coefficient

Table 4.5: Simulation 2 with varying PMD co-efficients keeping other factors constant

Run	1	2	3	4	5	6	7	8
PMD Co-eff	0.01	1.01	2.01	3.01	4.01	5.01	6.01	7.01
BER	$9.46e^{-30}$	$9.46e^{-40}$	$9.46e^{-40}$	$3.88e^{-36}$	$4.71e^{-5}$	$2.56e^{-9}$	$3.29e^{-7}$	0.011
Q Value	21.072	23.000	22.850	21.946	11.909	15.477	13.984	7.270

Figures 4.25 to 4.31 below shows the effect of PMD in an optical fiber link of 100 km.

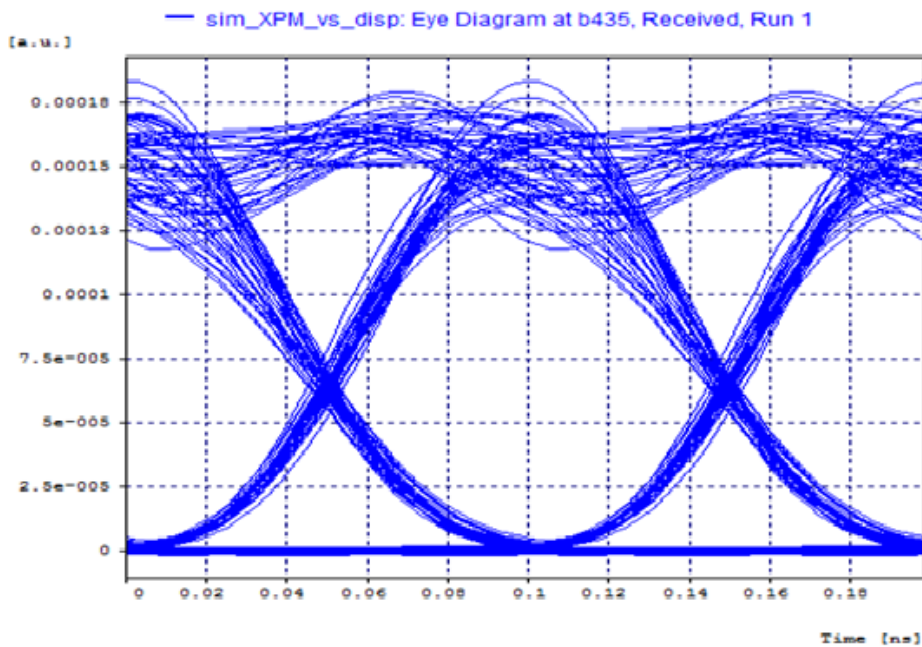


Figure 4.25: Eye diagram at run 1 showing a Q value of 21.072053 dB

Figure 4.25 above shows the eye diagram having a Q value of 21.072053 dB at run1. The effect PMD is analyzed by performing a parametric run which shows the time varying property of PMD.

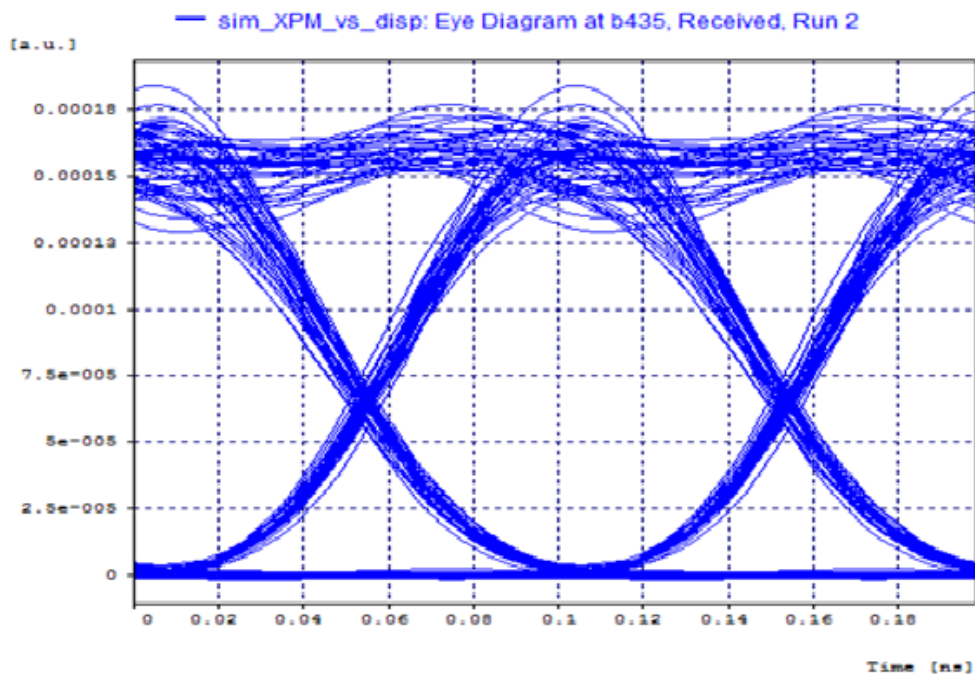


Figure 4.26: Eye diagram at run 2 showing a Q value of 23.00 dB shows that the due to the time varying effect the eye diagram changes and thus Q value also changes

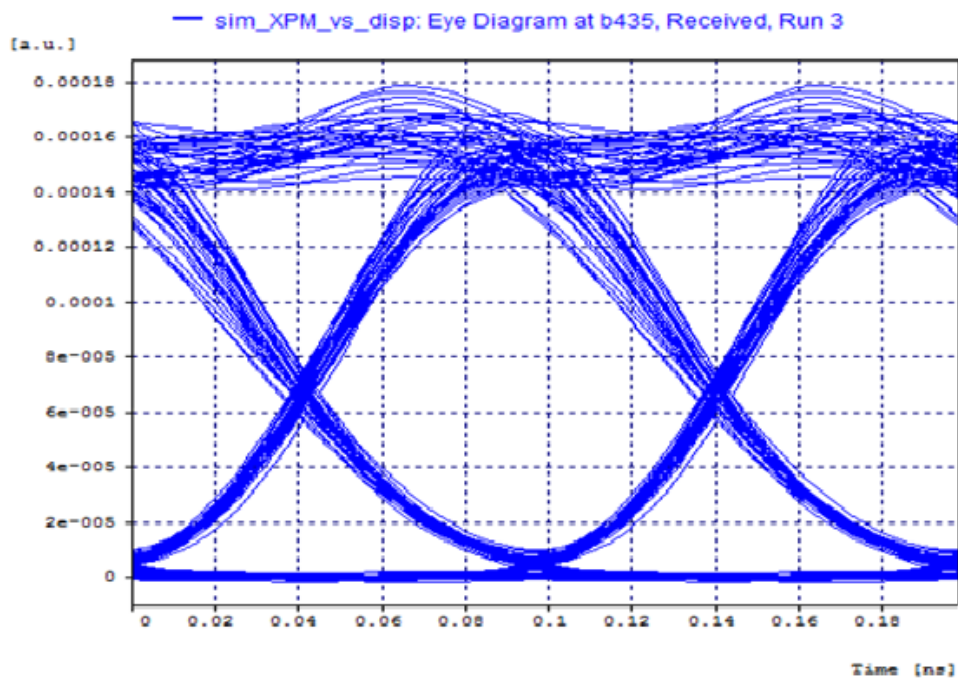


Figure 4.27: Eye diagram at run 3 showing a Q value of 22.850229 dB showing variations

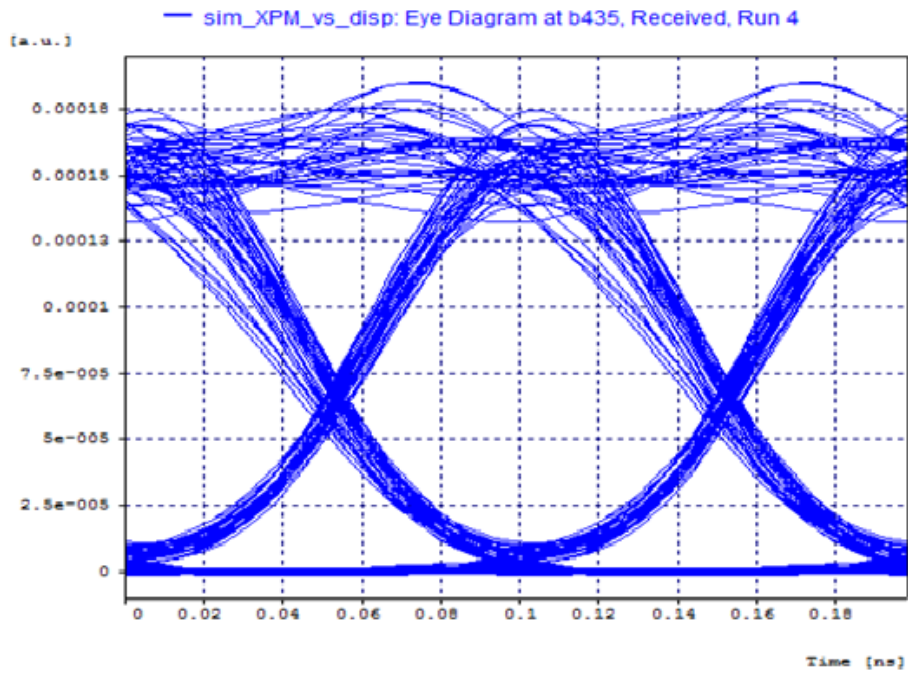


Figure 4.28: Eye diagram at run 4 showing a Q value of 21.946904 dB

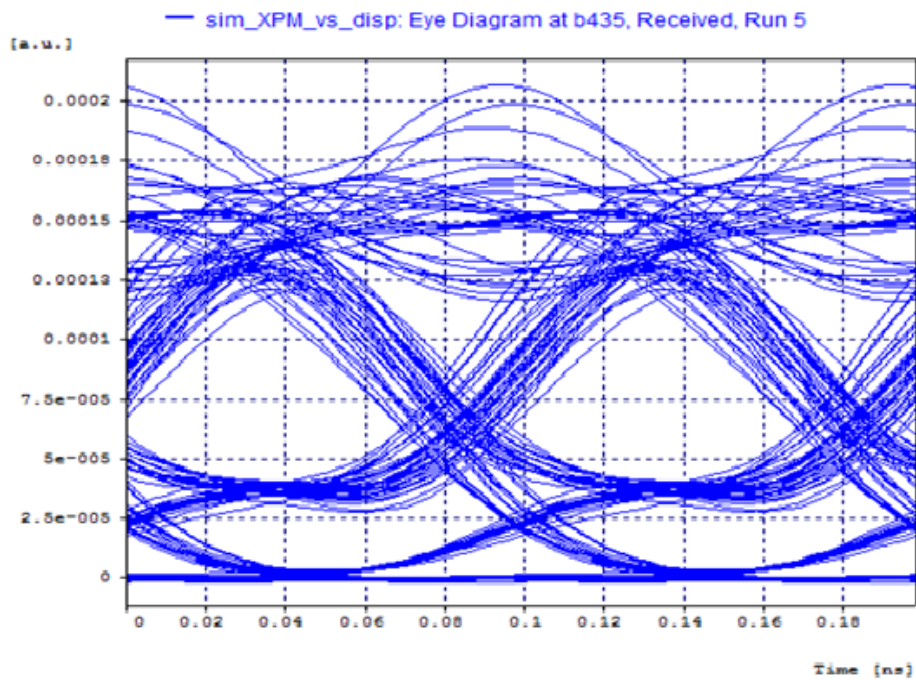


Figure 4.29: Eye diagram at run 5 showing a Q value of 11.909151 dB

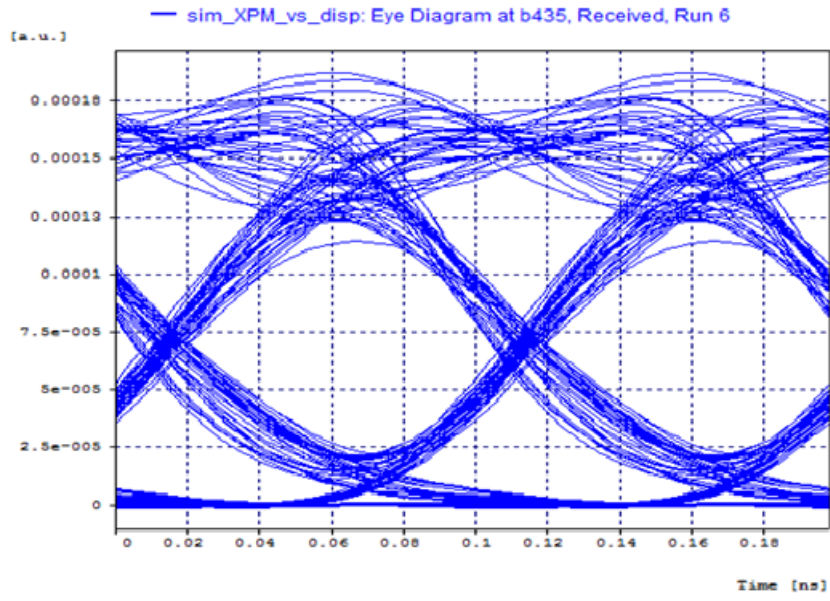


Figure 4.30: Eye diagram at run 6 showing a Q value of 15.477207 dB

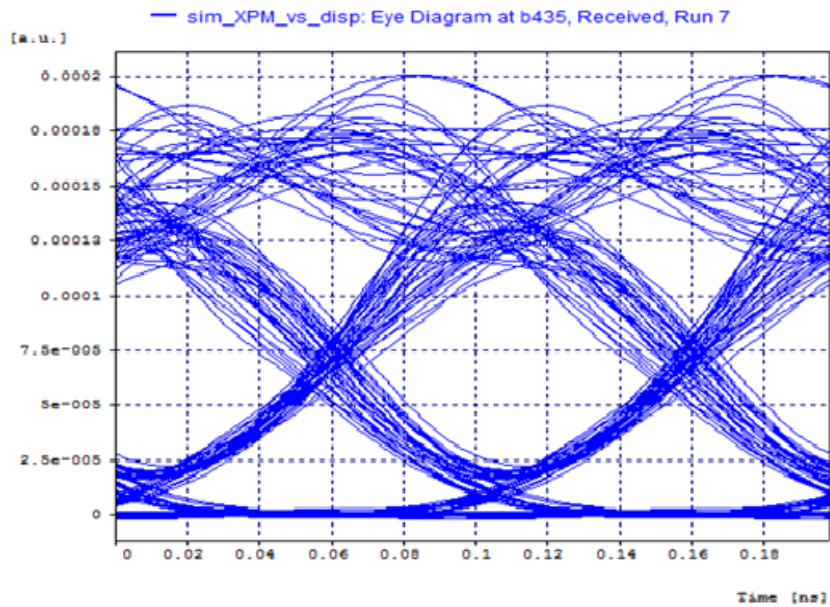


Figure 4.31: Eye diagram at run 7 showing a Q value of 13.984685 dB

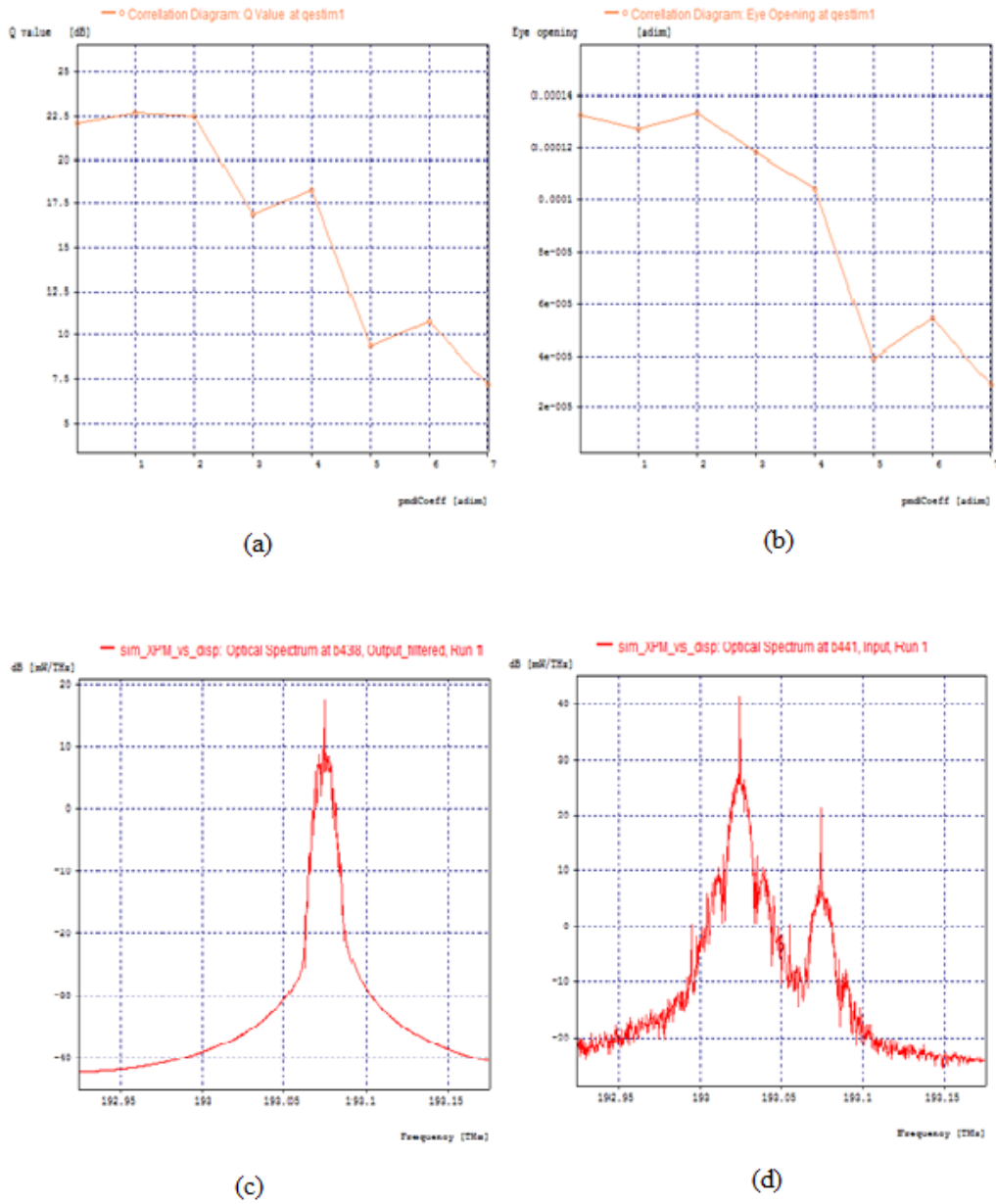


Figure 4.32: (a) Graph (b) Eye Opening Graph (c) Optical Spectrum for Transmitted Signal (d) Optical Spectrum for Received Signal for simulation 2 is shown

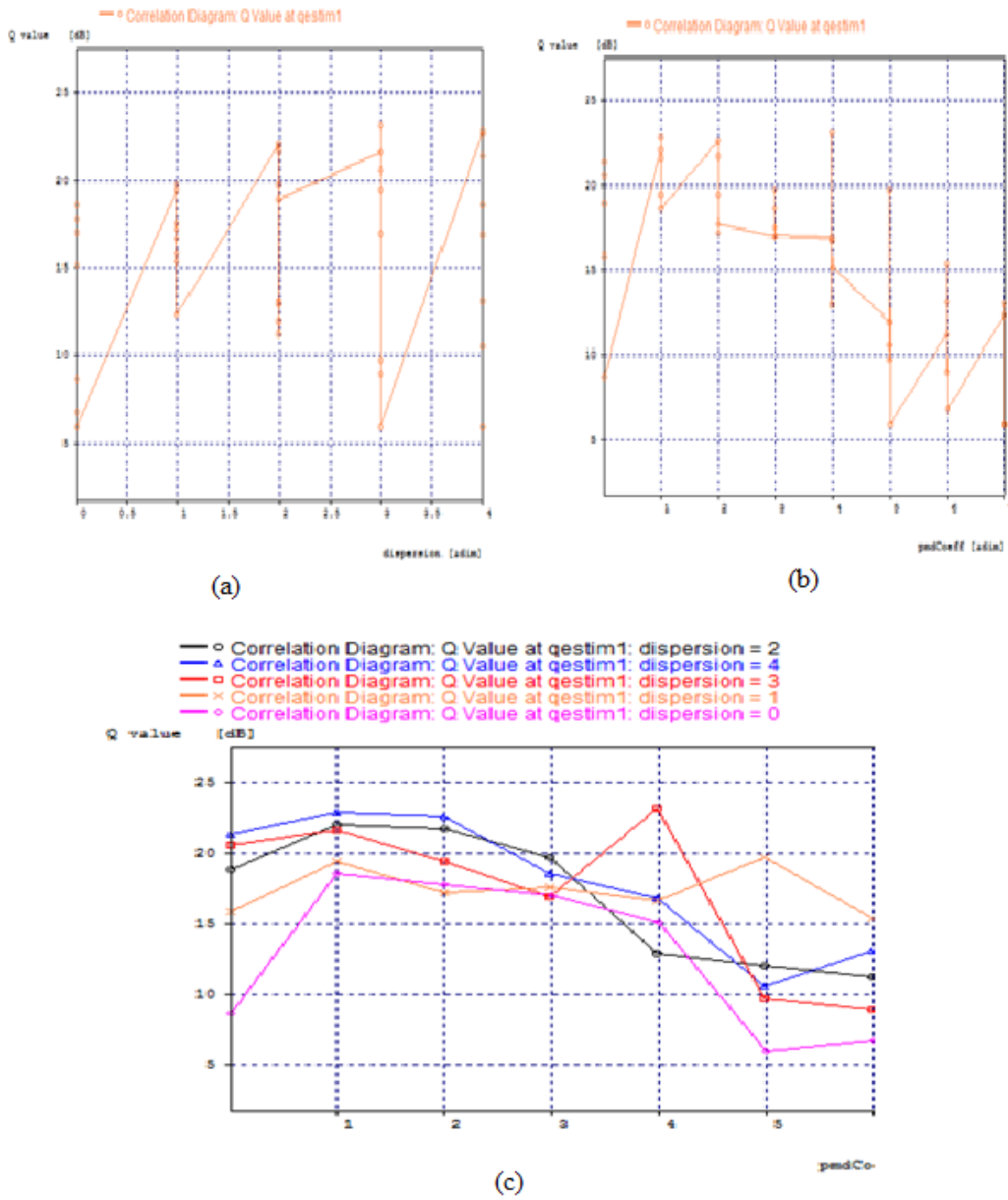


Figure 4.33: (a) combined effect of Q value and dispersion (b) combined effect of Q value and PMD (c) combined effect of Q value PMD and dispersion for simulation 3 is shown

4.11 Summary

The above simulations are based on the analysis and optical compensation of polarization mode dispersion. The impact of XPM on the 1st-order PMD compensator is numerically simulated for a two-channel WDM system with the bit rate in each channel of 40-Gbit/s. Simulation results show that a 1st-order PMDC does not change the distribution of the remaining EOP in a single channel system. In a DWDM system, the XPM effect from the pump channel does not affect the EOP distribution much before the 1st-order PMD compensation; but the EOP distribution will disperse over the whole EOP range when a 1st-order PMD compensator is used to compensate for the DGD of the preceding fiber link. This indicates that the occurrence probability of larger EOPs will increase heavily due to the XPM effect after the 1st-order PMD compensation. Furthermore, in a WDM system, the larger the input average optical power in the pump channel, the severer the impact of XPM on 1st-order PMD compensation. When the XPM-inducing input average optical power in the pump channel reaches 0dBm, the impact of XPM on the 1st-order PMD compensator is visible.

CHAPTER 5

CONCLUSION AND FUTURE WORK

5.1 Conclusion of this Study

A rigorous analysis has been carried out to explain the optical line coding scheme, quantify the effect of XPM, modeling the system to apply the line coding scheme and finally to quantify the effect of the application of line coding scheme in a multiple channel DWDM scheme. We have also discussed the effect of PMD in DWDM system induced by XPM and how they affect PMD impairments and PMD mitigation.

The application of line coding in optical communication system exhibits promising features that will be useful for future high speed, long distance optical networks. The multilevel line coding schemes especially Novel Optical line code of order one show an improvement of about 1.3 dB at different lengths. The parameters of the optical communication system model discussed in this study conform to the real life optical systems. At longer distance, high bit rate and lower channel spacing the XPM effect become more dominant causing higher BER. It has been observed that the performance of conventional DWDM system without employing appropriate line coding show more ISI, the performance is further deteriorated when channel spacing is less and input power per channel is high. Line coding scheme is found an effective tool in combating the nonlinear effects by reducing the dispersion effects. Two line coding schemes; Duobinary and Novel Optical coding were described in detail. These schemes are implemented in the modeled system to combat the effect of XPM successfully. Out of these two schemes, Novel Optical line coding of order one is found more effective. A remarkable improvement in system performance can be achieved by this scheme. Maximum allowable input power per channel is much higher than that of a system without line coding. The balanced configuration of the system including the encoder, transmitter, amplifier, receiver and decoder yields a system with lower BER even at lower channel spacing and longer distance which enables larger link length at higher band width.

Therefore, these schemes will also be attractive for DWDM networks.

PMD is a time changing quantity which causes a serious problem that limits distances. The PMD in a fiber link is analyzed through various eye diagrams by parametric run in OptSim simulation which confirms the degradation of system performance at higher bit rates. An optical compensation method by which the effect of PMD can be mitigated is shown as an increase in Q value and decrease in BER from the eye diagrams of the simulation.

5.2 Future Work

In our work we have assumed that the fibers used in the transmission system are perfect without considering FWM, SRS, SBS, PMD, etc. Therefore, a study on how line coded DWDM system performs after considering those nonlinear effects is of immediate of interest. In the calculation of bit error rate (BER), we have not encountered the response of the optical filters and amplifier noise, and if fiber amplifiers are used, then FWM effect in these fibers will also have to be taken into account. Moreover, we have analyzed the systems considering only a repeater-less network. So there is an opportunity to analyze the multi-channel multi-repeater systems and the combined systems considering amplifier noise along with shot noise, thermal noise and FWM noise. Future studies may include dispersion management schemes with line coding schemes to combat the nonlinear effects.

REFERENCES

- [1] Senior J. M., *Optical Fiber Communication* 2nd Edition, New Delhi, Prentice-Hall of India, 2002.
- [2] Kao K. C., Hockham G. A., *Dielectric Fiber Surface Waveguides for Optical Frequencies*, Proceedings of the IEE, vol. 133, pp.1151-1158, July 1966.
- [3] Trischitta, M. Colas, M. Green, G. Wuzniak, J. Arena, *The TAT-12/13 cable network*, IEEE Communication Magazine, vol.34, no.2, pp.24-28, February 1996.
- [4] Marcuse D., Chraplyvy A. R., Tkach R. W., *Dependence of Cross-Phase Modulation on Channel Number in Fiber WDM Systems*, Journal of Lightwave Technology, vol.12, no.5, pp.885-890, May 1994.
- [5] Chiang T. K., *Cross-phase modulation in dispersive fibers: theoretical and experimental investigation of the impact of modulation frequency*, IEEE Photonics Technology Letters, vol.6, no.6, pp.733-736, June 1994.
- [6] Chiang T. K., *Cross-Phase Modulation in Fiber Links with Multiple Optical Amplifiers and Dispersion Compensators*, Journal of Lightwave Technology, vol.14, no.3, pp.249-259, March 1996.
- [7] Song K., Premaratne M., *Effects of SPM, XPM and Four Wave Mixing in L-Band ED-FAs on Fiber-Optic Signal Transmission*, IEEE Photonics Technology Letters, Vol 12, No 12, pp. 1630-1632, December 2000.
- [8] Cartaxo A. V. T., *Impact of Modulation Frequency on Cross Phase Modulation Effect in IM/DD WDM Systems*, IEEE Photonics Technology Letters, vol.10, no.9, pp.1268-1270, September 1998.
- [9] Cartaxo A. V. T., *Cross Phase Modulation in Intensity Modulation - Direct Detection WDM systems with Multiple Optical Amplifiers and Dispersion Compensators*, Journal of Lightwave Technology, Vol. 17, No. 2, , pp. 178-190, February 1999.

- [10] Djordjevic B. I., *Transmission Limitations of WDM Transmission Systems with Dispersion Compensated Links in the Presence of Fiber Nonlinearities*, IEEE Photonics Technology Letters, vol.1, no.2, pp. 496 - 499, March 2001.
- [11] Norimatsu S. and Yamamoto T., *Waveform Distortion Due to Stimulated Raman Scattering in Wide Band WDM Transmission Systems*, Journal of Lightwave Technology, vol.19, no.2, 226-236 February 2001.
- [12] Bellotti G., *Intensity Distortion Induced by Cross-Phase Modulation and Chromatic Dispersion in Optical-Fiber Transmissions with Dispersion Compensation*, IEEE Photonics Technology Letters, vol.10, no.12, pp.1745-1747, December 1998.
- [13] Kowalewski M., Marciniak M. and Sedlin A., *Nonlinear Interactions in Wavelength Multiplexed Optical Fiber Telecommunications Systems*, Journal of Optics, Pure Applications, pp 319-326, February 2000.
- [14] Lakoba T. I. and Agrawal G. P., *Optimization of the Average-Dispersion Range for Long-Haul Dispersion-Managed Systems*, Journal of Lightwave Technology, vol.18, no.11, pp 1504-1512 November 2000.
- [15] Ten S., Enns K. M., Grochocinski J. M., Burtsev S. P. and Silva V. L., *Comparison of Four Wave Mixing and Cross Phase Modulation Penalties in dense WDM at 2.5 GBits/s*, Journal of Lightwave Technology, vol.19, no.5, pp 679-685 May 2000.
- [16] Betti S., Giacon M. and Nardini M., *Effect of Four Wave Mixing on WDM Optical Systems: A Statistical Analysis*, IEEE Photonics Technology Letters, vol.18, no. 8, pp.745-747, August 2003.
- [17] Thiele H. J., Killey R. I. and Bayvel P., *Pump-Probe Investigation of Cross Phase Modulation in Standard-Fibre, Dispersion Compensated WDM Recirculating Loop*, Conference on Lasers and Electro-Optics, pp.305-306, May, 1999.
- [18] Hoon K., *Cross Phase Modulation Induced Nonlinear Phase Noise in WDM Direct Detection DPSK Systems*, Journal of Lightwave Technology, vol. 21, no. 8, pp 1126-1137 August 2003.

- [19] Sang S. L., Hyun J. L., Wanseok S. and Seung G. L., *Stimulated Brillouin Suppression Using Cross Phase Modulation Induced by an Optical Supervisory Channel in WDM Links*, IEEE Photonics Technology Letters, vol. 13, no. 7, pp.145-149, July 2001.
- [20] Keang P. H., Channel Capacity of WDM Systems Using Constant Intensity Modulation Formats, Proceedings of Optical Fiber Communications Conferences, May 2002.
- [21] Wang Z., Bodtker E. and Jacobson G., *Effects of Cross Phase Modulation in Wavelength Multiplexed SCM Video Transmission Systems*, Electronic Letters, vol. 31, no. 10, pp 893-896 October 1995.
- [22] Belloti G., Varani M., Francia C. and Bononi A., *Intensity Distortion Induced by XPM and Chromatic Dispersion in Optical Fiber Transmission with Dispersion Compensation*, IEEE Photonics Technology Letters, Vol 10, No 12, pp. 605-607, Dec 1998.
- [23] Hui R., Demarest K. R. and Allen C. T., *Cross Phase Modulation in Multispan WDM Optical Fiber Systems*, Journal of Lightwave Technology, vol. 17, no. 6, pp 1018-1026, June 1999.
- [24] Thiele H. J., Killy R. I. and Bayvel P., *Investigation of XPM Distortion in Transmission over Installed Fiber*, IEEE Photonics Technology Letters, Vol 12, No 6, pp 669 -671, June 2000.
- [25] Hui R., Wang Y., Demarest K. and Allen C., *Frequency Response of Cross Phase Modulation in Multispan WDM Optical Fiber Systems*, IEEE Photonics Technology Letters, Vol 10, No 9, pp 1271 -1273, September 1998.
- [26] Majumder S. P., Gangopadhyay R., Alam M. S. and Prati G., *Performance of Linecoded Optical Hetrodyne FSK Systems with Nonuniform Laser FM Response*, Journal of Lightwave Technology, Vol. 13, No. 4, pp. 628-638, April 1995.
- [27] Agrawal G. P., *Nonlinear Fiber Optics*, Second Ed., Academic Press, San Diego, 1995. pp. 5-20, 267-288.
- [28] Chraplyvy, *Impact of Nonlinearities on Lightwave Systems*, Optics and Photonics News, vol.5, pp.16-21, May 1994.

- [29] Kurtzke C., *Suppression of Fiber Nonlinearities by Appropriate Dispersion Management*, IEEE Photonics Technology Letters, vol.5, pp. 1250-1253, 1993.
- [30] Ezmir M. R. Majumder S. P. and Muhammad A. F., *Eye Penalty Due to Cross-Phase Modulation (XPM) in a Single Segment WDM IM/DD Transmission System*, Faculty of IT, Multimedia University, Malaysia.
- [31] Pal B., Gangopadhyay R. and Prati G., *Analytical Evaluation of Transmission Penalty Due to Group Velocity Dispersion, Self-Phase Modulation and Amplifier Noise in Optical Heterodyne CPFSK Systems*, Journal of Lightwave Technology, Vol. 18, No. 4, pp. 530-539, April 2000.
- [32] Binh L. N. and Perera D., *Modelling Platform for Ultra-Long Ultra-High-Speed Dispersion-Managed DWDM Optical Fibre Communication Systems*, Technical Report, MECSE-13-2003, Monash University.
- [33] R. Udayakumar, V. Khanaa and T. Saravanan., *Analysis of Polarization Mode Dispersion in Fibers and its Mitigation using an Optical Compensation Technique*.
- [34] Arun Kumar. Ajoy Ghatak., *Polarization of Light with Applications in Optical Fibers*.
- [35] Sergey Ten , Merrions Edward, WP5051 *An Introduction to the Fundamentals of PMD in Fiber*
- [36] <http://optics.synopsys.com/rsoft/application-gallery/pmd-in-highbit-rate-systems.html>, [05 December 2013].